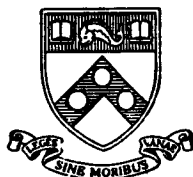


Final Report

STUDY OF GSFC RADIO FREQUENCY
INTERFERENCE DESIGN GUIDELINE
FOR
AEROSPACE COMMUNICATIONS SYSTEMS

25 April 1967

Contract No.: NAS5-9896



GPO PRICE \$ _____

CFSTI PRICE(S) \$ _____

Hard copy (HC) 3.00

Microfiche (MF) .65

Prepared by:

ff 653 July 65

The Moore School of Electrical Engineering

UNIVERSITY of PENNSYLVANIA

PHILADELPHIA, PENNSYLVANIA 19104

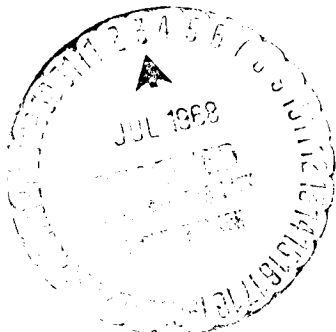
For

Goddard Space Flight Center

GREENBELT, MARYLAND

Moore School Report No. 68-21

UNCLASSIFIED



N 68-27646

(THRU)

(CODE)

(CATEGORY)

(ACCESSION NUMBER)

(PAGES)

(NASA CR OR TMX OR AD NUMBER)

FACILITY FORM 602

Final Report

STUDY OF GSFC RADIO FREQUENCY INTERFERENCE (RFI)
DESIGN GUIDELINE FOR AEROSPACE COMMUNICATIONS SYSTEMS

25 April 1967

Contract No.: NAS5-9896

Prepared by:

THE MOORE SCHOOL OF ELECTRICAL ENGINEERING
University of Pennsylvania
Philadelphia, Pa. 19104

N68 27646

For

GODDARD SPACE FLIGHT CENTER
Greenbelt, Maryland

Moore School Report No. 68-21

UNCLASSIFIED

TABLE OF CONTENTS

	<u>Page</u>
I. SCOPE OF STUDY PROGRAM AND PROGRESS	1
II. STATE OF WORK UNDERWAY AND RECOMMENDATIONS FOR CONTINUATION	4
1. Frequency and Load Assignment	4
2. Continuation of Studies of Interference Effect ...	5
III. TECHNICAL REPORTS	7
1.0 Tracking Errors Caused by Interference to the Minitrack System	8
1.1 Description of Minitrack System	8
1.2 Interference Effects	11
1.2.1 CW Interference	11
1.2.2 Broadband Interference	25
1.3 Conclusions	30
2.0 A Study of the Phase Locked Loop with Interference	40
2.1 Introduction	40
2.2 The Phase Locked Loop with Interference-- An Infinite Series Approach	41
2.3 The Effect of Interference on the Acquisition Time and Pull-in Range of the Phase Locked Loop--A Quasi-Stationary Approach	54
2.4 Phase Plane Solutions to the Second Order Phase Lock Loops with Interference	67
2.5 Appendix A	91
2.6 Appendix B	94
2.7 References	97

LIST OF FIGURES

<u>Figure</u>		<u>Page</u>
1-1	ψ_1 and ψ_2 Identify Angles Measured in Minitrack System	32
1-2	Relation Between Delay and Inclination Angle	33
1-3	Block Diagram of 136 MHz Minitrack Receiver	34
1-4	Various Inputs to the Post-Detection Filter	35
1-5	Angular Errors Obtained Through Phasor Diagrams ..	36
1-6	Phase Errors Created by CW and Broadband Interference	38
1-7	Phase Errors for Small X; Expansion of Lower Part of Fig. 1-6	39
2-1	Model for the Phase Locked Loop	98
2-2	Second Order Loop Filter	99
2-3	Model for the Phase Locked Loop	99
2-4	Output Spectrum of an Ideal Limiter with Limiter Filter Characteristic and Loop Filter Characteristic Superimposed	99
2-5	Effective Loop Gain with Interference Versus the Relative Interference Amplitude	100
2-6	The Acquisition and Process: The Spectral Analysis Viewpoint and the Composite Signal Viewpoint	101
2-7	Limiter Output Spectrum with Loop Filter Characteristic Superimposed	102
2-8	Instantaneous Frequency Input to Loop with $\cos \omega t + a \cos (\omega + \delta) t$ At Input to Limiter With a as a Parameter	103
2-9	Instantaneous Frequency Input to Loop with $\cos \omega t + a \cos (\omega + \delta) t$ At Input to Limiter With a as a Parameter	104
2-10	Instantaneous Frequency Input to Loop with $\cos \omega t + a \cos (\omega + \delta) t$ At Input to Limiter With a as a Parameter	105

<u>Figure</u>		<u>Page</u>
2-11	Instantaneous Frequency Input to Loop with $\cos \omega t + a \cos (\omega + \delta) t$ At Input to Limiter With a as a Parameter	106
2-12	Instantaneous Frequency Input to Loop with $\cos \omega t + a \cos (\omega + \delta) t$ At Input to Limiter With a as a Parameter	106
2-13	Piecewise Linear Approximation to Instantaneous Frequency	107
2-14	Phase Plane Solution to Second Order Loop Equation	108
2-15	Change in Average Frequency Caused by Phase Locked Loop	109
2-16	Peak to Peak Fluctuation in Input and Output Frequency As a Function of a	110
2-17	Approximate Frequency Input	111
2-18	Output Frequency Error for Input of Fig. 2-17	112
2-19	Approximate Input Frequency	113
2-20	Normalized Approximation to Input Frequency	113
2-21	Phase Plane Solution to Second Order Loop Equation with Trajectory for Input of Figs. 2-19 and 2-20 Superimposed	114
2-22	Graphical Integration	115
2-23	Graphical Integration	116
2-24	Graphical Integration	117
2-25	Graphical Integration	117
2-26	Graphical Integration	117
2-27	Output Frequency Error for Input of Figs. 2-19 and 2-20	118

I. SCOPE OF STUDY PROGRAM AND PROGRESS

A study of radio frequency interference in GSFC ground installations has been underway at the Moore School of Electrical Engineering of the University of Pennsylvania since June 25, 1965. The purpose of this work was to identify the major sources of radio interference at the GSFC stations, to analyze the severity of the interference, and to propose methods of minimization. The output of the study was to be a document presenting guidelines for interference minimization suitable for use by equipment designers and system planners. Such a document has been completed and submitted. Discussed in the document are: 1) mechanisms of generation of unwanted emissions, 2) receiver susceptibility mechanisms, 3) equipment design for interference minimization, 4) methods of interference measurement, and 5) site selection for avoiding areas of concentration of radio sources.

During the course of this work, data on actual interference encounters at the various ground stations were made available to us. These data were summarized and presented as function of time of occurrence, place of occurrence, and type of interference for the years 1964-1966. A report entitled "Summary of STADAN Network Radio Frequency Interference Events" containing the results of the data analysis was issued early in 1967.

To a large measure the interference encountered at GSFC satellite tracking and data acquisition stations is a result of the simultaneous appearance of two (or more) satellites in the field of view of the ground station which have equal or nearly equal frequency

assignments. This was anticipated in the early stages of the study and borne out by the interference data. Accordingly, methods of predicting and of minimizing such interference were studied. The prediction studies resulted in a computer program which uses the anticipated locations of all the satellites aloft and the electrical parameters of the satellite transmitters to determine future interference encounters. In addition a statistical study was undertaken which had as its purpose the development of a frequency assignment plan which minimizes the probability of interference. The results of the latter two studies are reported in the second interim report on this contract, Chapter 5, dated 30 April 1966. Since this work was reported, additional attention was given to this problem expanding it to include load assignment as well as frequency assignment. Since the continuation of this work is a major effort a brief statement of the status of the work and the direction it might take in the future is given in Section II.

While mechanisms of generation of unwanted emissions and mechanisms of entry into receivers have received much attention in the past the information of the effect of interference on the receiver output is usually found to be insufficient. We have therefore given attention to 1) the tracking errors caused by interference in the Minitrack system, and 2) the behavior of phase locked loops subjected to interference. The first of these problems was discussed, in part, in the second interim report on this contract, Section 3.3.2. Since the publication of that report the work was completed and a technical report

prepared. This report is included here under Section III, Part 1 entitled "Tracking Errors Caused by Interference to the Minitrack System." The problem of the phase locked loop was mentioned in Section 3.3.1 of the second interim report but was not pursued there in any detail. Since the publication of that report several methods of analyzing the interference effect were studied and are presented here under Section III, Part 2 entitled "A Study of the Phase Locked Loop with Interference."

II. STATE OF WORK UNDERWAY AND RECOMMENDATIONS FOR CONTINUATION

1. Frequency and Load Assignment

As pointed out above, the problem of optimum frequency assignment has received some attention; the second interim report, Section 5.2 contains the details of this work. A method of assignment was outlined but the detailed procedure, which will require a computer program, remains to be developed. Furthermore, it appears reasonable to go a step further and to propose that the overall system be optimized with a view to maximizing the information transfer between satellite and ground. The study should provide a basis for

- (1) locating new stations;
- (2) assigning ground stations to a given satellite for tracking and/or data collections;
- (3) assignment of frequencies.

These decisions should be made subject to a number of constraints, among which are

- (1) existing ground locations;
- (2) orbital elements;
- (3) transmitter and receiver characteristics (power, information rate, etc.);
- (4) available bands;
- (5) storage capabilities of satellites;
- (6) satellite priority.

Solution of the problem depends mainly on the choice of a suitable mathematical model for the total space-ground system.

The model considered is a probabilistic model. Satellites are assumed to enter and stay in the region of view of a ground station according to a probability law. Information is transferred from a satellite to a ground station when the former is in the region of view of the latter and there is no interference from other satellites. In case of interference a satellite, it is assumed, may be ordered to store information until another pass at a certain cost, depending on the amount of information stored and on the storage time.¹ The cost of the information lost depends on (a) the satellite it has been collected by, and (b) the time at which it is supposed to be transmitted. It is desired to minimize the average cost, where the average is taken with respect to time, satellites and ground stations. The variables in this problem are the parameters of the joint probability distribution of the information transferred during successive passes.

2. Continuation of Studies of Interference Effect

Analyses of the effect of interference are often made tractable by using convenient, but not necessarily realistic, assumptions about the nature of the interference and the system through which it passes. It is therefore essential that experiments be carried out to demonstrate the validity of the analysis. In certain instances the mathematical model is so formidable that no one cares to undertake analysis; the only alternative is to use experiment.

Experiments can be carried out directly, or indirectly on simulated models. The latter method has shortcomings too since it does

¹ If the total information required to be stored exceeds the storage capacity information will be lost and a cost is associated with the loss.

not involve the actual device, but it is a middle ground between pure analysis and direct experiment.

We believe it will be of great value to initiate an experimental program leading to results of output interference effect on the various components of the STADAN system. Tracking and measurement errors in the Minitrack system and the Range and Range-Rate system ought to be found. Error probabilities and other measures of output noise should be found for the data acquisition devices. The tracking errors, acquisition time, and loss of lock in phase-locked loops should also be found.

III. TECHNICAL REPORTS

1.0 TRACKING ERRORS CAUSED BY INTERFERENCE TO THE MINITRACK SYSTEM

2.0 A STUDY OF THE PHASE LOCKED LOOP WITH INTERFERENCE

1.0 TRACKING ERRORS CAUSED BY INTERFERENCE TO THE MINITRACK SYSTEM

1.1 Description of Minitrack System

The Minitrack system, which forms a basic part of the STADAN network, is used to determine satellite orbits by means of a series of independent angle measurements that are made at different ground stations.

The Minitrack system basically consists of a radio interferometer which has two antenna arrays orthogonally aligned along east-west and north-south baselines. These interferometer arrays provide measurements of the angles ψ_1 and ψ_2 in Fig. 1-1. The elevation and bearing of the satellite can then be obtained by means of the following relations:

$$\tan^2 \theta = \cot^2 \psi_1 + \cot^2 \psi_2 \quad (1-1)$$

$$\sin^2 \phi = \frac{\cot^2 \psi_1}{\cot^2 \psi_1 + \cot^2 \psi_2} \quad (1-2)$$

The interferometer array obtains a measurement of the angle ψ by measuring the phase delay which results when the wavefront arriving from the satellite intersects the receiving array at the angle ψ (see Fig. 1-2). This phase delay is created due to the time needed for the wavefront to progress from element x of the array to element y. If $\Delta\phi'$ represents the phase delay, then

$$\Delta\phi' = 2\pi \frac{a}{\lambda} \quad (1-3)$$

where ' λ ' is the wavelength and 'a' represents the "radio path difference" expressed in wavelengths. From Fig. 1-2 it can be seen that

$$\cos \psi = \frac{a}{d} = \frac{a}{n\lambda}$$

Hence,

$$\cos \psi = \frac{\Delta\phi'}{2\pi n} \quad (1-4)$$

Equation (1-4) represents the basic equation from which the angle ψ can be computed.

The angular resolution of the interferometer array increases with the distance 'd' between the elements of the array; the best resolution is obtained for a separation of many wavelengths. In the Minitrack system, the so-called "fine" antenna, which has an element separation distance of $n = 46$ wavelengths, provides the maximum system resolution. The maximum phase difference $\Delta\phi'$ is obtained when $\psi = 0$ and $a = d = n\lambda$. From (1-3) we see this to be $\Delta\phi'_{\max} = 2\pi n$. The electrical phase measuring system will determine $\Delta\phi'$ modulo 2π . That is

$$\Delta\phi' = 2\pi k + \phi_1, \quad k = 0, 1, 2, \dots, n = 46$$

and the system measures ϕ_1 , an angle which is less than 2π in magnitude. The corresponding value of ψ is from (1-4)

$$\cos \psi = \frac{k}{n} + \frac{\phi_1}{2\pi n} \quad (1-4a)$$

The component $\frac{k}{n}$ represents the ambiguity arising in the measurement and is resolved through the use of low resolution antennas. Two such

antenna systems are in use, a "medium" antenna in which $n = 4$, and a coarse antenna in which $n = 3.5$. Hence, for the "medium" antenna $\cos \psi$ is given by (from (1-4))

$$\cos \psi = \frac{\Delta\phi''}{8\pi} \quad (1-4b)$$

Similarly for the "coarse" antenna,

$$\cos \psi = \frac{\Delta\phi'''}{7\pi} \quad (1-4c)$$

Subtracting (1-4c) from (1-4b) gives

$$\cos \psi = \frac{\Delta\phi'' - \Delta\phi'''}{\pi} \quad (1-5)$$

It is evident that $(\Delta\phi'' - \Delta\phi''')$ will decrease monotonically from 180° when $\psi = 0^\circ$ to 0° when $\psi = 90^\circ$. Equation (1-5) gives, therefore, an unambiguous measurement of ψ and is used to determine the value of $\frac{k}{n}$ (eq. (1-4a)) in the "fine" measurement. Since $\frac{k}{n}$ ($n = 46$) changes in discrete units of $\frac{1}{46}$ it is essential that the error in the ambiguity resolving measurements be less than this amount if error in the measurement of k is to be avoided. In the work to follow the view is taken that the ambiguity channels must not have an error in the measurement of each of the angles $\Delta\phi''$ and $\Delta\phi'''$ of more than 1° .

Continuous measurements of the three phase shifts $\Delta\phi'$, $\Delta\phi''$, and $\Delta\phi'''$ are obtained using analog phase meters. These measurements are periodically sampled at fixed increments of time and fed into a digital computer.

1.2 Interference Effects

In recent months, a large number of incidents have been recorded in which unwanted radio signals have caused interference to the Minitrack system, thereby destroying the ability of a ground station to both track a satellite and gather telemetry data from it. This interference falls into one of two categories: a) co-channel interference originating from other satellites which are also transmitting in the 136-138 MHz space research band and which happen to be passing over the ground station at the same time as the desired satellite and b) adjacent channel interference originating from aircraft transmitters which operate in the 118-136 MHz aeronautical mobile band and which happen to be flying in the vicinity of the ground station. The errors created in the Minitrack system by these forms of CW interference (CW) are analyzed in the following section. A further section (1.2.2) is similarly devoted to the errors caused by broadband interference such as might be created by modulated signal sources or high-voltage power lines.

1.2.1 CW Interference

Figure 1-3 gives a simplified block diagram of the interferometer system. The following assumptions will be made in order to simplify the calculations which follow:

- 1) The IF and post-detection filters have rectangular pass-band characteristics.
- 2) The angle measurements are unaffected by noise in the measuring system.

If both the desired and undesired (interfering) signal are simultaneously present, then the input to the receiver from antenna x is given by

$$V_{ix} = A_D \cos \omega_D t + A_U \cos (\omega_U t - \xi) \quad (1-6a)$$

where A_D = amplitude of wanted signal

A_U = amplitude of unwanted signal

ω_D = frequency of wanted signal

ω_U = frequency of unwanted signal

ξ = phase lag of the unwanted signal relative to the wanted signal.

Similarly, the input signal from antenna y is given by

$$V_{iy} = A_D \cos (\omega_D t - \phi_D) + A_U \cos (\omega_U t - \phi_U - \xi) \quad (1-6b)$$

where ϕ_D = interferometer phase delay for desired signal

ϕ_U = interferometer phase delay for undesired signal.

These signals are then converted down to a lower IF frequency in the two mixers.

For the x channel, the mixer output is:

$$V_{ox} = \alpha A_D \cos \Omega_D t + \alpha A_U \cos (\Omega_U t - \xi) \quad (1-7a)$$

where Ω_D and Ω_U are the respective IF frequencies for desired and undesired signals and α is the mixer gain ($\alpha < 1$).

The mixer output in the y channel is shifted in frequency with respect to the x channel output by $\omega_o = 2\pi(100)$ rds/sec. Hence the y channel output is given by:

$$V_{oy} = \alpha A_D \cos [(\Omega_D + \omega_o)t - \phi_D] + \alpha A_U \cos [(\Omega_U + \omega_o)t - \phi_U - \xi] \quad (1-7b)$$

Both of these signals are now combined and amplified in the IF amplifier. If the amplifier gain is G, then the amplifier output is

$$V_{IF} = \alpha G A_D \left\{ \cos \Omega_D t + \cos [(\Omega_D + \omega_o)t - \phi_D] \right\} + \alpha G A_U \left\{ \cos (\Omega_U t - \xi) + \cos [(\Omega_U + \omega_o)t - \phi_U - \xi] \right\} \quad (1-8)$$

If Ω_U is outside the 10 KHz bandwidth, of the IF amplifier, then the undesired component of V_{IF} is eliminated, and there are consequently no measurement errors. In this case, the input to the detector is given by

$$E_i = \alpha G A_D \left\{ \cos \Omega_D t + \cos [(\Omega_D + \omega_o)t - \phi_D] \right\} \quad (1-9)$$

Assuming that the detector is a square law device, then

$$E_o = k E_i^2. \quad \text{Hence,}$$

$$\begin{aligned} E_o &= k \alpha^2 G^2 A_D^2 \left\{ \cos \Omega_D t + \cos [(\Omega_D + \omega_o)t - \phi_D] \right\}^2 \\ &= K A_D^2 \left\{ \cos 2\Omega_D t + \frac{1}{2} \cos [2(\Omega_D + \omega_o)t - 2\phi_D] \right. \\ &\quad \left. + \cos [2\Omega_D t + \omega_o t - \phi_D] + \cos (\omega_o t - \phi_D) \right\} \quad (1-10) \end{aligned}$$

where $K \equiv k\alpha^2 G^2$

The detector output E_o is now fed to the post-detection filter, which is a band-pass filter centered at ω_o , with a bandwidth $bG = 10$ Hz. Such a filter is only able to pass the lowest frequency component of E_o ; all the other components fall well outside the pass-band of this filter and are consequently rejected.

Hence, the output from the post-detection filter is

$$V_u = KA_D^2 \cos (\omega_o t - \phi_D) \quad (1-11)$$

which contains ϕ_D , the unknown phase difference from which the angle ψ is computed.

Now consider the case in which Ω_U falls within the 10 KHz IF bandwidth (assume also that $(\Omega_U + \omega_o)$ falls within the bandwidth). In this case, E_i is given by (1-8). The detector output will therefore be:

$$\begin{aligned} E_o = kE_i^2 = k\alpha^2 G^2 A_D^2 \left\{ \cos \Omega_D t + \cos \left[(\Omega_D + \omega_o)t - \phi_D \right] \right\}^2 \\ + k\alpha^2 G^2 A_U^2 \left\{ \cos (\Omega_U t - \xi) + \cos \left[(\Omega_U + \omega_o)t - \phi_U - \xi \right] \right\}^2 \\ + 2k \alpha^2 G^2 A_U A_D \left\{ \cos \Omega_D t + \cos \left[(\Omega_D + \omega_o)t - \phi_D \right] \right\} \left\{ \cos (\Omega_U t - \xi) \right. \\ \left. + \cos \left[(\Omega_U + \omega_o)t - \phi_U - \xi \right] \right\} \quad (1-12) \end{aligned}$$

As before, the post-detection filter will only pass the low frequency components. Hence, if eq. (1-12) is expanded and all frequency components containing Ω_D and Ω_U are eliminated, we are left with:

$$\begin{aligned}
V_u = & K A_D^2 \cos (\omega_o t - \phi_D) + K A_U^2 \cos (\omega_o t - \phi_U) \\
& + K A_D A_U \left\{ \cos (\Delta t - \xi) + \cos \left[(\Delta + \omega_o) t - \phi_U - \xi \right] \right. \\
& \left. + \cos \left[(\pm \Delta \mp \omega_o) t + \phi_D - \xi \right] + \cos \left[\Delta t + \phi_D - \phi_U - \xi \right] \right\} \quad (1-13)
\end{aligned}$$

where $\Delta \equiv (\pm \Omega_D \mp \Omega_U)$

The first two terms in expression (1-13) for V_u contain only the frequency ω_o , so that these terms always appear at the output of the post-detection filter. The remaining four terms, however, contain signal components with frequencies Δ , $\Delta + \omega_o$ and $\pm \Delta \mp \omega_o$. Whether or not these components appear at the filter output, depends on the value of the difference frequency Δ relative to the filter bandwidth $\beta = 2\pi b$.

In Fig. 1-4, these three spectral components are shown for six different values of Δ . The six different spectra of Fig. 1-4 will now be grouped into four categories and the error in phase difference will be separately computed for each of the four cases.

Case A

In this particular case, none of the three spectral components fall within the filter pass-band. Using Fig. 1-4, this case corresponds to spectrum Nos. 2, 4, and 6.

Hence, in case A, the last four terms of V_u do not appear, so that V_u is defined only by the first and second terms of (1-12); i.e.,

$$V_{uA} = K A_D^2 \left\{ \cos (\omega_o t - \phi_D) + X^2 (\omega_o t - \phi_U) \right\} \quad (1-14)$$

where $X = \frac{A_U}{A_D}$

Figure 1-5a represents a phasor diagram in which V_u is represented by two phasors rotating at frequency ω_o . OA and OC represent the desired and undesired components of V_u , while OB represents the resultant signal which appears at the filter output. The angle ϵ_A represents the phase error caused by the undesired signal OA. From Fig. 1-5a it is immediately apparent that

$$\tan(\phi_D + \epsilon_A) = \frac{\sin \phi_D + X^2 \sin \phi_U}{\cos \phi_D + X^2 \cos \phi_U} \quad (1-15)$$

Hence,

$$\tan(\phi_D + \epsilon_A) = \frac{\tan \phi_D + \tan \epsilon_A}{1 - \tan \phi_D \tan \epsilon_A} = \frac{\sin \phi_D + X^2 \sin \phi_U}{\cos \phi_D + X^2 \cos \phi_U} \quad (1-16)$$

Solving for $\tan \epsilon_A$ gives

$$\tan \epsilon_A = \frac{X^2 \sin \phi'}{1 + X^2 \cos \phi'} \quad (1-17)$$

where $\phi' = \phi_U - \phi_D$

Equation (1-16) therefore defines the error ϵ_A for case A.

Figures 1-6 and 1-7 show curves of the error ϵ_A plotted against X (in db) for different values of ϕ' .

If X is small (case where $A_D \gg A_u$), then the resulting error ϵ_A will be small. Consequently, (1-17) reduces to

$$\epsilon_A = \tan^{-1} \frac{X^2 \sin \phi'}{1 + X^2 \cos \phi'} \approx X^2 \sin \phi' \quad (1-17a)$$

It was pointed out above that an angular error of 1° is to be viewed as the tolerable maximum in the ambiguity channels. This implies a large signal-to-noise ratio ($\frac{1}{X}$) in (1-17) and one for which the approximation used is valid. Furthermore, ϕ' will take on many different values during a pass so that it would be reasonable to assure that in the worst case ϵ_A should not exceed the tolerable maximum. Since

$$\epsilon_{A \max} \cong X^2$$

we conclude that the signal-to-interference ratio should be equal to or greater than 17.6 db to hold $\epsilon_{A \max}$ to less than 1° .

Case B

This case corresponds to spectrum No. 1 of Fig. 1-4, in which both the $(\omega_o - \Delta)$ and $(\omega_o + \Delta)$ components are present at the filter output. The total output is now given by

$$V_{u_B} = K A_D^2 \left\{ \cos (\omega_o t - \phi_D) + X^2 \cos (\omega_o t - \phi_U) \right. \\ \left. + X \cos [(\omega_o + \Delta)t - \phi_U - \xi] + X \cos [(\omega_o - \Delta)t + \phi_D - \xi] \right\} \quad (1-18)$$

Case B is vectorially represented in Fig. 1-5b. The lower left half of the diagram is the same as that shown in Fig. 1-5a and corresponds to the first two terms of (1-18). The upper right half of the diagram represents

the two additional components; phasor BF rotates clockwise with a frequency Δ , while phasor BD rotates anticlockwise with the same frequency. Since the magnitudes of BF and BD are the same, the resultant BE does not rotate but points continuously in the same direction; that is at an angle $\frac{\psi_1 + \psi_2}{2} = \xi + \frac{\phi'}{2}$ with respect to the horizontal phase reference. Phasor OE represents the combined output signal and $\epsilon_B(t)$ represents the resulting phase error for case B. As phasors BD and BF rotate about B, the point E moves along the line BEG and passes through B (at the two extremities, the point E is at a distance of $2X$ on either side of B). The error $\epsilon_B(t)$ therefore changes periodically with time. An expression for $\epsilon_B(t)$ will now be obtained. From Fig. 1-5b, it can be seen that

$$\begin{aligned} \tan[\phi_D + \epsilon_B(t)] &= \frac{\tan \phi_D + \tan \epsilon_B}{1 - \tan \phi_D \tan \epsilon_B} \\ &= \frac{\sin \phi_D + X^2 \sin \phi_U + X(\sin \psi_1 + \sin \psi_2)}{\cos \phi_D + X^2 \cos \phi_U + X(\cos \psi_1 + \cos \psi_2)} \end{aligned} \quad (1-19)$$

where

$$\psi_1(t) = (\xi - \phi_D + \Delta t)$$

$$\psi_2(t) = (\xi + \phi_U - \Delta t)$$

Evaluating $\tan \epsilon_B(t)$ gives

$$\tan \epsilon_B(t) = \frac{X^2 \sin \phi' + 2X \sin (\xi + \frac{\phi'}{2} - \phi_D) \cos (\Delta t - \frac{\phi}{2})}{1 + X^2 \cos \phi' + 2X \cos (\xi + \frac{\phi'}{2} - \phi_D) \cos (\Delta t - \frac{\phi}{2})} \quad (1-20)$$

where $\phi' = \phi_U - \phi_D$ and $\Phi = \phi_U + \phi_D$

The maximum error is obtained when E is at one of its extremities, i.e., either when $(\Delta t - \frac{\Phi}{2}) = 0$, or π . Hence, the maximum error is given by

$$\hat{\epsilon}_B(t) = \left| \tan^{-1} \frac{X^2 \sin \phi' \pm 2X \sin (\xi + \frac{\phi'}{2} - \phi_D)}{1 + X^2 \cos \phi' \pm 2X \cos (\xi + \frac{\phi'}{2} - \phi_D)} \right| \quad (1-20a)$$

where the maximum is the larger of the two values taken on by $\epsilon_B(t)$.

It can be anticipated that $X \ll 1$ and that

$$\hat{\epsilon}_B(t) \doteq 2X \left| \sin (\xi + \frac{\phi'}{2} - \phi_D) \right| \quad (1-21)$$

Furthermore, as the satellite progresses through its orbit, the angle in (1-21) will very likely pass through $-\pi/2$ or $\pi/2$. Thus

$$\left[\hat{\epsilon}_B(t) \right]_{\max} \doteq 2X$$

If the latter is to be less than 1° then the signal-to-interference ratio, $\frac{1}{X}$, has to be 41.2 db.

This estimate of the signal-to-interference ratio takes the pessimistic view that everything will be at its worst. The measurements are repeated every second and successive measurements are averaged in a computer so that it is unlikely that each sample entering into the average will be taken exactly when E in the Fig. 1-5b is at its extremity. It would be more appropriate to treat the angle $(\Delta t - \frac{\Phi}{2})$ in (1-20) as a random variable uniformly distributed in 2π and to derive

a suitable statistical conclusion. Again, for $X \ll 1$, we write in place of (1-20)

$$\epsilon_B(t) \doteq 2X \sin \left(\xi + \frac{\phi'}{2} - \phi_D \right) \cos \left(\Delta t - \frac{\Phi}{2} \right) \quad (1-22)$$

Written in this manner, the time average of $\epsilon_B(t)$ over a cycle is zero. This is only approximately correct; it can be shown that the time average of (1-20) is not zero (it differs, also, from ϵ_A defined in (1-17a) and shown in Fig. 1-5b).

Now, the final computed output angle is obtained by using 145 "fine channel" measurements and 29 "ambiguity channel" measurements taken over a 29-second period. We have argued that 1° error in the ambiguity channel establishes the tolerable input interference level. Therefore, we compute the angular error for the ambiguity channel taking into account the averaging over 29 successive measurements each given by (1-22).

The error criterion is here treated as follows. Each measurement of $\epsilon_B(t)$ will depend on $(\Delta t - \frac{\Phi}{2})$ which we are treating as a uniform random variable. The variance of $\epsilon_b(t)$ is therefore from (1-22)

$$\sigma_{\epsilon_b}^2 = X^2 \sin^2 \left(\xi + \frac{\phi'}{2} - \phi_D \right) \quad (1-23)$$

Now, we view the $n = 29$ successive measurements as independent samples which are averaged to give $\overline{\epsilon_b}$. The variance of this latter quantity is

$$\frac{\sigma^2}{\epsilon_b} = \frac{X^2}{n} \sin^2 \left(\xi + \frac{\phi'}{2} - \phi_D \right) \quad (1-24)$$

Assuming we are at a part of the orbit where $\xi + \frac{\phi'}{2} - \phi_D = k \frac{\pi}{2}$, k odd, the variance will be maximum. We write it then

$$\left[\frac{\sigma}{\epsilon_b} \right]_{\max} = \frac{X}{\sqrt{n}} \quad (1-24a)$$

Finally, we let the permissible angular error of 1° , equal

$2 \left[\frac{\sigma}{\epsilon_B} \right]_{\max}$. Since $\overline{\epsilon_B}$ will be approximately normally distributed this means that there will be about 5% probability that $|\overline{\epsilon_B}| > 1^\circ$. Thus,

$$X \doteq \frac{\sqrt{n}}{2} \cdot 2 \left[\frac{\sigma}{\epsilon_b} \right]_{\max} = \frac{29}{2} (1^\circ)$$

and

$$X \doteq -26.7 \text{ db}$$

For this case, then, it is advisable to have a signal-to-noise ratio of about 9 db greater than in the previous case. It should be recalled that the case treated is one in which the desired and undesired signal frequencies are separated by an amount less than the post-detection filter bandwidth of about 10 Hz.

Case C

This case corresponds to spectrum No. 3 of Fig. 1-4 in which the signal components of frequency Δ are present at the filter output. The total output for this case is therefore given by

$$\begin{aligned} V_{u_c} = K A_D^2 \bigg\{ & \cos(\omega_o t - \phi_D) + X^2 \cos(\omega_o t - \phi_U) \\ & + X \cos(\Delta t - \xi) + X \cos(\Delta t - \phi' - \xi) \bigg\} \end{aligned} \quad (1-25)$$

The phasor diagram for Case C is shown in Fig. 1-5c. In this case, BD and BF are both rotating in the same direction at a frequency $(\Delta - \omega_o)$. The resultant BE therefore also rotates about B at the same frequency. Consequently, the error $\epsilon_c(t)$ varies periodically with ϵ_A as its mean value. An expression for $\epsilon_c(t)$ can be obtained in the same way as in the last case. The result is

$$\tan \epsilon_c(t) = \frac{X^2 \sin \phi' - 2X \cos \frac{\phi'}{2} \sin (\Delta - \omega_o)t - \xi - \frac{\phi'}{2} - \phi_D}{1 + X^2 \cos \phi' + 2X \cos \frac{\phi'}{2} \cos (\Delta - \omega_o)t - \xi - \frac{\phi'}{2} - \phi_D} \quad (1-26)$$

The maximum error is obtained when BE is normal to OB for the situation shown in Fig. 1-5c

$$\psi_1(t) + \frac{\phi'}{2} = \epsilon_A + \frac{\pi}{2} \quad (1-27)$$

Substituting for $\psi_1(t)$ and solving for "t" gives

$$t = \frac{\xi + \frac{\phi'}{2} - \epsilon_A - \frac{\pi}{2}}{\Delta - \omega_o} \quad (1-28)$$

Substituting (1-28) into (1-26) gives the maximum error for Case C:

$$\tan \epsilon_c(t) = \frac{X^2 \sin \phi' + 2X \cos \frac{\phi'}{2} \sin (\phi_D + \epsilon_A + \frac{\pi}{2})}{1 + X^2 \cos \phi' + 2X \cos \frac{\phi'}{2} \cos (\phi_D + \epsilon_A + \frac{\pi}{2})} \quad (1-29)$$

Conclusions similar to those obtained in Case B can be drawn for Case C. For $X \ll 1$ (1-29) can be approximated by

$$\epsilon_c(t) \doteq 2X \cos \frac{\phi'}{2} \sin (\phi_D + \epsilon_A + \frac{\pi}{2})$$

The maximum value of the magnitude of $\epsilon_c(t)$ is

$$\left[\hat{\epsilon}_c(t) \right]_{\max} = 2X$$

If $\left[\epsilon_c(t) \right]_{\max}$ is to be limited to 1° the value of X is, as in Case B, 41.2 db.

Returning to (1-26), for $X \ll 1$

$$\epsilon_c(t) = -2X \cos \frac{\phi'}{2} \sin \left\{ (\Delta - \omega_o)t - \xi - \frac{\phi'}{2} - \phi_D \right\}$$

As in Case B, treating the angle in the braces as a random variable uniformly distributed in 2π , the maximum value of the variance of the average of n samples of $\epsilon_c(t)$ is

$$\left[\sigma \frac{\epsilon_c}{\epsilon_c} \right]_{\max} = \frac{X}{\sqrt{n}}$$

The signal-to-noise ratio required to keep $2 \left[\sigma \frac{\epsilon_c}{\epsilon_c} \right] < 1^\circ$ is 26.7 db.

Case D

This final case corresponds to Spectrum No. 5 of Fig. 1-4, in which the component of frequency $(\Delta - \omega_o)$ is present at the filter output. The total output is now given by

$$\begin{aligned} V_{u_D} = K A_D^2 \{ & \cos(\omega_o t - \phi_D) + X^2 \cos(\omega_o t - \phi_U) \\ & + X \cos[(\Delta - \omega_o)t + \phi_D - \xi] \} \end{aligned} \quad (1-30)$$

The phasor diagram for Case D is shown in Fig. 1-5d. Phasor BE rotates about B at a frequency $(\Delta - 2\omega_o)$ and the resulting error is now $\epsilon_D(t)$ which again varies periodically about ϵ_A as its mean value.

An expression for $\epsilon_D(t)$ can again be obtained as before:

$$\tan \epsilon_D(t) = \frac{X^2 \sin \phi' - X \sin \phi_D - X \sin [(\Delta - 2\omega_0)t + 2\phi_D - \xi]}{1 + X^2 \cos \phi' + X \cos \phi_D + X \cos [(\Delta - 2\omega_0)t + 2\phi_D - \xi]} \quad (1-31)$$

The maximum error is again obtained when BE is normal to

OB. For the situation shown in Fig. 1-5d this implies

$$\psi(t) = \epsilon_A + \frac{\pi}{2}$$

or when

$$t = \frac{\xi - \phi_D - \epsilon_A - \frac{\pi}{2}}{\Delta - 2\omega_0} \quad (1-32)$$

Substituting (1-32) in (1-31) gives the maximum error for

Case D:

$$\tan \epsilon_D(t) = \frac{X^2 \sin \phi' - X \sin \phi_D + X \sin (\epsilon_A + \frac{\pi}{2} - \phi_D)}{1 + X^2 \cos \phi' + X \cos \phi_D + X \cos (\epsilon_A + \frac{\pi}{2} - \phi_D)} \quad (1-33)$$

Once again for $X \ll 1$

$$\epsilon_D(t) \doteq X \left[\sin (\epsilon_A + \frac{\pi}{2} - \phi_D) - \sin \phi_D \right]$$

Recognizing that $\epsilon_A \ll \frac{\pi}{2}$

$$\epsilon_D(t) \doteq X \left[\cos \phi_D - \sin \phi_D \right]$$

The maximum value here is

$$\left[\hat{\epsilon}_d(t) \right]_{\max} = \sqrt{2} X$$

To hold $\left[\hat{\epsilon}_d(t) \right]_{\max}$ to 1° requires that X be about 38 db. Now using $X \ll 1$ with (1-31)

$$\epsilon_D(t) \doteq -X \left\{ \sin \phi_D - \sin \left[(\Delta - 2\omega_o)t + 2\phi_D - \xi \right] \right\}$$

In this case averaging $n = 29$ successive samples will reduce the effect of the second sine term in the braces but not the first. We take the view then that the error in this case is

$$\epsilon_D(t) \doteq X \sin \phi_D$$

At the point in the orbit where $\phi_D = (2k + 1)\pi/2$, k an integer,

$$\epsilon_D(t) \doteq X$$

and the required signal-to-noise ratio to hold $\epsilon_D(t)$ to within 1° is about 35 db.

1.2.2 Broadband Interference

A few cases have been recorded in which broadband interference from unwanted information bearing signal sources or high voltage power lines has temporarily disrupted the operation of the Minitrack system. It is therefore worth analyzing the effect of broadband noise on the system.

Let the broadband noise be given by the real part of:

$$A_U(t) e^{j \left\{ \omega_D t + \theta(t) \right\}} \quad (1-34)$$

Then, as before, the signal arriving from antenna X is given by the real part of

$$V_{ix} = A_D e^{j \omega_D t} + A_U(t) e^{j \left\{ \omega_D t + \theta(t) \right\}} \quad (1-35)$$

and the signal arriving from antenna Y is given by the real part of:

$$V_{iy} = A_D e^{j \omega_D (t - \tau_D)} + A_U(t - \tau_U) e^{j \omega_D (t - \tau_U)} e^{j \theta(t - \tau_U)} \quad (1-35a)$$

where τ_D and τ_U represent the time delays necessary for the desired and undesired waves to travel from antenna X to antenna Y (time required to cover distance "a" in Fig. 1-2).

Similarly, the two outputs from the mixer are given by the real parts of

$$V_{ox}(t) = \alpha A_D e^{j \Omega_D t} + \alpha A_U(t) e^{j \left\{ \Omega_D t + \theta(t) \right\}} \quad (1-36)$$

$$\begin{aligned} V_{oy}(t) = & \alpha A_D e^{j (\Omega_D + \omega_o)(t - \tau_D)} \\ & + \alpha A_U(t - \tau_U) e^{j (\Omega_D + \omega_o)(t - \tau_U)} e^{j \theta(t - \tau_U)} \end{aligned} \quad (1-36a)$$

In practice, the time delay τ_U does not exceed 0.5 μ sec, so that the change of $A(t)$ and $\theta(t)$ during the time τ_U may be neglected. Hence,

$$A_U(t - \tau_U) \approx A_U(t)$$

and

$$\theta(t - \tau_U) \approx \theta(t)$$

The two output signals are combined and amplified in the IF amplifier. If the time response of the IF amplifier circuit is given by

$$Gh(t)e^{j\Omega_D t}$$

then the amplifier output is given by the real part of

$$E_i(t) = \alpha G \int_{-\infty}^{+\infty} V_O(t') h(t - t') e^{j\Omega_D(t - t')} dt' \quad (1-37)$$

where

$$V_O(t') = V_{ox}(t') + V_{oy}(t')$$

Hence,

$$E_i(t) = \alpha G e^{j\Omega_D t} \left\{ A_D + \int_{-\infty}^{+\infty} A_U(t') e^{j\theta(t')} h(t - t') dt' + A_D e^{j\omega_o(t - \tau_D)} + e^{j\omega_o(t - \tau_U)} \int_{-\infty}^{+\infty} A_U(t') e^{j\theta(t')} e^{-j\omega_o(t - t')} h(t - t') dt' \right\} \quad (1-38)$$

The two integrals in (1-38) differ only by the term $e^{-j\omega_o(t - t')}$. Since ω_o is very small compared with the IF bandwidth B, this term is approximately unity, so that the two integrals are identical.

Let these integrals be represented by $I(t)$. Then the amplifier output is given by the real part of

$$E_i(t) \approx \alpha G e^{j\Omega_D t} \left[A_D \left\{ 1 + e^{j(\omega_o t - \phi_D)} \right\} + I(t) \left\{ 1 + e^{j(\omega_o t - \phi_U)} \right\} \right] \quad (1-39)$$

where

$$\phi_D = (\omega_o + \Omega_D)\tau_D \quad \text{and} \quad \phi_U = (\omega_o + \Omega_D)\tau_u$$

The output from the detector is given by

$$E_o(t) = k \left| E_i(t) \right|^2 = k E_i E_i^* \quad (1-40)$$

Substitute (1-39) into (1-40) and simplify. Passing the detector output through the post-detection filter will eliminate all components in Ω_D . Hence, there remains

$$\begin{aligned} E_o(t) = K A_D^2 \left\{ 1 + \cos(\omega_o t - \phi_D) + K \left| I(t) \right|^2 1 + \cos(\omega_o t - \phi_U) \right. \\ \left. + K A_D \operatorname{Re} [I(t)] \cos(\omega_o t - \phi_D) + \cos(\omega_o t - \phi_U) + 1 + \cos \phi' \right\} \\ \left. + K A_D \operatorname{Im} [I(t)] \sin(\omega_o t - \phi_D) - \sin(\omega_o t - \phi_U) + \sin \phi' \right\} \quad (1-41) \end{aligned}$$

where $K = k \alpha^2 G^2$ and $\phi' = \phi_U - \phi_D$

The first term in (1-41) contains the desired signal component plus a dc component which will be rejected in the post-detection filter. The remaining terms in (1-41) are interference generated. Because the post-detection filter has a very narrow

bandwidth much of the interference output is negligible with the exception of a portion of the term $|I^2(t)| \cos(\omega_o t - \phi_u)$. If $I(t)$ is white Gaussian noise in a limited band with total power P_I , then $|I^2(t)|$ has a power spectrum which is an impulse function at zero frequency and a triangular function extending from zero frequency to twice the band of $I(t)$. The dispersed power in the triangular function contributes little in the narrow post-detection filter. The impulse function is a concentration of power (it contains $\frac{1}{3}$ the power in $I^2(t)$) and makes the major contribution. We can therefore say that at the post-detection filter output the major noise contribution is given by $\overline{|I^2(t)|} \cos(\omega_o t - \phi_u)$ where $\overline{|I^2(t)|}$ is the average value of the square of the noise output of the IF amplifier and is given by $2P_I$.

We can also argue that the last two terms in (1-41), which are continuous spectrum components, make contributions at the post-detection filter output of the same order as does the triangular component of $|I^2(t)|$ and are also negligible. Furthermore, the contribution to the angular error resulting from all the continuous spectrum components in (1-41) is time-varying and will be reduced in the computer processing. It will be recalled that the computer averages 29 successive measurements in the ambiguity channel thus reducing the rms value of the time varying components by an additional factor of $\sqrt{29}$. Hence, the final filter output is approximately

$$E_o(t) = K A_D^2 \left\{ \cos(\omega_o t - \phi_D) + X^2 \cos(\omega_o t - \phi_U) \right\} \quad (1-42)$$

where

$$X^2 = \frac{2P_I}{A_D^2}$$

The expression for $E_o(t)$ now agrees with (1-14) for the CW interference case. Hence, the expression obtained for the error created by the noise will be the same as that obtained in Case A of the CW interference analysis, i.e.,

$$\tan \epsilon = \frac{X^2 \sin \phi'}{1 + X^2 \cos \phi'} \quad (1-43)$$

Hence, the curves of Figs. 1-6 and 1-7 are also applicable to the case of broadband noise. We conclude as we did in the discussion following (1-17a) that to have an error of less than 1° in the ambiguity channels necessitates a signal-to-noise ratio at the IF amplifier output of 17.6 db or more.

1.3 Conclusions

The foregoing study of the effects of CW and wideband interference to the Minitrack system has resulted in a number of expressions giving the angular measurement error as a function of signal-to-interference ratio and other pertinent quantities. Several significantly different cases were distinguished for CW interference. The most common case (Case A) is one in which the interference will appear in the IF amplifier band but is neither too close to the desired signal frequency (that is, it is separated from the desired signal by more than the post-detection filter bandwidth), nor do its cross products with the desired signal appear in the post-detection filter. The

other cases arise when one of these stipulations do not hold. Three such distinguishable situations (Cases B, C, D) can arise, but they are much less likely to occur than Case A.

The view is taken in this work that the Minitrack system has a threshold determined by the ambiguity resolving portion of the system. A safe condition was taken to be that condition wherein the electrical angles measured in the ambiguity channels is not in error by more than 1° . On this basis it was concluded that the required signal-to-noise ratio for CW interference in Case A and for broadband interference is 17.6 db. For the other three CW cases, the signal-to-interference ratio required may be as high as 35 db.

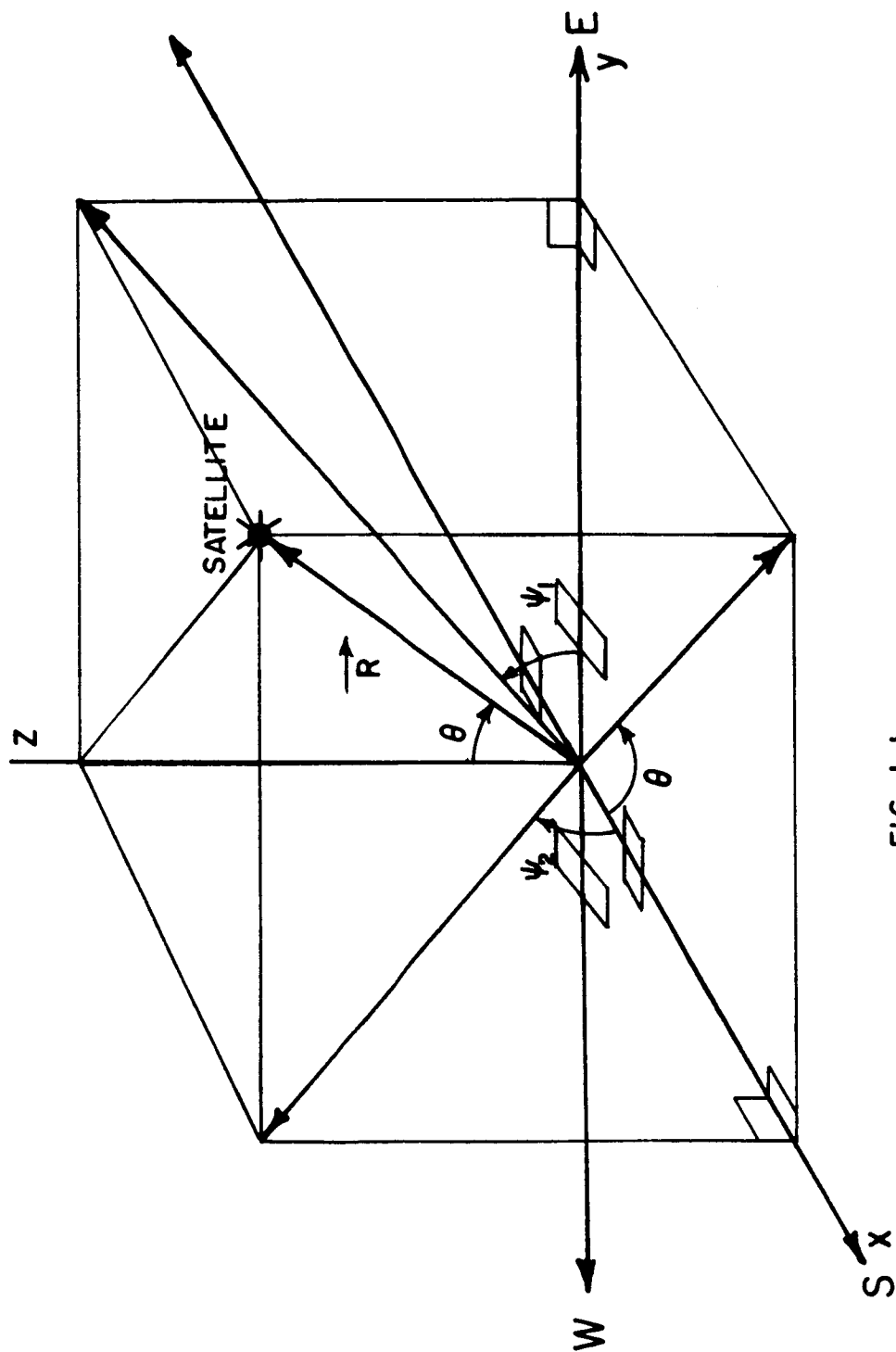


FIG. 1-1

ψ_1 AND ψ_2 IDENTIFY ANGLES MEASURED IN MINITRACK SYSTEM.

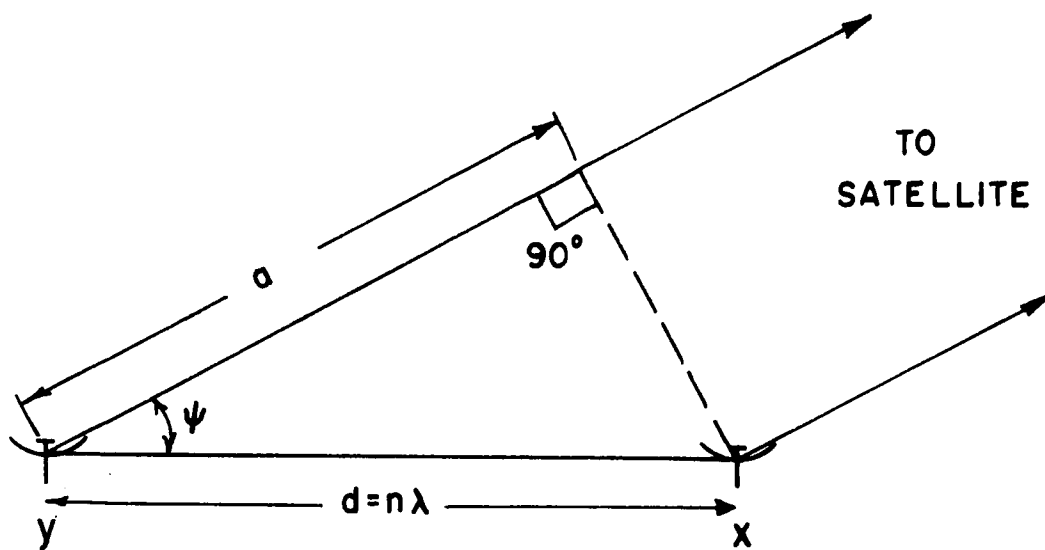


FIG. 1-2

RELATION BETWEEN DELAY AND INCLINATION ANGLE

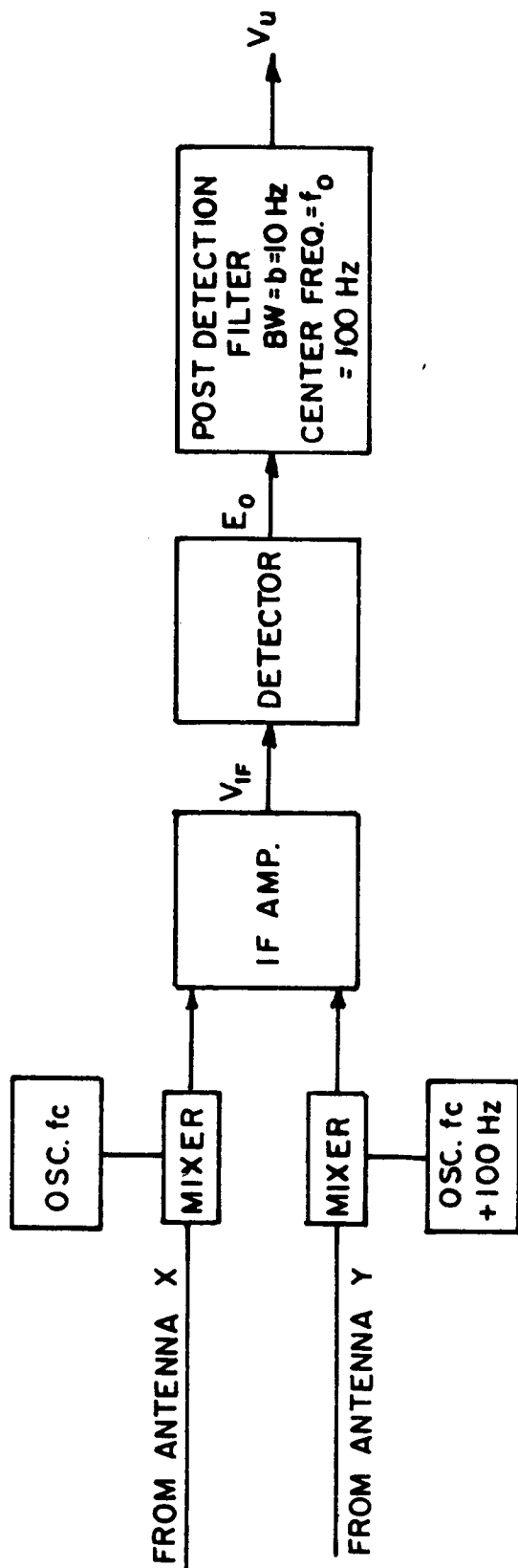


FIG. 1-3

BLOCK DIAGRAM OF 136 MHz MINITRACK RECEIVER

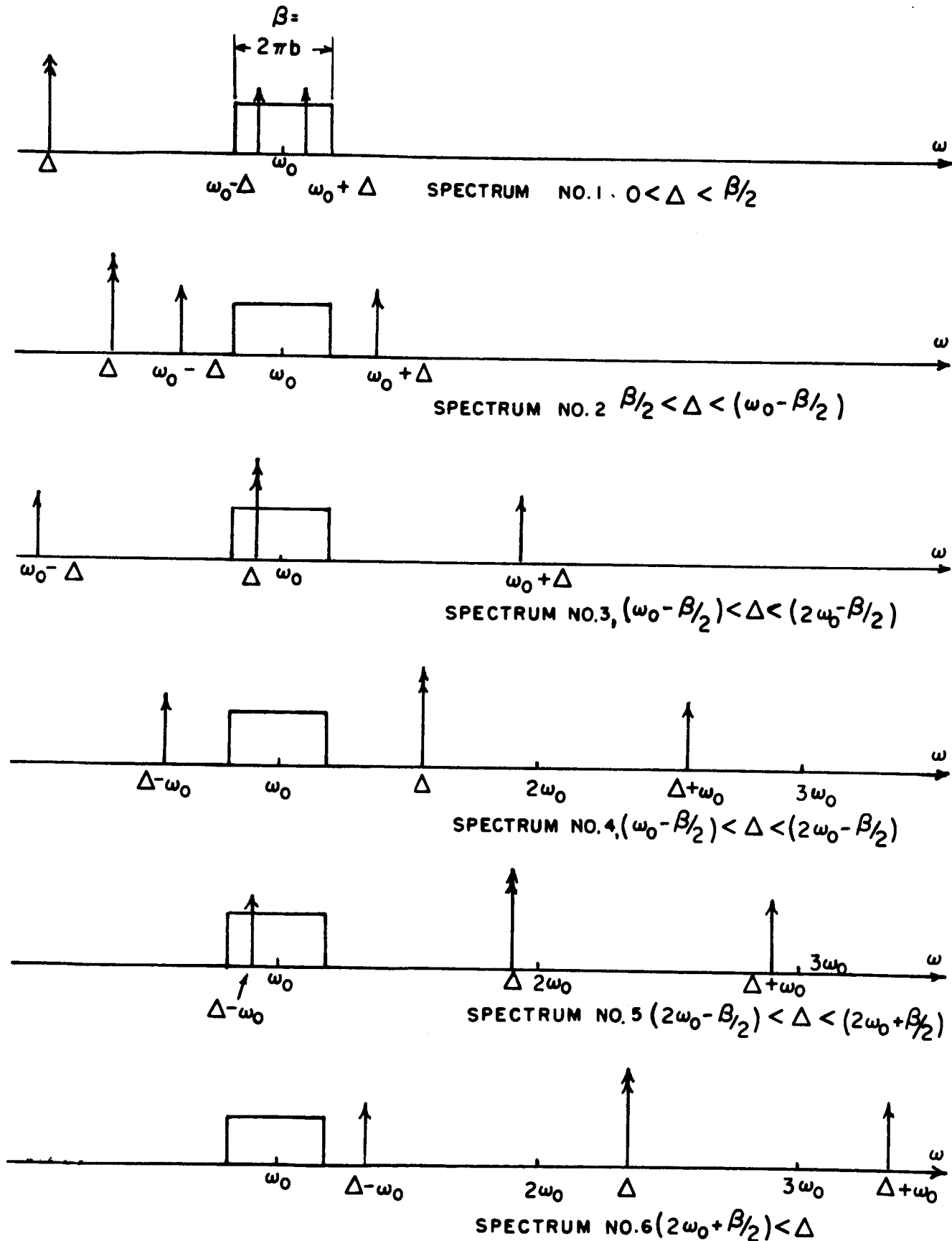
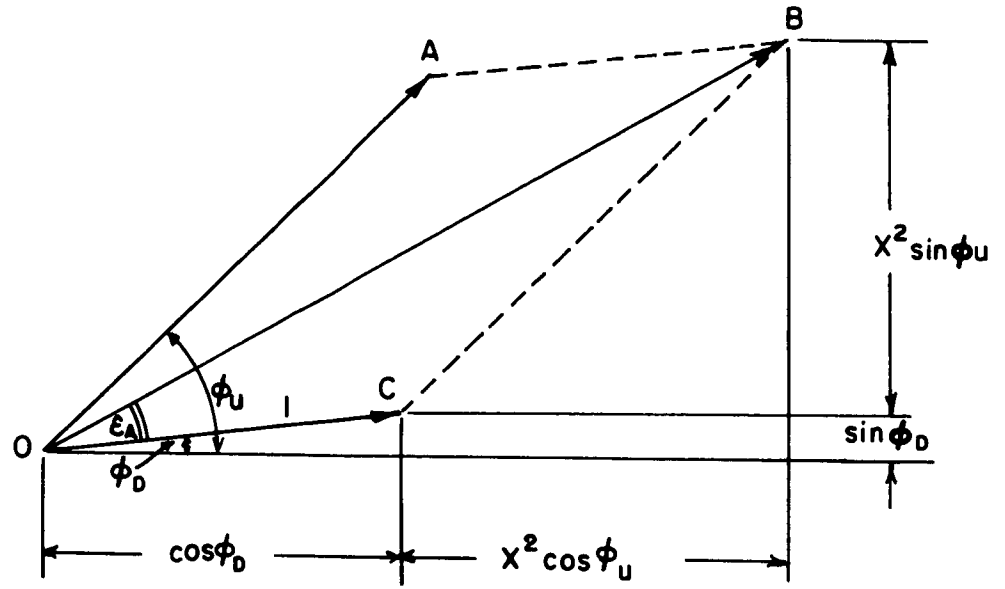
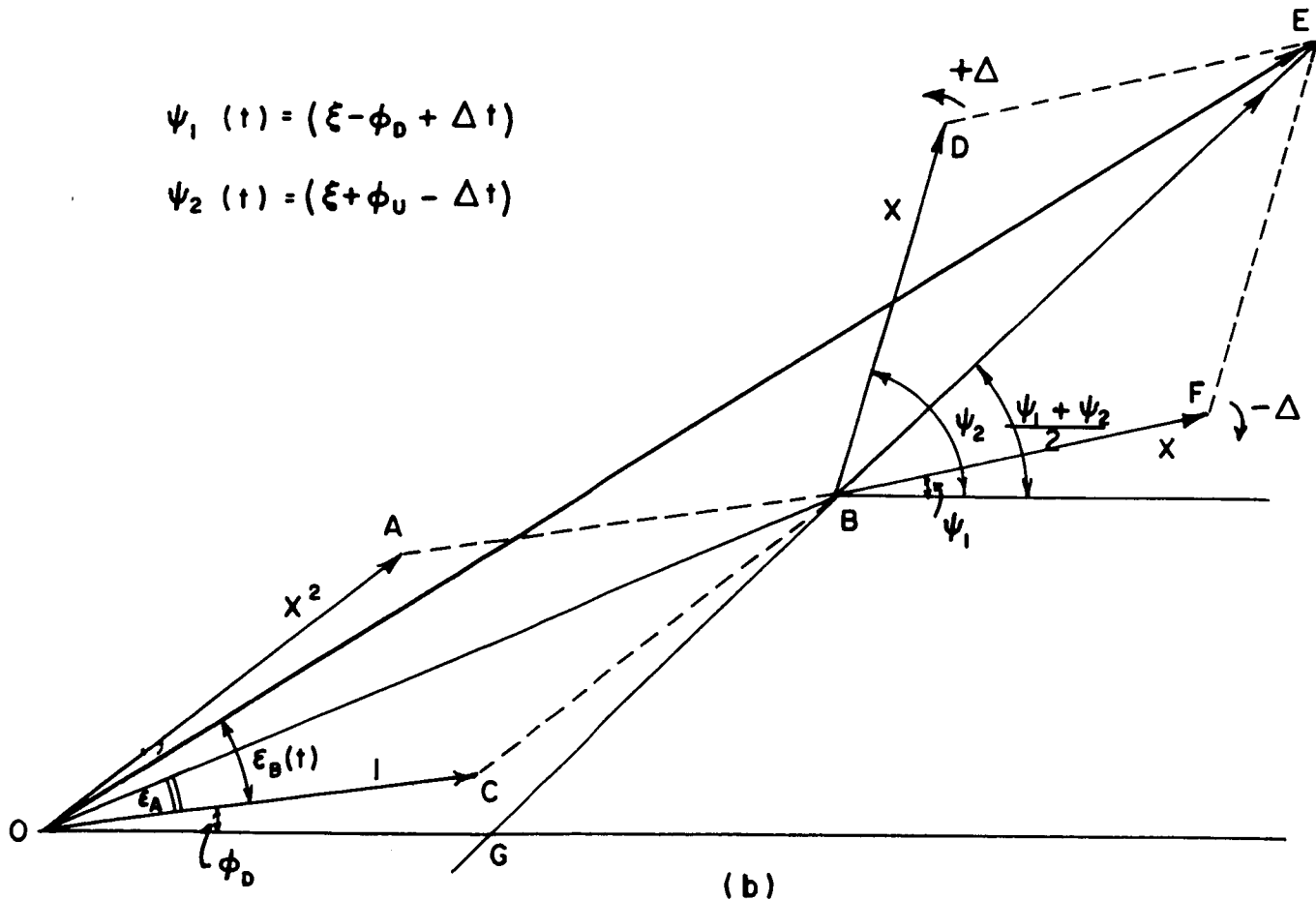


FIG. 1-4 VARIOUS INPUTS TO THE POST-DETECTION FILTER.

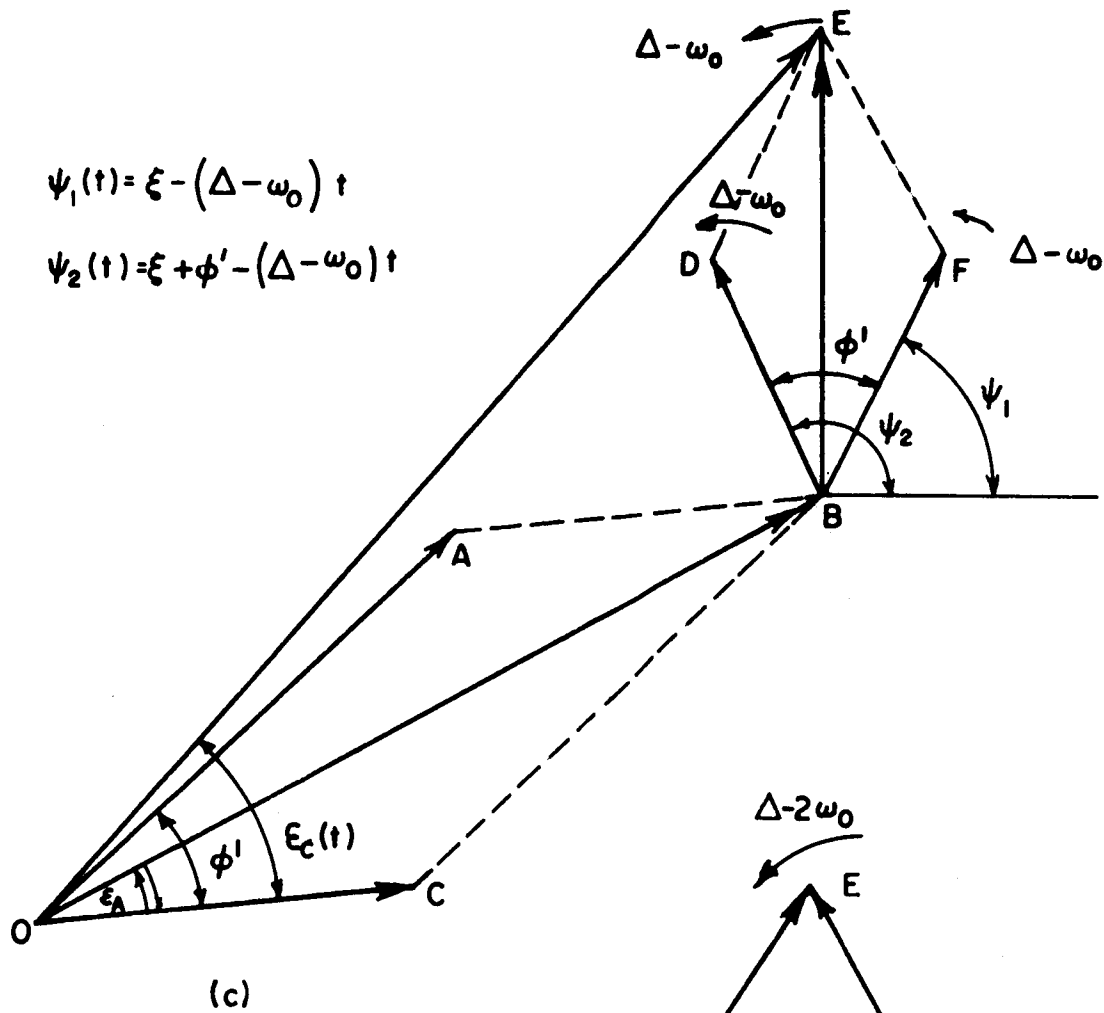


(a)



(b)

FIG. I-5 a&b ANGULAR ERRORS OBTAINED THROUGH PHASOR DIAGRAMS.



$$\psi(t) = \xi - \phi_D - (\Delta - 2\omega_0) t$$

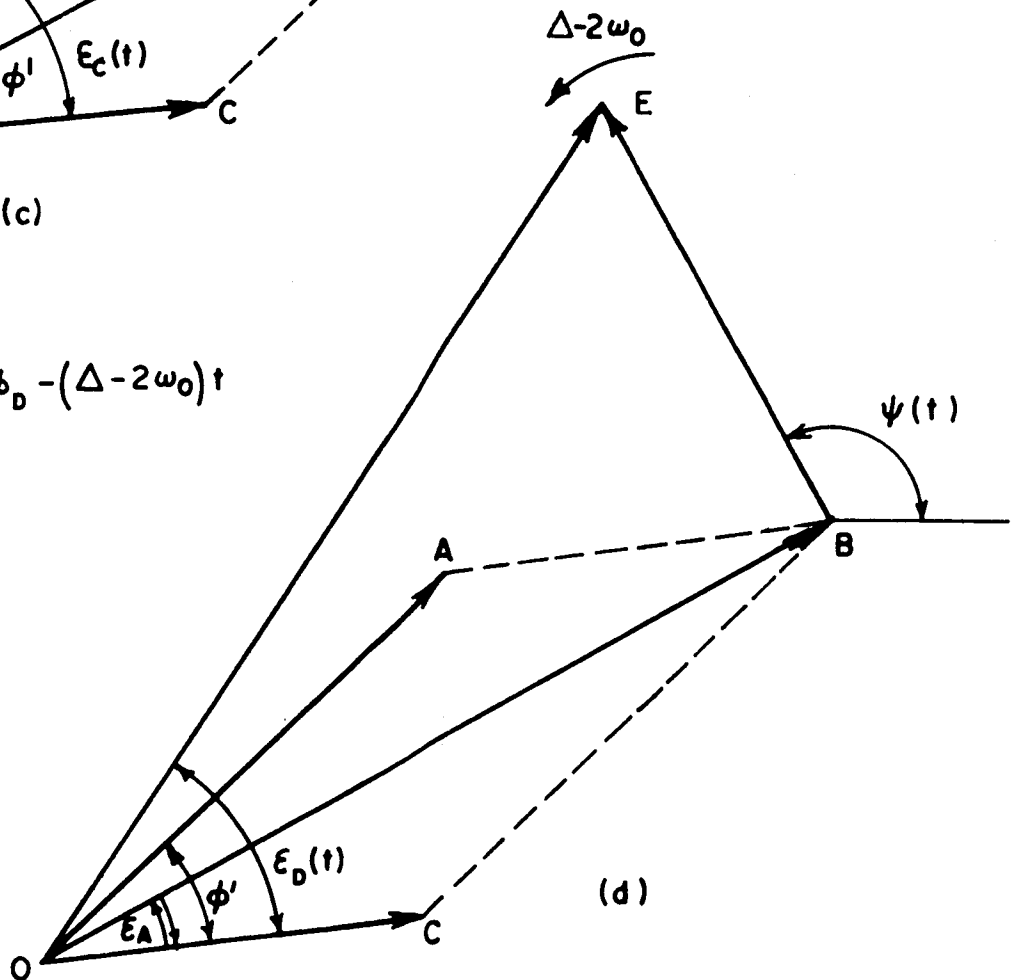


FIG. 1-5 (c & d)

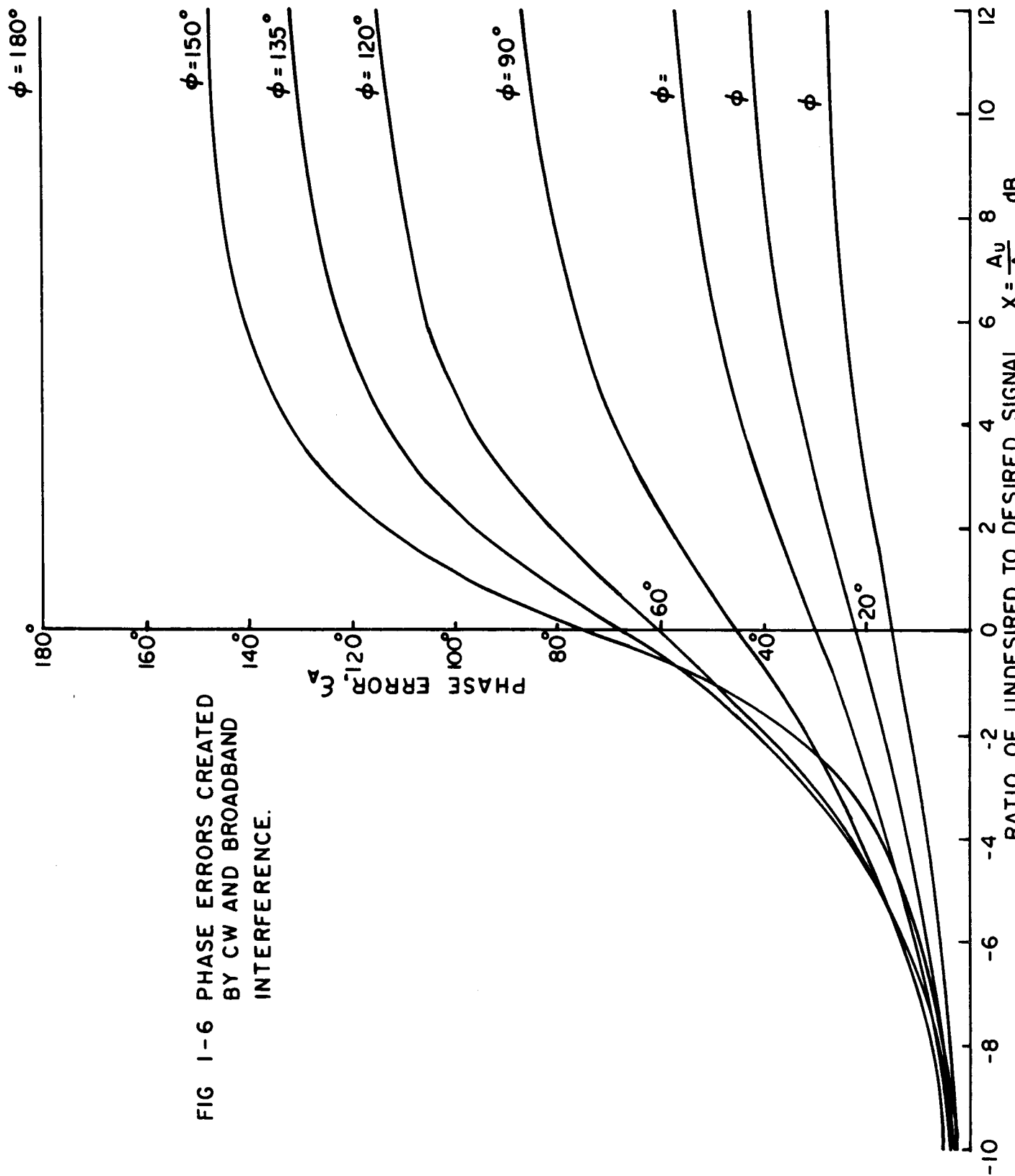


FIG 1-6 PHASE ERRORS CREATED BY CW AND BROADBAND INTERFERENCE.

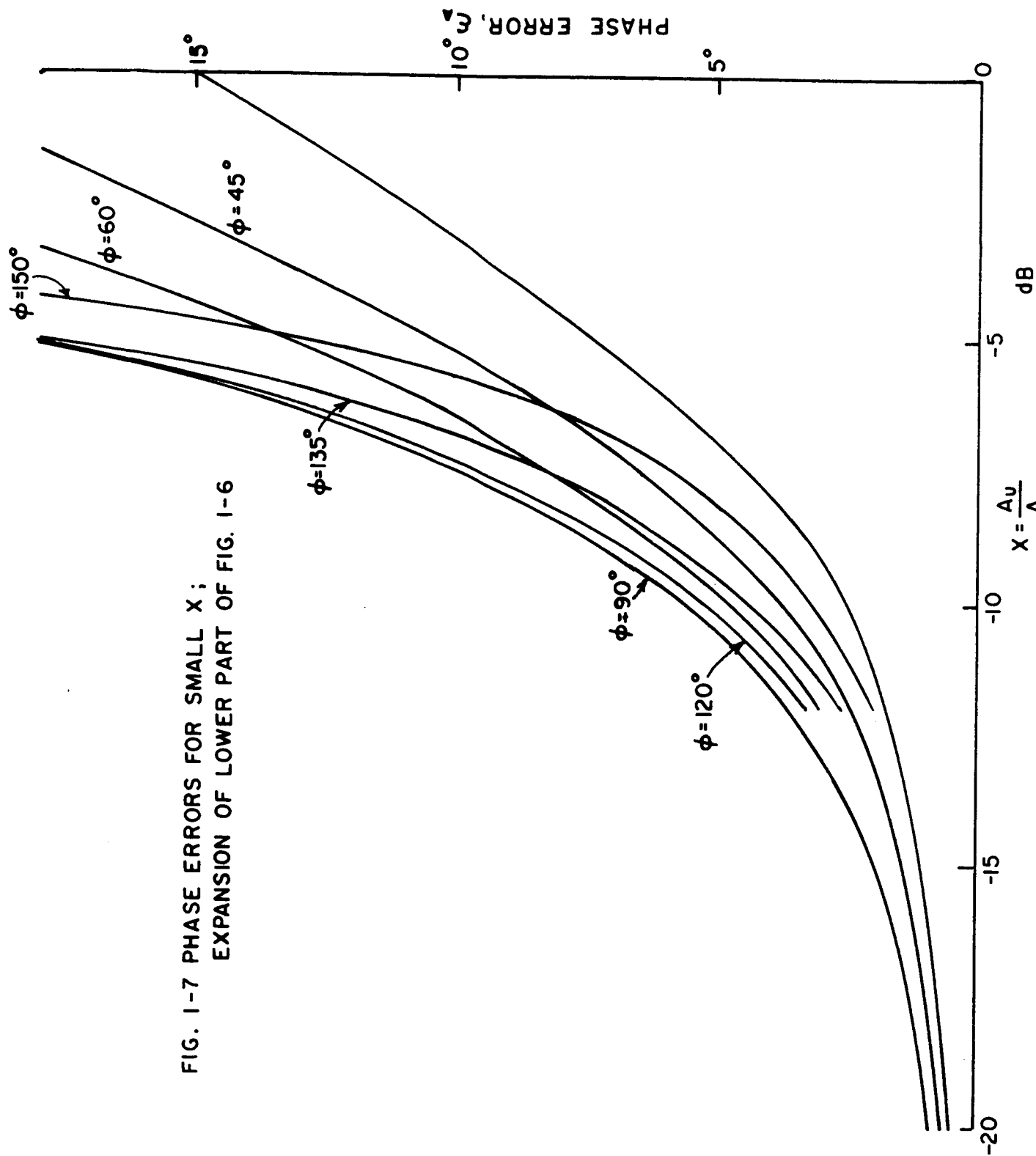


FIG. 1-7 PHASE ERRORS FOR SMALL X ;
EXPANSION OF LOWER PART OF FIG. 1-6

2.0 A STUDY OF THE PHASE LOCKED LOOP WITH INTERFERENCE

2.1 Introduction

The phase locked loop is an important element in modern communication systems, and has been given much study in the past ten years. Much of this work has been devoted to the acquisition and tracking properties in the presence of noise. Very little work has been devoted to the analysis of the phase locked loop in the presence of interference from other communication signal sources.

The behavior of the phase locked loop with interference present is an important practical matter. In many actual situations, interference has caused the loop to lose track, track the interfering signal, or fluctuate in such a manner as to obscure or completely destroy the information being transmitted.

A study of the operation of the phase locked loop in the presence of interference should attempt to answer the questions; under what conditions will the interference disrupt the tracking procedure to such a degree as to cause a loss of information, and what can be done to reduce the effect of the interference.

The answer to the first question is obscured by the fact that different amounts of disturbance can be tolerated depending on the specific use of the phase locked loop. It is the aim of this paper to develop techniques of analysis for use with the phase locked loop in the presence of interference. Expressions for the output phase fluctuations caused by an interfering carrier and the effect of the interfering carrier on pull-in range and acquisition time are sought.

The following three approaches are used: an infinite series solution to the linearized loop equation, a quasi stationary approach, and a phase plane approach.

2.2 The Phase Locked Loop with Interference--An Infinite Series Approach

The differential equation for the phase locked loop (PLL) preceded by a limiter for the case of an unmodulated carrier plus an unmodulated interference at the input yields an unwieldy nonlinear differential equation. But by assuming the effect of the interference to be small a series solution for the output phase can be obtained and from this, insight into the loop operation with interference present can be obtained. The model for the phase locked loop is given in Fig. 2-1.

The effect of the limiter is easily seen by rewriting the signal at point 1.

$$\cos \omega t + a \cos (\omega + \delta)t = \sqrt{1 + a^2 + 2a \cos \delta t} \cos \left\{ \omega t + \tan^{-1} \frac{a \sin \delta t}{1 + a \cos \delta t} \right\} \quad (2-1)$$

The limiter removes the amplitude variations. Therefore, the signal at point 2 is

$$\cos \phi = \cos \left(\omega t + \tan^{-1} \frac{a \sin \delta t}{1 + a \cos \delta t} \right) \quad (2-2)$$

The voltage at point 3 is filtered and passed through the voltage controlled oscillator (VCO) to give the voltage at point 4

which, using operational notation, is

$$-2 \sin (\omega_o t + \frac{KF(S)}{S} \sin \phi)$$

But the product of the voltages at points 2 and 4 gives the voltage at point 3

$$\cos \Theta (-2 \sin(\omega_o t + \frac{KF(S)}{S} \sin \phi)) = \sin \phi \quad (2-3)$$

This leads to

$$\sin(\Theta - \omega_o t - \frac{KF(S)}{S} \sin \phi) = \sin \phi$$

where the double frequency term is taken to be outside the bandwidth of the system. Equating the angles we get

$$S\phi + KF(S) \sin \phi = S\Theta - S \omega_o t \quad (2-4)$$

Substituting for Θ from (2-2) and defining

$$\theta = \tan^{-1} \frac{a \sin \delta t}{1 + a \cos \delta t}$$

we obtain

$$S\phi + KF(S) \sin \phi = \omega - \omega_o + \dot{\theta} \quad (2-5)$$

$\dot{\theta}$ can be expanded in an infinite series to give¹

$$\dot{\theta} = \delta \sum_{n=1}^{\infty} (-1)^{n+1} a^n \cos n\delta t \quad (a < 1) \quad (2-6)$$

Assume ϕ has the form of a constant term plus a fluctuating term.

$$\phi = \phi_o + \psi(t) \quad (2-7)$$

Then using (2-5) and (2-6)

$$S\psi + KF(S) (\sin \phi_o \cos \psi + \cos \phi_o \sin \psi) = \delta \sum_{n=1}^{\infty} (-1)^{n+1} a^n \cos n\delta t + \omega - \omega_o \quad (2-8)$$

Assuming the fluctuations about the dc value of the phase error are small then

$$\dot{\psi} + KF(S) (\sin \phi_o + \cos \phi_o \psi) = \delta \sum_{n=1}^{\infty} (-1)^{n+1} a^n \cos n\delta t + \omega - \omega_o \quad (2-9)$$

For the case of the first-order loop $F(S) = 1$.

Assuming an infinite series for the output phase fluctuations

$$\psi = \sum_{n=1}^{\infty} A_n \cos (n\delta t + \alpha_n) \quad (2-10)$$

and substituting into the differential equation yields (see Appendix A for details)

$$\alpha_n = \tan^{-1} \frac{-n\delta}{K \cos \phi_o} \quad (2-11)$$

and

$$A_n = \frac{(-1)^{n+1} \delta a^n}{K \cos \phi_o \sqrt{1 + \left(\frac{n\delta}{K \cos \phi_o} \right)^2}}$$

where

$$\phi_o = \sin^{-1} \left(\frac{\omega - \omega_o}{K} \right) \quad (2-12)$$

ϕ_o is the solution for no interference present. The complete solution for ϕ is

$$\begin{aligned} \phi &= \phi_o + \delta \sum_{n=1}^{\infty} \frac{(-1)^{n+1} a^n}{\sqrt{(K \cos \phi_o)^2 + (n\delta)^2}} \cos (n\delta t + \tan^{-1} \frac{-n\delta}{K \cos \phi_o}) \\ &= \phi_o + \delta \sum_{n=1}^{\infty} \frac{(-1)^{n+1} a^n}{(n\delta)^2 + K^2 \cos^2 \phi_o} (K \cos \phi_o \cos n\delta t \\ &\quad + n\delta \sin n\delta t) \end{aligned} \quad (2-13)$$

Note that the output phase for the first order loop with low levels of interference is a periodic fluctuation of zero average value about the

phase error that would be present if there were no interference. Also, note that, if the assumption that the fluctuations due to the interference are small, were not made, the average effect of the interference would not be expected to be zero since the nonlinear sine function would weight positive and negative fluctuations unevenly.

To examine the limiting behavior for very large δ the following approximation is made

$$\frac{1}{(n\delta)^2 + K^2 \cos^2 \phi_0} \doteq \frac{1}{(n\delta)^2} \quad (2-14)$$

for

$$\delta^2 \gg (K \cos \phi_0)^2$$

which upon substitution into the solution for ϕ (eq. (2-13)) and by noting that

$$\theta = \sum (-1)^{n+1} \frac{a^n}{n} \sin n\delta t \quad (2-15)$$

$$\int \theta \, dt = - \sum (-1)^{n+1} \frac{a^n}{n^2 \delta} \cos n\delta t$$

yields

$$\phi \doteq \phi_0 + \theta - K \cos \phi_0 \int \theta \, dt \quad (\delta^2 \gg K^2 \cos^2 \phi_0) \quad (2-16)$$

To compare the fluctuations due to the interference before and after the phase lock loop, examine

$$\frac{[\phi - \phi_o]_{\text{peak}}}{\theta_{\text{peak}}}$$

$$[\phi - \phi_o]_{\text{peak}} = \left[\sum_{n=1}^{\infty} \frac{\delta (-1)^{n+1} a^n}{\sqrt{(n\delta)^2 + (K \cos \phi_o)^2}} \cos \left[n\delta t + \tan^{-1} \frac{-n\delta}{K \cos \phi_o} \right] \right]_{\text{peak}}$$

if $a \ll 1$, the first term dominates

$$[\phi - \phi_o]_{\text{peak}} \doteq \frac{a \delta}{\sqrt{(\delta)^2 + (K \cos \phi_o)^2}}$$

Taking only the first term in (2-15) for θ ,

$$[\theta]_{\text{peak}} = a$$

$$\frac{[\phi - \phi_o]_{\text{peak}}}{[\theta]_{\text{peak}}} = \frac{\delta}{\sqrt{(\delta)^2 + (K \cos \phi_o)^2}} = \frac{1}{\sqrt{1 + \left(\frac{K \cos \phi_o}{\delta}\right)^2}} \quad (2-17)$$

Note that the phase locked loop always decreases the peak-to-peak fluctuations when $a \ll 1$. Also note that as δ gets large the effectiveness of the PLL diminishes as far as reducing the peak-to-peak fluctuations of the interference.

To compare the mean square fluctuation caused by the interference before and after the PLL, compute

$$\begin{aligned} \frac{1}{\frac{2\pi}{\delta}} \int_0^{\frac{2\pi}{\delta}} \psi^2(t) dt &= \frac{1}{\frac{2\pi}{\delta}} \int_0^{\frac{2\pi}{\delta}} \left[\sum \frac{(-1)^{n+1} a^n}{\sqrt{(K \cos \phi_o)^2 + (n\delta)^2}} \cos(n\delta t) \right. \\ &\quad \left. + \tan^{-1} \frac{-n\delta}{K \cos \phi_o} \right]^2 dt = \sum_1^{\infty} \frac{\frac{\delta^2 a^{2n}}{2}}{(K \cos \phi_o)^2 + (n\delta)^2} \end{aligned} \quad (2-18)$$

If $a \ll 1$, the first term dominates

$$\frac{1}{\frac{2\pi}{\delta}} \int_0^{\frac{2\pi}{\delta}} \psi^2(t) dt \doteq \frac{\frac{\delta^2 a^2}{2}}{(K \cos \phi_o)^2 + \delta^2} \quad (2-19)$$

The mean square fluctuation before entering the phase locked loop is

$$\begin{aligned} \frac{1}{\frac{2\pi}{\delta}} \int_0^{\frac{2\pi}{\delta}} \theta^2 dt &= \frac{\delta}{2\pi} \int_0^{\frac{2\pi}{\delta}} \left[\sum_1^{\infty} (-1)^{n+1} \frac{a^n}{n} \sin n\delta t \right]^2 \\ &= \sum_1^{\infty} \frac{a^{2n}}{2n^2} \end{aligned} \quad (2-20)$$

If $a \ll 1$, the first term dominates

$$\frac{\delta}{2\pi} \int_0^{\frac{2\pi}{\delta}} \theta^2 dt = \frac{a^2}{2} \quad (2-21)$$

Therefore, the ratio is

$$\frac{\text{mean square } \psi(t)}{\text{mean square } \theta(t)} = \frac{\sum_1^{\infty} \frac{a^{2n}}{2} \frac{\delta^2}{(K \cos \phi_o)^2 + (n\delta)^2}}{\sum_1^{\infty} \frac{a^{2n}}{2}} \quad (2-22)$$

This ratio is less than one regardless of the values of a and δ . That is, the PLL always reduces the mean square phase fluctuation caused by the interference and this effect diminishes for larger δ . For $a \ll 1$

$$\frac{\text{mean square } \psi(t)}{\text{mean square } \theta(t)} = \frac{\delta^2}{\delta^2 + (K \cos \phi_o)^2} \quad (2-23)$$

Let us return to the differential equation (2-4) to examine the behavior of the second order loop with interference.

$$S\phi + KF(S) \sin \phi = S\Theta - \omega_o \quad (2-4)$$

For the second order loop let

$$F(S) = 1 + \frac{\tau}{S}$$

which when substituted into (2-4) and the equation is simplified yields

$$S^2\phi + KS \sin \phi + K\tau \sin \phi = S^2\Theta - S\omega_o \quad (2-24)$$

Eliminating the operational notation gives

$$\ddot{\phi} + K\dot{\phi} \cos \phi + K\tau \sin \phi = \ddot{\Theta} \quad (2-25)$$

Letting $\Theta = \omega t + \theta$ finally yields

$$\ddot{\phi} + K\dot{\phi} \cos \phi + K\tau \sin \phi = \ddot{\theta} \quad (2-26)$$

If we precede as before and let $\phi(t) = \phi_o + \psi(t)$, expand $\sin \phi$ and $\cos \phi$ and then let $\cos \psi(t) \doteq 1$ and $\sin \psi(t) \doteq \psi(t)$, we

find we cannot solve the equations. If, however, we make the cruder approximation that $\cos \phi \doteq 1$ and $\sin \phi \doteq \phi$, we can proceed to solve the equation. This approximation is not as crude as it appears since, when the second order loop is in phase lock, the phase error is zero. Therefore, the approximation is that the fluctuations about the phase error that exists when no interference is present, are small. This is the same approximation we made for the first order loop.

Therefore, we make the approximation $\cos \phi \doteq 1$ and $\sin \phi \doteq \phi$, then equation 2-26 becomes

$$\ddot{\phi} + K\dot{\phi} + K_T\phi = \ddot{\theta} \quad (2-27)$$

As before, we represent the input phase, θ , by an infinite series, equation 2-15. Differentiating twice yields,

$$\ddot{\theta} = \delta^2 \sum_{n=1}^{\infty} (-1)^n n a^n \sin n\delta t \quad (2-28)$$

We assume a solution of the form

$$\phi = \phi_0 + \sum_{n=1}^{\infty} A_n \sin (n\delta t + \alpha_n) \quad (2-29)$$

Substituting (2-29) into (2-27) and solving for A_n and α_n yields (see Appendix B for details)

$$\phi_0 = 0$$

$$\alpha_n = \tan^{-1} \frac{Kn\delta}{n^2\delta^2 - K\tau} \quad (2-30)$$

$$A_n = (-1)^{n+1} n\delta^2 a^n$$

The output phase is then

$$\begin{aligned} \phi &= \sum_{n=1}^{\infty} \frac{(-1)^{n+1} n\delta^2 a^n}{\sqrt{(nK\delta)^2 + (n^2\delta^2 - K\tau)^2}} \sin \left(n\delta t + \tan^{-1} \frac{Kn\delta}{n^2\delta^2 - K\tau} \right) \\ &= \sum_{n=1}^{\infty} \frac{(-1)^{n+1} n\delta^2 a^n \{ \sin n\delta t (n^2\delta^2 - K\tau) + \cos n\delta t (Kn\delta) \}}{(nK\delta)^2 + (n^2\delta^2 - K\tau)^2} \quad (2-31) \end{aligned}$$

For the second order PLL, the output phase is again a periodic fluctuation of zero average value about the value of the phase error that would be present if there were no interference.

In the case of the second order loop we might still expect the average value of the output phase to be zero even if we had not approximated $\cos \phi \doteq 1$ and $\sin \phi \doteq \phi$, since for the second order loop the steady state phase error with no interference present, ϕ_o , is zero.

If $\delta^2 \gg K\tau$ and $\delta^2 \gg K^2$, then

$$A_n \doteq \frac{(-1)^{n+1} a^n}{n}$$

and

$$\alpha_n = \tan^{-1} \frac{Kn\delta}{n^2\delta^2 - K\tau} \doteq \tan^{-1} \frac{Kn\delta}{n^2\delta^2} \doteq \tan^{-1}(0) = 0$$

then

$$\phi = \sum_{n=1}^{\infty} \frac{(-1)^{n+1} a^n}{n} \sin n\delta t = \theta$$

that is

$$\begin{aligned} \phi &\doteq \theta \quad \text{for } \delta^2 \gg K\tau \\ &\quad \delta^2 \gg K \end{aligned} \tag{2-32}$$

Returning for a moment to the solution to the first order loop, equation (2-13), we have

$$\phi = \phi_o + \delta \sum_{n=1}^{\infty} \frac{(-1)^{n+1} a^n}{(n\delta)^2 + K^2 \cos^2 \phi_o} \left\{ K \cos \phi_o \cos n\delta t + n\delta \sin n\delta t \right\} \tag{2-13}$$

If $\delta^2 \gg K$

$$\begin{aligned} \phi &\doteq \phi_o + \sum_{n=1}^{\infty} \frac{(-1)^{n+1} a^n}{n} \sin n\delta t \\ &\doteq \phi_o + \theta \end{aligned} \tag{2-33}$$

We see that for $\delta^2 \gg K$, the phase fluctuations of the first order loop and the second order loop are identical. This is an important result which will be arrived at from another viewpoint later.

To examine the ratio $\phi_{\text{peak}} : \theta_{\text{peak}}$ for the second order loop, we assume $a \ll 1$. Then the first term of the series solutions (2-31) and (2-15) will dominate. Then

$$\frac{\phi_{\text{peak}}}{\theta_{\text{peak}}} = \frac{\frac{\delta^2 a}{[(K\delta)^2 + (\delta^2 - K\tau)^2]^{1/2}}}{a} = \frac{\delta^2}{\sqrt{(K\delta)^2 + (\delta^2 - K\tau)^2}} \quad (2-34)$$

If δ is very large this ratio approaches one. If δ is very small the ratio approaches zero.

This ratio is greater than one if $(2\tau - K)\delta^2 > K\tau^2$.

If $K > 2\tau$ this will never happen.

The mean square output phase fluctuation is

$$\frac{1}{\frac{2\pi}{\delta}} \int_0^{\frac{2\pi}{\delta}} \phi^2(t) dt = \frac{1}{2} \sum_{n=1}^{\infty} \frac{\frac{n^2 \delta^4 a^{2n}}{2}}{(nK\delta)^2 + (n^2 \delta^2 - K\tau)^2} \quad (2-35)$$

Forming the ratio mean square ϕ : mean square θ we have

$$\frac{\text{mean square } \phi}{\text{mean square } \theta} = \frac{\sum_{n=1}^{\infty} \frac{\frac{n^2 \delta^4 a^{2n}}{2}}{(nK\delta)^2 + (n^2 \delta^2 - K\tau)^2}}{\sum_{n=1}^{\infty} \frac{a^{2n}}{2n^2}} \quad (2-36)$$

if $a \ll 1$ the first terms dominate and we have

$$\frac{\text{mean square } \phi}{\text{mean square } \theta} = \frac{\delta^4}{[(K\delta)^2 + (\delta^2 - K\tau)^2]} \quad (2-37)$$

For large δ this ratio approaches one and for small δ this ratio approaches zero. As for (2-34) this ratio is greater than one, if

$$(2\tau - K)\delta^2 > K\tau^2$$

For the second order loop it has been shown that for large δ the output phase fluctuations are approximately the input phase fluctuations. It has also been shown that for large δ the second order loop output is the same as the first order loop output when carrier plus interference are present at the input. It was also demonstrated that if $K < 2\tau$, it is possible that the peak-to-peak output phase fluctuations are greater than the input peak-to-peak phase fluctuations in the second order loop. Similarly, the mean square phase fluctuations of the output can be greater than those of the input in the second order loop. This contrasts with the case for the first order loop where the peak-to-peak and mean square output phase fluctuations are always less than those of the input.

2.3 The Effect of Interference on the Acquisition Time and Pull-in Range of the Phase Locked Loop--A Quasi-Stationary Approach

There have been many studies completed considering the acquisition behavior of phase locked loops with no interference present. In this section one of these approaches will be briefly reviewed. Then several cases of acquisition in the presence of interference will be reduced to the case of acquisition without interference and the effects of the interference pointed out.

The approach we are going to follow is that of Meer².

Meer's approach is to demonstrate that for large frequency errors the second order loop can be considered as a first order loop with a slowly varying bias. With this approximation an expression for acquisition time is developed from which he deduces the pull-in range. Briefly, his approach is as follows:

The first order loop equation is

$$S\phi + mK \sin \phi = \Delta \omega \quad (2-38)$$

where $\Delta \omega = \omega - \omega_0$ is the initial frequency error.

K is the loop gain

$m = \lim_{S \rightarrow \infty} F(S)$ is the high frequency (HF) gain of the filter

$H \equiv mK$ is the HF loop gain

$\rho_0 \equiv \frac{\Delta \omega}{H}$ is the normalized initial frequency error.

For the first order loops (2-38) has two solutions. For

$$|\Delta \omega| < H$$

$$\phi(t) = \frac{2 \tan^{-1} \left[\sin \phi_s - \tan \frac{\phi_o}{2} \right] \tanh \left(t \cos \frac{\phi_s}{2} \right) + \cos \phi_s \tan \frac{\phi_o}{2}}{\left[1 - \sin \phi_s \tan \frac{\phi_o}{2} \right] \tanh \left(t \cos \frac{\phi_s}{2} \right) + \cos \phi_s} \quad (2-39)$$

where ϕ_s is the steady state error

$$\phi_s \equiv \sin^{-1} \frac{\Delta\omega}{H} = \sin^{-1} \rho_o$$

$\phi(t)$ was plotted for several values of initial phase, ϕ_o , and it was found that $\phi(t)$ settles to ϕ_s in less than $\frac{10}{H}$ sec in most cases.

Outside the synchronization range, $\Delta\omega > H$, the solution is

$$\frac{\sqrt{(\Delta\omega)^2 - H^2}}{2} t = \left[\tan^{-1} \left(\frac{\Delta\omega \tan \frac{\phi}{2} - H}{\sqrt{(\Delta\omega)^2 - H^2}} \right) \right] \phi_o \quad (2-40)$$

From this a plot of $\sin \phi(t)$ is made and is found to be periodic, with period

$$T_o = \frac{2\pi}{\sqrt{(\Delta\omega)^2 - H^2}} \quad (2-41)$$

From equation (2-38) the average value of $\sin \phi$ over a period of length, T_o , is

$$\frac{T_o}{\sin \phi} = \frac{\Delta\omega}{H} - \sqrt{\left(\frac{\Delta\omega}{H}\right)^2 - 1} = \rho_o - \sqrt{\rho_o^2 - 1} \quad (2-42)$$

where

$$\overline{g[\phi(t)]}^{T_o} \equiv \frac{1}{T_o} \int_0^{T_o} g(\phi(t)) dt$$

Next the second order loop is considered. It is given by

$$\tilde{F}_2(s) = \frac{1 + \tau_1 s}{1 + \tau_i s} = \tilde{M}_2 + \frac{1 - \tilde{M}_2}{1 + \tau_i s} = \tilde{M}_2 + \tilde{G}_2(s) \quad (2-43)$$

where

$$\tilde{M}_2 \triangleq \frac{\tau_1}{\tau_i}, \quad \tilde{G}_2(s) \triangleq \frac{1 - \tilde{M}_2}{1 + \tau_i s}$$

\tilde{M}_2 is the high frequency gain and $\tilde{G}_2(s)$ is a low pass filter.

Using this expression for the second order loop filter the second order loop differential equation is

$$s\phi + H_2 \sin \phi = \Delta\omega - \tilde{G}_2(s) \tilde{K}_2 \sin \phi \quad (2-44)$$

where $H_2 = \tilde{M}_2 \tilde{K}_2$

If we define $\omega_i(t) \equiv \Delta\omega - \tilde{G}_2(s) \tilde{K}_2 \sin \phi \quad (2-45)$

then (2-44) becomes

$$s\phi + H_2 \sin \phi = \omega_i(t)$$

Next Meer argues that for large initial $\Delta\omega$ the filter capacitor is a short. Recall that the second order loop filter is given by Fig. 2-2, where

$$G_2(S) = \frac{1 + MRCS}{1 + RCS}$$

$$\lim_{S \rightarrow \infty} G_2(S) = M$$

$$G_2(0) = 1$$

If the filter capacitor is a short, then the phase detector output is that of a first order loop. Therefore, from the earlier analysis of the first order loop, there is initially a low frequency component out of the phase detector given by (2-42) with period given by (2-41). Along with this low frequency component are components at the fundamental and harmonics of the beat frequency, $\frac{2\pi}{T_0}$. But only the low frequency component gets through the filter $\tilde{G}_2(S)$, ergo

$$\tilde{G}_2(S) \sin \phi(t) \doteq G_2(S) \frac{T_0}{\sin \phi(t)} \quad (2-46)$$

and

$$\omega_i(t) \doteq \Delta\omega - \tilde{K}_2 \tilde{G}_2(S) \frac{T_0}{\sin \phi(t)} \quad (2-47)$$

Meer then proceeds to demonstrate that as long as $1.8 B_n < \omega_i$ where B_n is the noise bandwidth $\omega_i(t)$ is a slowly varying term and under these conditions, the second order loop can be treated as a first order loop with a slowly changing bias.

With this point established

$$S\phi + H_2 \sin \phi = \omega_i(t)$$

is treated as a first order loop equation with an initial frequency

error $\omega_i(t)$. Then at any instant the low frequency component of the phase detector output is

$$\frac{T}{\sin \phi} = \frac{\omega_i}{H} - \sqrt{\left(\frac{\omega_i}{H}\right)^2 - 1} \quad (2-48)$$

where T is

$$\frac{2\pi}{T} = \sqrt{\omega_i^2 - H^2} \quad (2-49)$$

Substituting (2-48) into (2-45) yields

$$\omega_i = \Delta\omega - \tilde{G}_2(s) \Re \left[\frac{\omega_i}{H} - \sqrt{\left(\frac{\omega_i}{H}\right)^2 - 1} \right] \quad (2-50)$$

If we define $\rho(t) = \frac{\omega_i(t)}{H}$ and $\rho(0) = \rho_0 = \frac{\Delta\omega}{H}$ and substitute for $\tilde{G}_2(s)$ and separate variables, we get,

$$\frac{dt}{\tau_i} = \frac{d\rho}{\rho_0 - \rho + \frac{1 - \tilde{M}}{\tilde{M}} (\sqrt{\rho^2 - 1} - \rho)} \quad (2-51)$$

Integration of (2-51) between the limits ρ_0 and the minimum value of ρ for which the quasi-static condition is satisfied gives a part of the total acquisition time.

This portion is called the frequency acquisition time, t_f . The remaining time to acquisition is called the phase acquisition time t_ϕ . The total acquisition time, t_a , is then

$$t_a = t_\phi + t_f$$

Meer then justifies using $\rho = 1$ as the upper limit of integration for eq. (2-51) and accepting $t_{\phi} \leq \frac{10}{H}$ as a bound for t_{ϕ} .

The solution of eq. 51) from $\rho = \rho_0$ to $\rho = 1$ is given by Richman³ and is presented graphically by Meer.

The pull-in limit, the value of ρ for which the acquisition time goes to infinity, is obtained by finding the real zeroes of the denominator of eq. (2-51) which yields

$$\Delta\omega_{\rho} = H \sqrt{\frac{2\tilde{K}}{H} - 1}$$

which depends only on the dc gain \tilde{K} and the high frequency gain H .

At this point, we have presented the results of Meer's investigation of the acquisition behavior of phase locked loops with no interference present. We have found the acquisition time to be a function of initial frequency error, dc loop gain and the HF gain of the circuit and we have found the pull-in range as a function of the dc loop gain and the HF gain of the circuit. In light of these results, we proceed to examine the behavior of the phase locked loop in the presence of interference.

Returning to the model of the PLL it is of interest to examine the spectrum of the signal after it has passed through the limiter but before it has entered the feedback loop. The model for the loop is shown in Fig. 2-3. For simplicity we assume that initially the frequency out of the VCO is zero. Therefore, $\Delta\omega$ represents the initial frequency deviation

$$\cos \Delta\omega t + a \cos (\Delta\omega + \delta)t = A(t) \cos (\Delta\omega t + \theta(t)) \quad (2-53)$$

$$a < 1$$

where

$$\theta = \tan^{-1} \frac{a \sin \delta t}{1 + a \cos \delta t}$$

and

$$A(t) = \sqrt{1 + a^2 + 2a \cos \delta t}$$

The amplitude variations are lost in the limiter. The frequency spectrum at the output of the ideal limiter can be found by expanding $\cos [\Delta\omega t + \theta(t)]$.

$$\cos [\Delta\omega t + \theta(t)] = \sum_{n=-\infty}^{\infty} B_n(a) \cos (\Delta\omega - n\delta)t \quad (2-54)$$

Reference 4 contains ten place tables of $B_n(a)$ computed by J. Granlund.

The output spectrum of the limiter contains a component at the desired signal frequency, the interfering signal frequency and harmonics of the difference frequency.

Case 1

First let us consider the case in which

$$\cos \Delta\omega t + a \cos (\Delta\omega + \delta)t$$

is present at the input but that the bandwidth of the limiter is such as to discard all but the component at the desired frequency.

Referring to eq. (2-54) it is easily seen that this will be the case when (see Fig. 2-4)

$$|\Delta\omega - n\delta| > B_\ell \quad (2-55)$$

for all integers $n \neq 0$

The effect of the interference is that the amplitude of the desired frequency component is reduced by a factor $B_0(a)$ over what it would be if there was no interference present. This effect can be absorbed into the loop gain and the problem considered to be that of acquisition with no interference present. The inequality (2-55) will always be satisfied if it is satisfied for $n = 1$.

$$|\delta - \Delta\omega| > B_\ell$$

which is always satisfied when

$$\delta > 2B_\ell \quad (2-56)$$

Referring to equation (2-52) we have, when $\delta > 2B_\ell$

$$\Delta\omega_p = H \sqrt{\frac{2 \tilde{K} B_0(a)}{H} - 1} \quad (2-57)$$

To find the effect on acquisition time reference to Richman's or Meer's results, using the effective gain $B_0(a) \tilde{K}$, should be made. $B_0(a)$ as a function of a is plotted in Fig. 2-5.

Case 2

Acquisition in the Presence of Interference with a WideBand Limiter

Again $\cos \Delta\omega t + a \cos (\Delta\omega + \delta)t$ is present at the input but now all the spectral components will be present after the limiter.

$$\cos (\Delta\omega t + \theta(t)) = \sum_{-\infty}^{\infty} B_n(a) \cos (\Delta\omega - n\delta)t$$

where

$$\theta = \tan^{-1} \frac{a \sin \delta t}{1 + a \cos \delta t}$$

We may think of this signal in two ways: as a signal with spectral components of magnitude $B_n(a)$ corresponding to a frequency $\Delta\omega - n\delta$ for all integers n ; or we may take the composite signal viewpoint, that is, we may think of the signal as a single line, of constant amplitude moving about its average value $\Delta\omega$ in the frequency domain.

Taking the composite signal viewpoint we note that the amplitude of $\cos (\Delta\omega t + \theta(t))$, the limiter output has a constant value which has the same magnitude that a sinusoid of constant frequency would have at the limiter output.

The first order loop equation with $\cos (\Delta\omega t + \theta(t))$ at the input is

$$S\phi + \tilde{M} \tilde{K} \sin \phi = S(\Delta\omega t + \theta(t)) = \Delta\omega + \frac{d}{dt} \tan^{-1} \frac{a \sin \delta t}{1 + a \cos \delta t} \quad (2-58)$$

For the first order loop with constant frequency input we had

$$\begin{aligned} \frac{T_o}{\sin \phi} &= \frac{\Delta\omega}{H} - \sqrt{\left(\frac{\Delta\omega}{H}\right)^2 - 1} = \rho_o - \sqrt{\rho_o^2 - 1} \\ &\doteq \frac{1}{2\rho_o} \quad \text{if } 4\rho_o^4 \gg 1 \end{aligned} \quad (2-59)$$

or

$$\frac{T_o}{\sin \phi} \doteq \frac{H}{2\Delta\omega}$$

Averaging equation (2-58) over T_o when $\Delta\omega \ll \delta$ also yields

$$\frac{T_o}{\sin \phi} \doteq \frac{H}{2\Delta\omega} = \frac{1}{2\rho_o} \quad (2-60)$$

since

$$T_o = \frac{2\pi}{\sqrt{(\Delta\omega)^2 - H^2}} \quad (2-61)$$

Thus when

$$\Delta\omega \ll \delta, \quad T_o \gg \frac{2\pi}{\delta} \equiv T_\delta \quad (2-62)$$

and

$$\frac{1}{T_o} \int_0^{T_o} \dot{\theta}(t) dt = \frac{1}{T_o} \int_0^{\left[\frac{T_o}{T_\delta}\right] T_\delta} \dot{\theta}(t) dt + \frac{1}{T_o} \int_{\left[\frac{T_o}{T_\delta}\right] T_\delta}^{T_o} \dot{\theta}(t) dt \quad (2-63)$$

But the first integral is exactly zero and the second integral is very nearly zero for $T_o \gg T_\delta$. Thus eq. (2-60) is seen to be true.

Therefore, the dc voltage on the VCO in the asynchronous mode for the first order loop with time varying frequency is determined by $\Delta\omega$ which is the average value of the input frequency.

Now following Meer's argument, for large values of frequency error the second order loop acts like a first order loop. Thus the dc voltage on the VCO is,

$$\sin \phi = \frac{H}{2\Delta\omega}$$

and since the loop filter is very narrow band

$$\tilde{G}_2(S) \sin \phi = G_2(S) \overline{\sin \phi} \quad (2-64)$$

and the argument proceeds as before in eqs. (2-47) through (2-52).

Since the composite signal amplitude is the same as the limiter output amplitude that a single sine wave of constant frequency would have, and since for large frequency errors the loop tries to acquire the average frequency, the pull-in limit is

$$\Delta\omega_p = H \sqrt{\frac{2\tilde{K}}{H} - 1} \quad (2-65)$$

where in this case $\Delta\omega_p$ represents the maximum average frequency that the loop will begin to acquire. The acquisition time is the same as if no interference were present.

The physical picture of the acquisition process is as follows. The large frequency error produces a dc voltage on the VCO, the VCO responds by increasing its frequency which when mixed with the input spectrum shifts it toward zero frequency. The frequency error, $\omega_i(t)$, decreases. Meer has shown that as long as

$$1.8 B_n < \omega_i(t)$$

$\omega_i(t)$ is slowly changing. As long as this situation is satisfied, the whole spectrum is being slowly shifted toward zero frequency. (see Fig. 2-6).

Before this process can be completed with the acquisition of the average frequency a component at one of the harmonics of the difference frequency will be shifted into the passband of the filter and will be acquired.

If the desired component is the first frequency component shifted into the filter passband, the loop will acquire the desired frequency. This occurs when (see Fig. 2-7).

$$|\Delta\omega - \delta| > 2\pi B_n \quad (2-66)$$

and

$$|\Delta\omega| < \delta$$

otherwise a harmonic of $\Delta\omega$ plus the difference frequency may be acquired. But conditions (2-66) are always satisfied when (2-63) is satisfied, that is when we can make the approximation

$$\frac{T_o}{\sin \phi} = \frac{1}{2\rho_o}$$

when interference is present.

When a frequency component has been acquired, that is $\omega_{VCO} = \omega_{comp.}$, there is still a voltage on the VCO due to all the components outside the noise bandwidth of the filter. This voltage causes the VCO to change its frequency which shifts the component out of phase lock. The phase error generates a voltage which tends to shift the

component back into phase lock. As the phase error is reduced by this restoring voltage the other frequency components again generate a voltage which tends to shift the component back out of lock, etc. The interference then causes a fluctuation in the phase error, never allowing it to go to zero.

We have considered the acquisition problem for two limiting cases of the limiter bandwidth. The first case was very narrow band, so that only the desired component of the limiter spectrum was allowed to enter the feedback loop. In the second case, the entire limiter spectrum was allowed to enter the feedback loop. These two situations had the common property that the input waveform could be represented by a cosine of constant amplitude and a time varying frequency. For all limiter bandwidths which pass more than one component but not all of them, the signal into the feedback loop must be represented in the form of a cosine with time varying amplitude and frequency.

$$A(t) \cos \theta_1(t)$$

If we rederive our differential equation using a sinusoidal input with time varying amplitude and frequency we obtain

$$S\phi + H(S) A(t) \sin \phi = S \theta_1(t)$$

We can no longer reduce the phase detector output for the first order loop to that of the constant frequency sinusoid since the phase detector output contains the amplitude fluctuations.

For Case 2, we have found that the PLL attempts to acquire the average frequency of $\cos(\Delta\omega t + \theta(t))$ provided $\Delta\omega + \dot{\theta}(t)$ is less than $\Delta\omega_p$, the pull in range (2-65). This process continues until a component of the spectrum is shifted into the passband of the lowpass filter, $\tilde{G}_2(s)$.

Further, we found that when $|\Delta\omega| \ll \delta$, the relations of Meer for pull-in range and acquisition time are still valid.

Acquisition when interference is present does not imply that the output phase error is zero however. In section 2.2 it was demonstrated that the output phase fluctuates periodically about $\phi = 0$ and in this section a physical description of the process was given.

2.4 Phase Plane Solutions to the Second Order Phase Lock Loops with Interference

As we have seen in preceeding sections the analysis of the second order PLL with or without interference is mathematically difficult. The nonlinear differential equation can only be solved when special simplifying assumptions are made. The use of graphical techniques, however, can be made to yield graphical solutions to the exact differential equation in the case of no interference. Viterbi,⁵ has presented phase plane solutions for the second order loop with constant and linearly varying frequency inputs.

For the case of single carrier interference, or for any other frequency input, we have two paths open to us. We can resolve the differential equation for the specific desired input frequency, or we can approximate the input frequency with a piecewise linear approximation

and utilize Viterbi's results. For the case of single carrier interference, we have found it convenient to use the second approach.

In this section, we use a piecewise linear approximation to the input frequency for the case of a desired signal with no modulation at a frequency ω_0 and an interfering signal with no modulation separated in frequency by an amount δ and with relative amplitude a . With this piecewise linear approximation we use the phase plane solutions to the second-order loop with no interference to obtain the output frequency error.

For large peak-to-peak variations in the input frequency, expressions for the average change in frequency and for the peak-to-peak variation in frequency are found as a function of a , the relative amplitude.

Figures 2-8 to 2-12 show plots of the instantaneous frequency input for values of $a = .9, .8, .7, .6, .5$ with δ as a parameter for the case of single carrier interference of relative magnitude, a , and frequency separation from the desired signal, δ .

For large values of a , we can approximate the input frequency by a rectangular wave having the same positive and negative peaks and the same average value as the exact instantaneous frequency. The approximation for $a = .9$ is shown in Fig. 2-12.

Viterbi has presented the phase plane solutions for several types of loop filters for both constant and linearly varying frequency inputs. The differential equation for the PLL with no interference and with constant frequency input is

$$\ddot{\phi} + K F(S) \sin \phi = \Omega \quad (2-67)$$

where

ϕ is the phase error

K is the loop gain

F(S) is the loop filter

Ω is the initial frequency error.

For the second order loop

$$F(S) = 1 + \frac{\tau_1}{S}$$

With this substitution, eq. (2-67) becomes

$$S^2 \phi + (KS + \tau_1 K) \sin \phi = S \Omega \quad (2-68)$$

letting $\tau_1 K = \omega_n^2$ and $K = 2\rho \omega_n$

where, in servo terminology,

ω_n is the undamped natural frequency

ρ is the damping factor

of the linearized servo loop.

With these substitutions and without operational notation, eq. (2-68) becomes

$$\frac{d^2 \phi}{dt^2} + 2\rho \omega_n \cos \phi \frac{d\phi}{dt} + \omega_n^2 \sin \phi = 0 \quad (2-69)$$

Normalizing the time $t = \frac{\tau}{2\rho \omega_n}$ and defining $\dot{\phi} = \frac{d\phi}{d\tau} = \frac{1}{2\rho \omega_n} \frac{d\phi}{dt}$,

we get

$$\ddot{\phi} + \dot{\phi} \cos \phi + \frac{1}{4\rho^2} \sin \phi = 0 \quad (2-70)$$

Now for purposes of plotting, let $\phi = x$, $\dot{\phi} = y$ then $y = \dot{x}$ and $\ddot{\phi} = \dot{y}$.

Equation (2-70) then becomes

$$\dot{y} + y \cos x + \frac{\sin x}{4\rho^2} = 0 \quad (2-71)$$

Viterbi has presented the trajectories, that is the locus of points of (x, y) i.e., of $(\phi, \dot{\phi})$, as the system relaxes from a large initial phase and frequency error $(\phi_o, \dot{\phi}_o)$ to its steady state condition of phase lock $(\phi_f = 0, \dot{\phi}_f = 0)$, for several values of ρ . Figure 2-13 was taken from Viterbi.⁵

Consider the case of the second order loop initially tracking the desired frequency, ω_o , and at time t_o the interference $a \cos (\omega_o + \delta)t$ appears at the input to the loop. We pose the question what happens to the phase and frequency errors.

The input frequency is of the type shown in Fig. 2-13. In general, the positive peak, C_+ , is $\frac{a \delta}{1+a}$, the negative peak, C_- , is $\frac{a}{1-a} \delta$. Let us also define the duration of the positive and negative peaks as T_+ and T_- respectively. Then $T_+ + T_- = T = \frac{2\pi}{\delta}$, then for time $t < t_o$, $(\phi, \dot{\phi}) = (0, 0)$. At $t = t_o$ the frequency error jumps from 0 to $\frac{a}{1+a} \delta$. For time $t_o < t < t_o + T_+$ the system relaxes along the trajectory determined by the new initial conditions $(0, \frac{a \delta}{1+a})$. At $t = (t_o + T_+)^-$ the coordinates of the system are $(\phi(t_o + T_+), \dot{\phi}(t_o + T_+))$ at $t = (t_o + T_+)^+$ the frequency error instantaneously drops from $\dot{\phi}[(t_o + T_+)^-]$ to $\dot{\phi}[(t_o + T_+)^+] - \frac{2a\delta}{1-a^2}$. The system coordinates

at $(t_0 + T_+)^+$. At $t = t_0 + T_+ + T_-$ another frequency jump of magnitude $\frac{a \delta}{1+a}$ occurs with the phase remaining constant. Continuing in this fashion the output phase and frequency error can be determined.

In most cases this is a tedious task since given the initial coordinates (x_1, y_1) and the phase plane trajectory at time t_1 it is not obvious which coordinates (x_2, y_2) on the trajectory the system is at on some later time, t_2 , since time is not explicitly indicated on the phase plane. A few methods for determining this are given in Truxal⁶. The most straightforward method is a graphical integration of

$$\tau_2 - \tau_1 = \int_{\tau_1}^{\tau_2} d\tau \quad (2-72)$$

with

$$y = \dot{x} = \frac{dx}{d\tau}$$

$$d\tau = \frac{dx}{y}$$

Therefore

$$\tau_2 - \tau_1 = \int_{x_1}^{x_2} \frac{1}{y} dx \quad (2-73)$$

$\tau_2 - \tau_1$, x_1 and the trajectory $y(x)$ are known. x_2 and y_2 are found by finding the point (x_2, y_2) on the curve $\frac{1}{y}$ at which the area under $\frac{1}{y}$ between x_1 and x_2 equals $\tau_2 - \tau_1$.

This method is illustrated later.

If the positive and negative jumps of the piecewise linear input carry the frequency error outside the phase acquisition region (the region between the two lines A - A in Fig.2-13, the phase

trajectory is almost periodic. This corresponds to the discussion in section 2.3 where $\Delta\omega$ is large and $\phi(t)$ is periodic. For large frequency errors, y , the periodic approximation is a good one. In this situation the phase error increases linearly with time and the graphical integration can be avoided. This is easily seen from the differential equation. Rewriting eq. (2-71)

$$\frac{\dot{y}}{x} = \frac{dy}{dx} = -\cos x - \frac{\sin x}{4\rho^2 y} \quad (2-74)$$

for $y \gg 1$ this becomes

$$\frac{dy}{dx} = -\cos x$$

$$y = -\sin x + c \quad (2-75)$$

also

$$y = \frac{dx}{d\tau}$$

$$d\tau = \frac{dx}{y} = \frac{dx}{c - \sin x}$$

$$\int_{t_0}^{t_f} d\tau = \int_{x_0}^{x_f} \frac{dx}{c - \sin x}$$

From Dwight Integral 436:00 (reference 7),

$$T_{dn} = t_f - t_o = \frac{2}{\sqrt{c^2 - 1}} \tan^{-1} \frac{c \tan \frac{x_f}{2} - 1}{\sqrt{c^2 - 1}} - \frac{2}{\sqrt{c^2 - 1}} \tan^{-1} \frac{c \tan \frac{x_o}{2} - 1}{\sqrt{c^2 - 1}}$$

$$\text{For } y \gg 1; \sqrt{c^2 - 1} \doteq |c| \quad \frac{1}{c} \ll 1$$

Then

$$x_f = c T_{dn} + x_o \quad (2-76)$$

Equation (2-76) is valid in the time interval from t_o to $t_1 = t_o + T_+$ and $c = c_+ = \frac{a}{1+a} \delta$ and the phase increases from x_o to $x_o + c_+ T_+$ in the time interval from t_1 to $t_2 = t_o + T_+ + T_-$. $c \doteq c_- = -\frac{a\delta}{1-a}$ and the phase "increases" from $x_o + c_+ T_+$ to $x_o + c_+ T_+ + c_- T_-$. The net increase in phase is $c_+ T_+ + c_- T_-$. But this is zero since it is the condition for the average frequency to be ω_o . Therefore the net change in phase over a period is zero and hence the output is approximately periodic with frequency δ .

The average frequency over a period is then

$$\omega_o + \frac{1}{T} \int_{t_o}^{t_1} c_+ - \sin(c_+ t - c_+ t_o + x_o) dt + \frac{1}{T} \int_{t_1}^{t_2} c_- - \sin(c_- t - c_- t_1 + x_o + c_+ T_+) dt$$

This expression can be simplified to

$$\omega_o + \frac{c_- - c_+}{c_+ c_- T} \left[\cos (x_o + c_+ T_+) - \cos x_o \right] \quad (2-77)$$

Therefore, the phase lock loop shifts the average frequency by an amount

$$\Delta \bar{f} = \frac{c_- - c_+}{c_+ c_- T} \left[\cos (x_o + c_+ T_+) - \cos x_o \right]$$

Let us keep a constant and see how $\Delta\bar{F}$ varies with δ under the constraints

$$c_+T_+ + c_-T_- = 0 \quad \text{and} \quad T_+ + T_- = \frac{2\pi}{\delta}$$

Writing c_+ and c_- in terms of a and δ we have, $c_+ = \frac{a}{1+a} \delta$ and $c_- = \frac{-a}{1-a} \delta$.

Substituting for c_+ and c_- in the constraint equations and solving for T_+ and T_- yields

$$T_+ = \frac{(1+a)\pi}{\delta} \quad \text{and} \quad T_- = \frac{\pi(1-a)}{\delta}.$$

Then, substituting for T_+ , T_- , c_+ , c_- in the expression for $\Delta\bar{F}$ gives

$$\begin{aligned} \Delta\bar{F} &= \frac{c_- - c_+}{c_+c_-T} \left[\cos(x_0 + c_+T_+) - \cos x_0 \right] \\ &= \frac{1}{a\pi} \left[\cos(x_0 + a\pi) - \cos x_0 \right] \\ &= \frac{1}{a\pi} \left[\cos x_0 (\cos a\pi - 1) - \sin x_0 \sin a\pi \right] \end{aligned}$$

If the loop was in phase lock initially $x_0 = 0$ and therefore

$$\Delta\bar{F} \bigg|_{x_0 = 0} = \frac{1}{a\pi} (\cos a\pi - 1) \quad (2-78)$$

The peak-to-peak fluctuation as a function of a, neglecting the effect of the sinusoidal fluctuation is

$$\text{peak-to-peak fluctuation} = \frac{2a}{1-a^2} \delta + \sin a\pi \quad a \leq \frac{1}{2}$$

$$= \frac{2a}{1-a^2} \delta + 1 \quad a \geq \frac{1}{2}$$

$\Delta \bar{f}$ as a function of \underline{a} and the peak-to-peak fluctuations of the input and output as a function of \underline{a} are presented in Figs. 2-15 and 2-16.

As \underline{a} increases both the integrals

$$\Delta \bar{f} = \frac{1}{c_+} \int_0^{a\pi} -\sin x \, dx + \frac{1}{c_-} \int_{a\pi}^0 -\sin x \, dx$$

increase as a^2 .

The weighting factors decrease as $\frac{1}{a}$, the net result being that $\Delta \bar{f}$ increases as \underline{a} for small \underline{a} .

After \underline{a} reaches the value $\frac{1}{2}$ the integral begin to increase much more slowly. Similarly $\frac{1}{c_+}$ approaches its minimum value of 2. However, $\frac{1}{c_-}$ continues to grow smaller and smaller overtaking the growth of the second integral and eventually swamping it out. At $a = .75$ the tradeoff between increasing integrals and decreasing weighting factors results in a maximum product of about $\Delta \bar{f} = .72$.

Looking at the physical process, the fluctuation superimposed on the input frequency by the PLL occurs because, when the system is displaced from phase lock a large frequency error exists. This results in a linearly increasing phase error. The sinusoidal phase detector

reacts to this linearly increasing phase error by transforming it into a sinusoidal fluctuation. This fluctuation is fed into the VCO and results in a sinusoidal fluctuation being imposed on the VCO frequency. This sinusoidal fluctuation is transferred to the output frequency by the mixer.

When \underline{a} is small the frequency error applied to the phase detector is small, the phase error increases slowly and not much of a fluctuation is transferred to the output frequency. As \underline{a} increases more of a phase error is accumulated and therefore a larger portion of the period of a sine wave is imposed on the output frequency. As $\underline{a} \rightarrow 1$, the phase error accumulated by a positive frequency peak of an input fluctuation that has zero average value is π . When \underline{a} is small the contributions from the positive and negative peaks add. However, as \underline{a} increases the finite contribution from the negative peak is swamped out because its time duration quickly approaches zero as $\underline{a} \rightarrow 1$. Somewhere between the sum of the two contributions is a maximum.

If we continue to think about the PLL in the same manner it is easy to see that as \underline{a} increases the peak-to-peak fluctuation in frequency will continue to increase until the phase error accumulated is $\frac{\pi}{2}$, at which point the phase detector is putting out its maximum voltage and the fluctuation imposed on the input frequency has reached its maximum value. As \underline{a} increases beyond this point the difference between the peak-to-peak fluctuation of the input and output maintains a constant value.

We have just examined the frequency error for the case of a rectangular frequency input that had an average value equal to the desired signal frequency. For the special case of large peak-to-peak fluctuations we found the average change in frequency and the peak-to-peak fluctuation caused by the PLL as a function of \underline{a} , the relative amplitude of the interference to the desired frequency. Let us now actually obtain a plot of the output phase fluctuations for a specific periodic rectangular frequency input.

If we assume that the positive and negative input frequency fluctuations carry the frequency error outside the phase acquisition region we can ignore the second term in the differential equation

$$\frac{dy}{dx} = -\cos x - \frac{\sin x}{4\rho^2 y} \quad (2-79)$$

which describes the second order loop with constant frequency input.

The solution to (2-79) under this assumption is given by

$$y = -\sin x + c \quad (2-80)$$

$$x_f = c T_{dn} + x_0 \quad (2-81)$$

For the positive pulse we have

$$c_+ = y_0 + \sin x_0$$

$$x_f = c_+ T_{d+} + x_0$$

$$y_f = c_+ - \sin x_f$$

For the negative pulse

$$c_- = y_1 + \sin x_1$$

$$x_2 = c_- T_{d-} + x_1$$

$$y_2 = c_- - \sin x_2$$

By repeating application of these equations a plot of output frequency error as a function of time is found. This was carried out and the resulting plot of output frequency error is given by Fig. 2-18 for the specific input of Fig. 2-17.

Referring to Fig. 2-18 we first note that the peak-to-peak fluctuation over a cycle increased by two normalized frequency units. For any c_+ and c_- , the peak-to-peak fluctuation will increase but it will not always be by 2 units over a cycle. Two is the maximum. The peak-to-peak fluctuation over several cycles will always increase by two if c_+ and c_- are such that they carry the frequency out of the phase acquisition region.

Let us examine the average positive peak over T_+ . We have

$$y = c_+ - \sin (c_+ t + x_0)$$

$$\bar{y}_+ = c_+ + \frac{1}{T_+} \int_0^{T_+} - \sin (c_+ t + x_0) dt$$

$$\bar{y}_+ = c_+ + \frac{1}{c_+ T_+} \cos x \bigg|_{x_0}^{x_0 + c_+ T_+}$$

$c_{++}T_+$ is the same for every positive peak. In our case $c_{++}T_+$ is $5.67 \frac{\text{rad}}{\text{norm. sec.}}$.

For the n^{th} cycle the initial phase is

$$x_{o,n} = n(c_{++}T_+ + c_{--}T_-) \quad n \geq 1$$

$$x_{o,0} = 0$$

if

$$\ell \ 2\pi + n(c_{++}T_+ + c_{--}T_-) = (n + m)(c_{++}T_+ + c_{--}T_-)$$

where n, m, ℓ are positive integers then the x_o 's repeat after m cycles and the output is periodic. The condition restated is

$$m(c_{++}T_+ + c_{--}T_-) = +\ell \ 2\pi$$

or

$$(c_{++}T_+ + c_{--}T_-) = \frac{\ell}{m} \ 2\pi \quad (2-82)$$

The average positive peak over T_+ is

$$\bar{y}_+ = c_+ + \frac{1}{c_{++}T_+} (\cos(x_o + c_{++}T_+) - \cos x_o) \quad (2-83)$$

where x_o takes on values

$$x_o = n(c_{++}T_+ + c_{--}T_-) - \ell \ 2\pi$$

n, ℓ integer

It has a finite number of values if (2-82) holds, otherwise it can take on an infinite number of values.

Maximizing \bar{y}_+ with respect to x_0 yields

$$\frac{1}{c_+ T_+} \left[-\sin(x_0 + c_+ T_+) + \sin x_0 \right] = 0$$

which results in

$$x_0 = \tan^{-1} \frac{\sin c_+ T_+}{1 - \cos c_+ T_+} + n\pi \quad (2-84)$$

The maximum average (over T_+) positive peak is then

$$\bar{y}_+ \Big|_{\max} = c_+ + \frac{1}{c_+ T_+} (\cos x_0 (\cos c_+ T_+ - 1) - \sin x_0 \sin c_+ T_+)$$

which reduces to

$$\bar{y}_+ \Big|_{\max} = c_+ + \frac{\sqrt{2}}{c_+ T_+} (1 - \cos c_+ T_+)^{1/2} \quad (2-85)$$

The exact same expression holds for $\bar{y}_- \Big|_{\max}$ if c_+ and T_+ are replaced by c_- and T_- respectively.

The value of \bar{y} averaged over a positive part of the cycle depends on the initial value of the phase x_0 . It takes on its maximum average value when x_0 has the value specified by eq. (2-84). This maximum value is given by (2-85).

If we average the positive peak over several cycles, we find

$$\bar{y}_+ = c_+ + \sum_{n=0}^{\infty} \frac{1}{c_+ T_+} \int_{x_{0,n}}^{x_{0,n} + c_+ T_+} (-\sin x) dx$$

where $x_{0,n} = n(c_+T_+ + c_-T_-) \triangleq n c$

If

$$(c_+T_+ + c_-T_-) \neq \frac{\ell}{m} 2\pi \quad (\ell, m \text{ integer})$$

then the sequence of $x_{0,n}$'s is not periodic.

Since there is apparently nothing to favor positive values of the integral over negative values, it seems reasonable to assume that the sum averages to zero.

Note: x_0 does not take on all values between zero and 2π since this would imply that

$$x_0 = nc - \ell 2\pi$$

$$\pi + x_0 = mc - \ell 2\pi$$

$$\pi = (m - n)c - (\rho - \ell) 2\pi$$

the sequence of x_0 's was periodic of period $2(m - n)$. This removes a countable infinity of points from the set of possible values for x_0 . Formulated more precisely

$$\overline{y}_+ = c_+$$

and

$$\sum_{n=0}^{\infty} \int_{x_{0,n}}^{x_{0,n} + c_+T_+} -\sin x \, dx = 0$$

if

$$\begin{aligned} \lim \\ M \rightarrow \infty \\ \Delta x \rightarrow 0 \end{aligned}$$

where

$$y_n = 1 \text{ if } x < nc - \ell 2\pi < x + \Delta x$$

$$= 0 \text{ otherwise}$$

$$z_n = 1 \text{ if } x + \pi < nc - \ell 2\pi < x + \Delta x + \pi$$

$$= 0 \text{ otherwise}$$

and

$$N_1 = \sum_0^M y_n \quad \text{and} \quad N_2 = \sum_0^M z_n$$

and

$$R = \frac{N_1}{N_2} \quad \ell \text{ and positive integer}$$

The average frequency of the output over a complete cycle of the input is

$$\begin{aligned} \frac{1}{T} \int_0^T y \, dt &= \frac{1}{T} \left\{ c_+ T_+ + \frac{1}{c_+} \int_{x_0}^{x_0 + c_+ T_+} -\sin x \, dx \right. \\ &\quad \left. + c_- T_- + \frac{1}{c_-} \int_{x_0 + c_+ T_+}^{x_0 + c_+ T_+ + c_- T_-} -\sin x \, dx \right\} \\ &= \frac{c_+ T_+ + c_- T_-}{T} + \frac{1}{T} \left(\frac{1}{c_+} - \frac{1}{c_-} \right) \cos (x_0 + c_+ T_+) - \frac{\cos x_0}{c_+ T} \\ &\quad + \frac{\cos (x_0 + c_+ T_+ + c_- T_-)}{c_- T} \end{aligned}$$

The first term represents the average frequency of the input, the others represent the effect of the PLL on the average frequency.

As in the previous discussion the average frequency over a cycle depends on the value of x_0 .

If the $x_{o,n}$'s are periodic, the average value over several cycles depends on the periodicity.

If the $x_{o,n}$'s are not periodic we argued that it is reasonable to assume that

$$\begin{aligned} \lim_{N \rightarrow \infty} \sum_{n=0}^N \frac{1}{c_+ T} \int_{x_{o,n}}^{x_{o,n} + c_+ T} -\sin x \, dx \\ + \frac{1}{c_- T} \int_{x_{o,n} + c_+ T}^{x_{o,n} + c_+ T + c_- T} -\sin x \, dx \\ \rightarrow 0 \end{aligned}$$

and therefore that the average over several cycles is $\frac{c_+ T + c_- T}{T_+ + T_-}$ which is the average frequency of the input.

In the two preceding discussions we discussed the reaction of the PLL to inputs whose frequency excursions carried the loop out of the phase acquisition region which allowed us to neglect a term in the differential equation. We now compute the output phase error to a rectangular frequency input whose average value is non-zero and whose positive excursions in frequency carry the loop outside the phase acquisition region but whose negative excursions do not.

The purpose of this discussion is to illustrate the use of the phase plane plot in computing output phase errors and to find the shape of the output pulse for a particular input frequency. The

instantaneous frequency of the input is chosen to be as illustrated in Fig. 2-19. It is normalized for a loop with high frequency gain $m = .01$, midband gain, $K = 1$, and 3 db loop bandwidth of 30 Hz and damping factor $\rho = .707$.

The normalized input frequency plot is shown in Fig. 2-20. This frequency input has a positive pulse of 583.09 cycles/normalized sec and no negative pulse.

For the duration of the positive pulse we can make the approximation that the nonlinear term in the differential equation (eq. 2-79), describing the loop is negligible. The solutions valid for the duration of the positive pulse are then given by (2-80) and (2-81)

$$y = -\sin x + c \quad (2-80)$$

$$x = c(t - t_0) + x_0 \quad (2-81)$$

As before we use equations (2-80) and (2-81) to relate phase and frequency errors just after the pulse appears to those just before it passes. To find the reaction of the loop for the period just after the pulse passes to just before the next pulse strikes we use the phase plane plot, Fig. 2-21, and the graphical integration technique described on page 71.

On the following pages, we calculate the output phase and frequency errors for several cycles of the input frequency of Figs. 2-19 and 2-20.

We assume the loop is initially in phase lock when the frequency input of Fig. 2-18 is applied. Then

$(x_0, y_0) = (0, 0)$, and the pulse of amplitude 583.09 strikes, then using eqs. (2-80) and (2-81),

$$c = 583.09 \text{ normalized frequency units}$$

$$x_f = c T_{dn} + x_0$$

$$x_f = (583.09)(2.2 \times 10^{-3}) + 0$$

$$= 1.28 \text{ radians}$$

$$y_f = c - \sin x_f = 583.09 - .96$$

$$(x_f, y_f) = (1.28, 583.09 - .96)$$

after the pulse passes we have

$$x_1 = x_f = 1.28 \text{ radian}$$

$$y_1 = y_f - c = -.96$$

$$\text{then } 1.28 \text{ rad at } \frac{\pi}{40} \frac{\text{radian}}{\text{phase unit}^*} = .0785 \frac{\text{radian}}{\text{phase unit}}$$

is 16.3 phase units on the phase plane plot (see Fig. 2-20). The phase and frequency error (x_1, y_1) just after the pulse has passed are known.

The system will now move toward the origin of the phase plane along the trajectory passing through (x_1, y_1) until it is disturbed by the pulse $T - T_d = .1$ sec later. The system coordinates at the time the pulse strikes for the second time can be determined from a graphical integration of

* A phase unit is the smallest division on the phase plane plot (see Fig. 2-20).

$$T - T_d = \int_{T_d}^T dT = \int_{x_1}^{x_2} \left(\frac{1}{y}\right) dx$$

This is carried out in Fig. 2-21 on which it is seen that the phase error decreases by 1.22 phase units and the frequency error does not change a significant amount. Therefore,

$$(x_2, y_2) = (1.18, -.96)$$

since

$$y_2 = (16.3 - 1.22)(.0785 \frac{\text{radian}}{\text{phase unit}}) - 1.18 \text{ radian}$$

As the pulse strikes for the second time

$$(x_2, y_2) \rightarrow (x_o, y_o)$$

i.e.,

$$(1.18, -.96) \rightarrow (1.18, 583.09, -.96)$$

The new c is

$$c = y_o + \sin x_o = 583.09 - .96 + .96 = 583.09$$

then

$$x_f = c T_{dn} + x_o = (583.09) 2.2 \times 10^{-3} + 1.18 = 2.46 \text{ radians}$$

and

$$y_f = c - \sin x_f = 583.09 - .63$$

After the pulse passes the new system coordinates, (x_1, y_1) , are

$$(x_1, y_1) = (2.46 \text{ radians} = 31.34 \text{ phase unit}, -.63)$$

proceeding exactly as before using Fig.2-22 we get

$$(x_2, y_2) = \begin{pmatrix} 2.39 \text{ radians} \\ \text{or} \\ 30.45 \text{ phase units} \end{pmatrix} \quad -.75$$

The pulse strikes for the third time changing

(x_2, y_2) to $(2.39, 5.83.09 - .75)$

The new c is

$$c = y_0 + \sin x_0 = 5.83.09 - .75 + .68 = 583.02$$

then

$$\begin{aligned} x_f &= (583.02) 2.2 \times 10^{-3} + 2.39 \\ &= 3.67 \text{ rad} \\ &= 3.67 - \pi .53 \end{aligned}$$

$$y_f = c - \sin x_f = 583.02 - .51 = 582.51$$

after the pulse has passed

$$(x_1, y_1) = (.53 + \pi, -.58)$$

Performing the graphical integration, Fig.2-23 yields

$$(x_2, y_2) = (\pi + .471, -.59)$$

The pulse strikes for the fourth time changing

$$(x_2, y_2) \text{ to } (\pi + .471, 583.09 - .59)$$

$$(x_0, y_0) = (\pi + .471, 582.5)$$

The new c is

$$c = y_0 + \sin x_0 = 582.5 - .45$$

$$c = 582.05$$

Then

$$x_f = (582.05) 2.2 \times 10^{-3} + \pi + .471$$

$$= \pi + 1.75 = \frac{3\pi}{2} + .179$$

$$y_f = c + \sin x_f = 582.05 + .98 = 583.03$$

$$(x_f, y_f) = (\frac{3\pi}{2} + .179, 583.03)$$

after the pulse passes the coordinates are

$$(x_1, y_1) = (\frac{3\pi}{2} + .179, - .06)$$

The graphical integration is performed in Fig. 2-24 to yield

$$(x_2, y_2) = (\frac{3\pi}{2} + .157, - .06)$$

The pulse strikes for the fifth time changing (x_2, y_2) to (x_0, y_0) .

$$(x_0, y_0) = (\frac{3\pi}{2} + .157, 583.03)$$

The new c is

$$c = y_o + \sin x_o = 583.03 - .99 = 582.04$$

$$\begin{aligned} x_f &= 582.04 (2.2 \times 10^{-3}) + \frac{3\pi}{2} + .157 \\ &= \frac{3\pi}{2} + 1.44 \end{aligned}$$

$$y_f = c - \sin x_f = 582.04 + .13 = 582.17$$

After the pulse passes we are left with

$$(x_1, y_1) = \left(\frac{3\pi}{2} + 1.44, - .92\right)$$

From Fig. 2-25

$$(x_2, y_2) = \left(\frac{3\pi}{2} + 1.35, - .81\right)$$

The pulse strikes for the sixth time changing (x_2, y_2) into (x_o, y_o)

$$(x_o, y_o) = \left(\frac{3\pi}{2} + 1.35, 582.28\right)$$

The new c is

$$c = y_o + \sin x_o = 582.28 - .22 = 582.06$$

$$x_f = 582.06 (2.2 \times 10^{-3}) + \frac{3\pi}{2} + 1.35 = 2\pi + 1.06$$

$$y_f = c - \sin x_f = 581.19$$

As the pulse passes the system coordinates become

$$(x_1, y_1) = (.87, - 1.90)$$

The resulting output frequency error is plotted in Fig.2-26 .

2.5 APPENDIX A

Series Solution to First Order Loop with Carrier and Interference Present
At the Input

The differential equation is (2-9)

$$\dot{\psi} + K \left[\sin \phi_o + (\cos \phi_o) \psi \right] = \delta \sum_{n=1}^{\infty} (-1)^{n+1} a^n \cos n\delta t + \omega - \omega_o \quad (2-9)$$

Assume a solution of the form (2-10)

$$\psi = \sum_{n=1}^{\infty} A_n \cos (n\delta t + \alpha_n) \quad (2-10)$$

Then

$$\dot{\psi} = - \sum_{n=1}^{\infty} A_n n\delta \sin (n\delta t + \alpha_n) \quad (A-1)$$

Therefore (2-9) becomes

$$\begin{aligned} & - \sum_{n=1}^{\infty} A_n n\delta \sin (n\delta t + \alpha_n) + K \sin \phi_o + \omega_o - \omega \\ & + K \cos \phi_o \sum_{n=1}^{\infty} A_n \cos (n\delta t + \alpha_n) = \delta \sum_{n=1}^{\infty} (-1)^{n+1} a^n \cos n\delta t \quad (A-2) \end{aligned}$$

Immediately we obtain

$$K \sin \phi_o + \omega_o - \omega = 0 \quad (A-3)$$

$$\phi_o = \sin^{-1} \left\{ \frac{\omega - \omega_o}{K} \right\} \quad (A-4)$$

Expanding $\sin(n\delta t + \alpha_n)$ and $\cos(n\delta t + \alpha_n)$ and collecting terms in (A-2) yields

$$\sum_{n=1}^{\infty} (-A_n n\delta \sin n\delta t \cos \alpha_n - A_n n\delta \sin \alpha_n \cos n\delta t + K \cos \phi_o A_n \cos n\delta t \cos \alpha_n + A_n K \cos \phi_o \sin n\delta t \sin \alpha_n) = \sum_{n=1}^{\infty} \delta(-1)^{n+1} a^n \cos n\delta t \quad (A-5)$$

Equating the coefficient of $\sin n\delta t$ to zero and equating the coefficients of the $\cos n\delta t$ terms gives

$$-A_n n\delta \cos \alpha_n - A_n K \cos \phi_o \sin \alpha_n = 0 \quad (A-6)$$

$$-A_n n\delta \sin \alpha_n + K \cos \phi_o A_n \cos \alpha_n = \delta(-1)^{n+1} a^n \quad (A-7)$$

Equation (A-6) gives

$$\alpha_n = \tan^{-1} \frac{-n\delta}{K \cos \phi_o} \quad (A-8)$$

Equation (A-7) gives

$$\begin{aligned} A_n &= \frac{\delta(-1)^{n+1} a^n}{-n\delta \sin \alpha_n + K \cos \phi_o \cos \alpha_n} \\ &= \frac{\delta a^n (-1)^{n+1}}{\cos \alpha_n [K \cos \phi_o - n\delta \tan \alpha_n]} \end{aligned} \quad (A-9)$$

But from equation (A-8)

$$\tan \alpha_n = \frac{-n\delta}{K \cos \phi_o} \quad (\text{A-10})$$

Therefore

$$\cos \alpha_n = \frac{K \cos \phi_o}{\sqrt{(n\delta)^2 + K^2 \cos^2 \phi_o}} \quad (\text{A-11})$$

Substituting (A-10) and (A-11) into (A-9) and simplifying gives

$$A_n = \frac{(-1)^n + 1}{\sqrt{(n\delta)^2 + (K \cos \phi_o)^2}} \delta a^n \quad (\text{A-12})$$

2.6 APPENDIX B

Series Solution to the Second Order Loop with Carrier and Interference Present at the Input

The differential equation is (2-27).

$$\ddot{\phi} + K \dot{\phi} + K \tau \phi = \ddot{\theta} \quad (2-27)$$

In which $\ddot{\theta}$ is given by (2-28).

$$\ddot{\theta} = \delta^2 \sum_{n=1}^{\infty} (-1)^n n a^n \sin n\delta t \quad (2-28)$$

Assume a solution of the form (2-29).

$$\phi = \phi_o + \sum_{n=1}^{\infty} A_n \sin (n\delta t + \alpha_n) \quad (2-29)$$

Then we have

$$\dot{\phi} = \sum_{n=1}^{\infty} A_n n\delta \cos (n\delta t + \alpha_n) \quad (B-1)$$

$$\ddot{\phi} = \sum_{n=1}^{\infty} -A_n (n\delta)^2 \sin (n\delta t + \alpha_n) \quad (B-2)$$

Substituting (2-28), (2-29), (B-1), and (B-2) in (2-27) yields

$$\begin{aligned}
& \sum_{n=1}^{\infty} -A_n (n\delta)^2 \sin(n\delta t + \alpha_n) + \sum_{n=1}^{\infty} K A_n n\delta \cos(n\delta t + \alpha_n) \\
& + K \tau \phi_0 + \sum_{n=1}^{\infty} K \tau A_n \sin(n\delta t + \alpha_n) = \sum_{n=1}^{\infty} \delta^2 n^2 (-1)^n a^n \sin n\delta t \quad (B-3)
\end{aligned}$$

Expanding $\sin(n\delta t + \alpha_n)$ and $\cos(n\delta t + \alpha_n)$ gives

$$\begin{aligned}
& -A_n (n\delta)^2 \sin n\delta t \cos \alpha_n - A_n (n\delta)^2 \cos n\delta t \sin \alpha_n + K \tau \phi_0 \\
& - K A_n n\delta \sin n\delta t \sin \alpha_n + K A_n n\delta \cos n\delta t \cos \alpha_n \\
& + K \tau A_n \sin n\delta t \cos \alpha_n + K \tau A_n \cos n\delta t \sin \alpha_n \\
& = \delta^2 (-1)^n n^2 a^n \sin n\delta t \quad (B-4)
\end{aligned}$$

Combining terms and equating coefficients of $\sin n\delta t$ and $\cos n\delta t$ equal to zero gives

$$\phi_0 = 0 \quad (B-5)$$

$$-A_n (n\delta)^2 \cos \alpha_n - K A_n n\delta \sin \alpha_n + K \tau A_n \cos \alpha_n = (-1)^n \delta^2 n a^n \quad (B-6)$$

$$-A_n (n\delta)^2 \sin \alpha_n + K A_n n\delta \cos \alpha_n + K \tau A_n \sin \alpha_n = 0 \quad (B-7)$$

From (B-7) we have

$$\alpha_n = \tan^{-1} \frac{K n \delta}{n^2 \delta^2 - K \tau} \quad (B-8)$$

$$\cos \alpha_n = \frac{n^2 \delta^2 - K \tau}{\sqrt{K^2 n^2 \delta^2 + (n^2 \delta^2 - K \tau)^2}} \quad (B-9)$$

From (B-6)

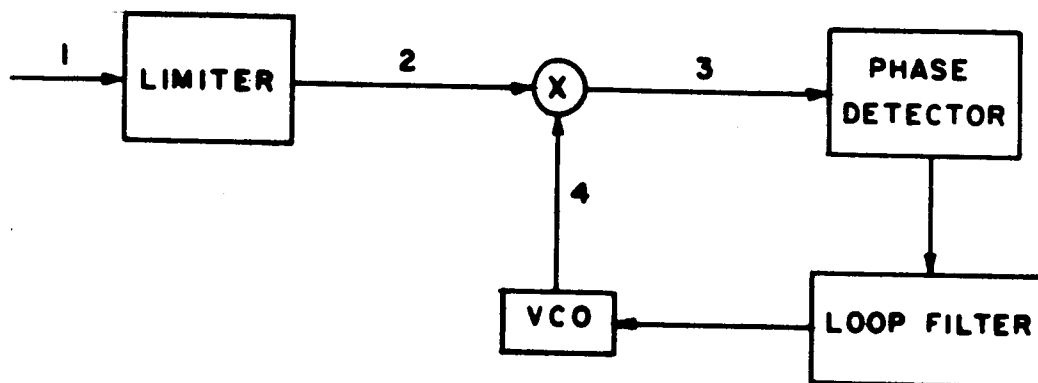
$$A_n = \frac{(-1)^n \delta^2 n a^n}{(K \tau - (n\delta)^2 - K n \delta \tan \alpha_n) \cos \alpha_n} \quad (B-10)$$

Substituting (B-8) and (B-9) in (B-10) gives

$$A_n = \frac{(-1)^{n+1} n \delta^2 a^n}{[(K n \delta)^2 + (n^2 \delta^2 - K \tau)^2]^{1/2}} = \frac{(-1)^{n+1} n \delta a^n}{\sqrt{(nK)^2 + \delta^2(n^2 - \frac{K\tau}{\delta^2})^2}} \quad (B-11)$$

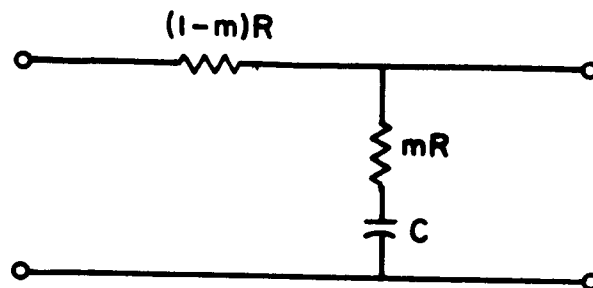
2.7 References

1. Panter, Philip, F., MODULATION, NOISE, AND SPECTRAL ANALYSIS, McGraw-Hill Book Co., New York, 1965.
2. Meer, S. Ahmed, "Analysis of Phase-Locked Loop Acquisition: A Quasi-Stationary Approach," IEEE International Convention Record, Part 7, New York, 1966.
3. Richman, D., "Color Carrier Reference Phase Synchronization Accuracy in NTSC Color Television," Proceedings of the Institute of Radio Engineers, Vol. 42, January, 1954.
4. Granlund, J., "Interference in Frequency Modulated Reception," MIT Research Laboratory Electronic Technical Report 42, January 20, 1949.
5. Viterbi, A. J., "Acquisition and Tracking Behavior of Phase Locked Loops," Symposium on Active Networks and Feedback Systems, Interscience Publishers, Evanston, Ill., 1961.
6. Truxal, J. G., AUTOMATIC FEEDBACK CONTROL SYSTEM SYNTHESIS, McGraw-Hill Book Co., New York, 1955.
7. Dwight, H. B., TABLES OF INTEGRALS AND OTHER MATHEMATICAL DATA, 4th Edition, Macmillan Company, New York, 1961.



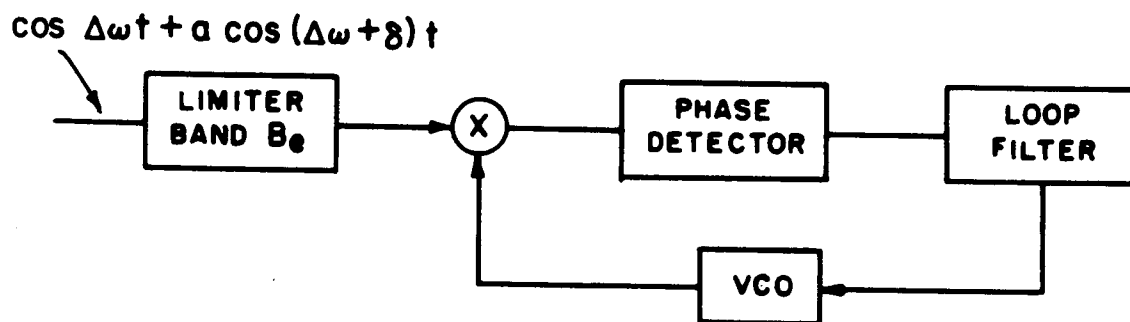
Model for the Phase Locked Loop

Figure 2-1



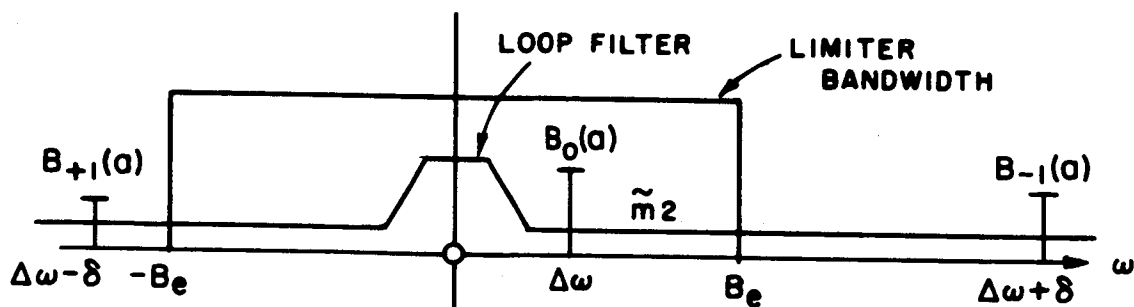
Second Order Loop Filter

Figure 2-2



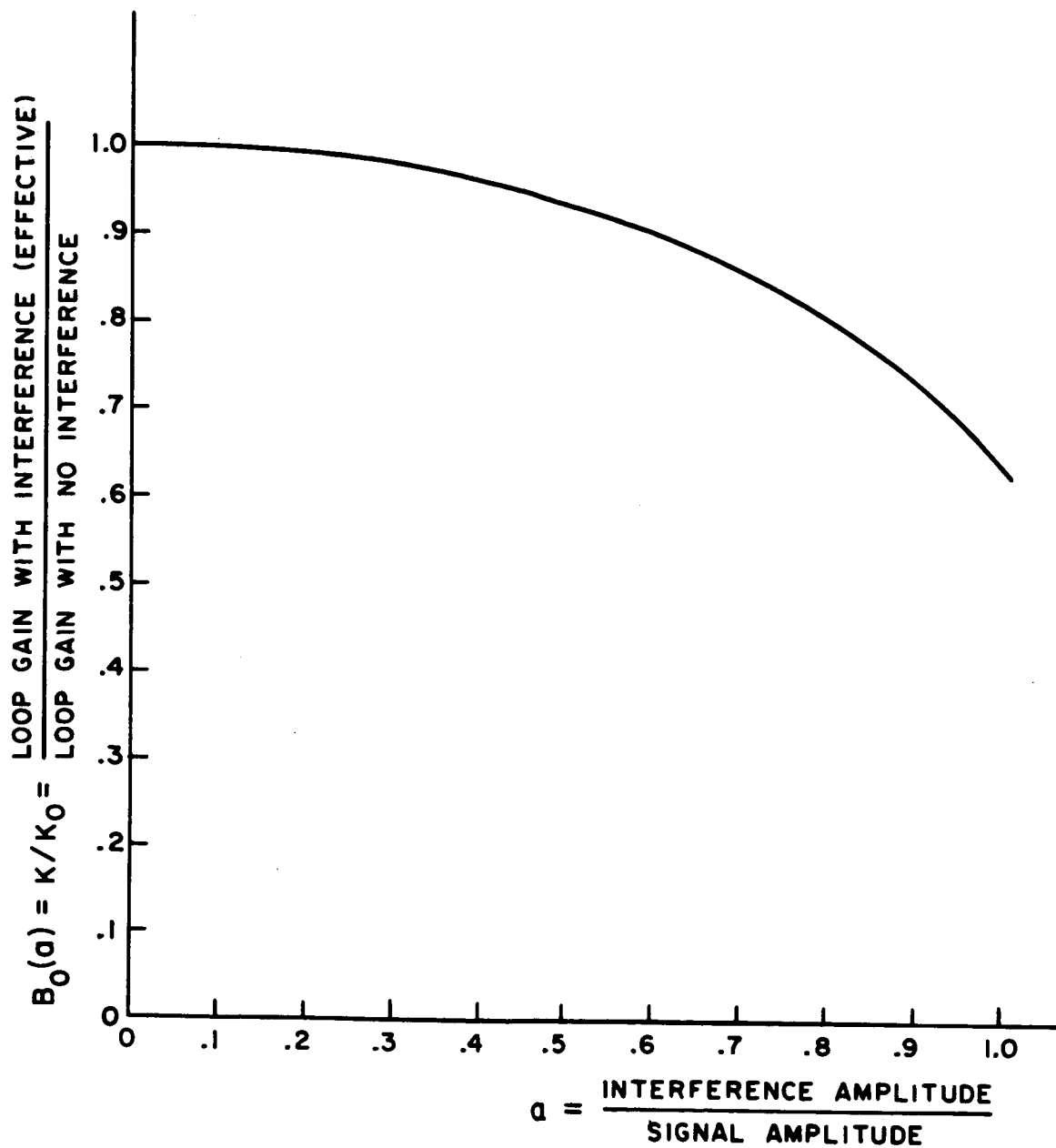
Model for the Phase Locked Loop

Figure 2-3



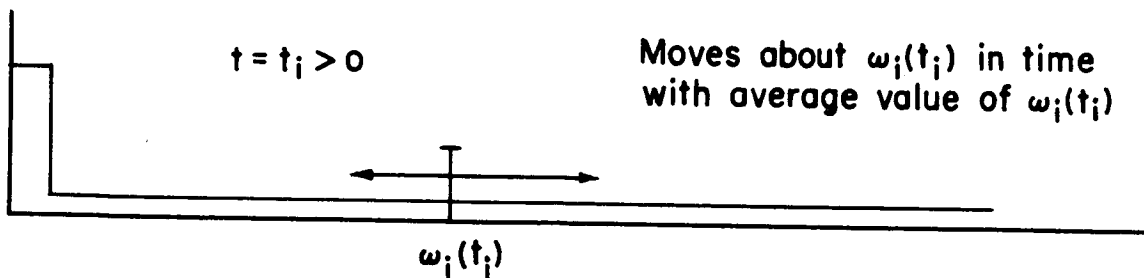
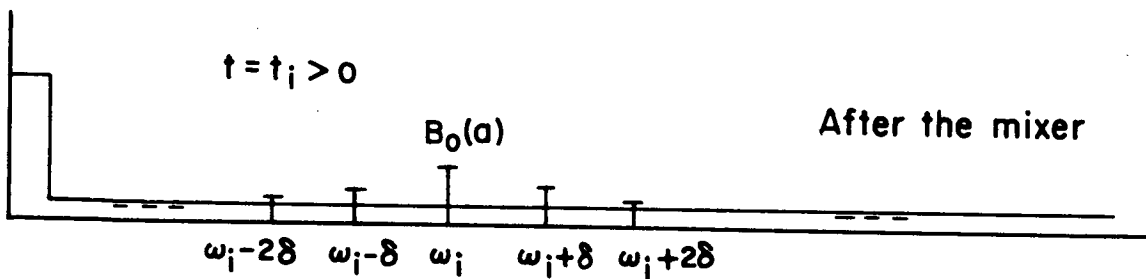
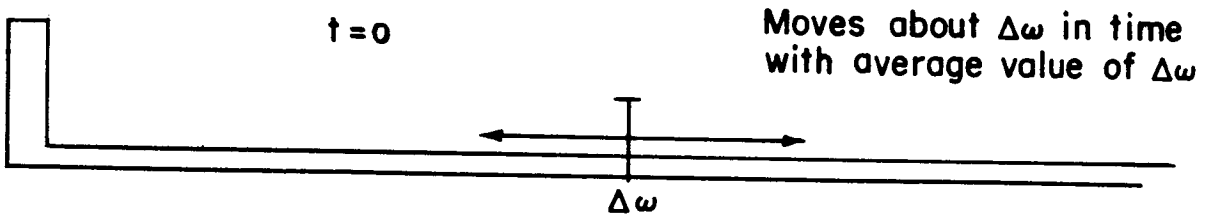
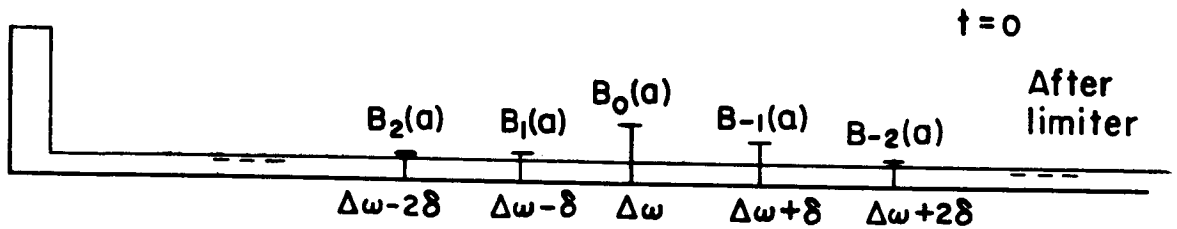
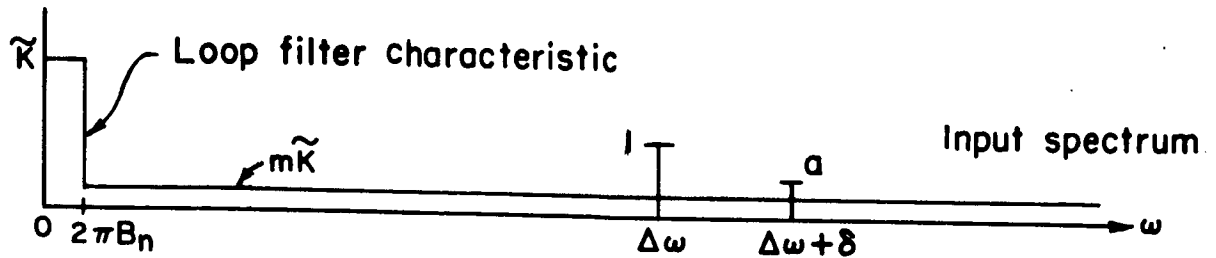
Output Spectrum of an Ideal Limiter with Limiter Filter Characteristic and Loop Filter Characteristic Superimposed

Figure 2-4

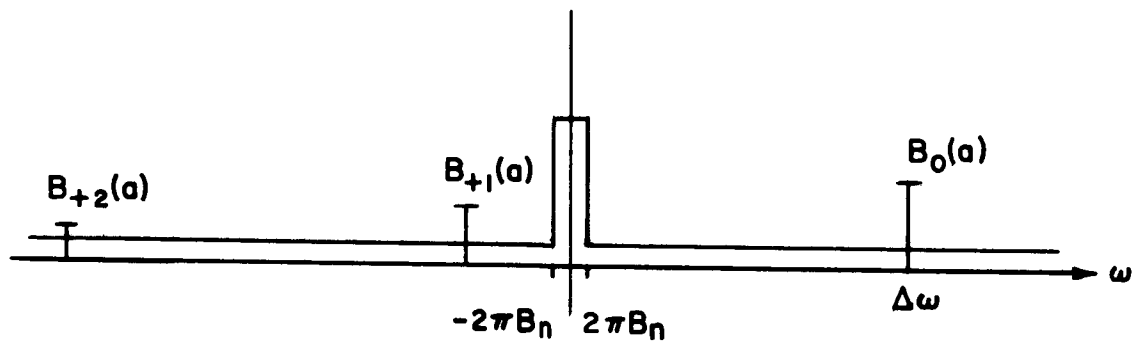


Effective Loop Gain with Interference
Versus the Relative Interference Amplitude

Figure 2-5

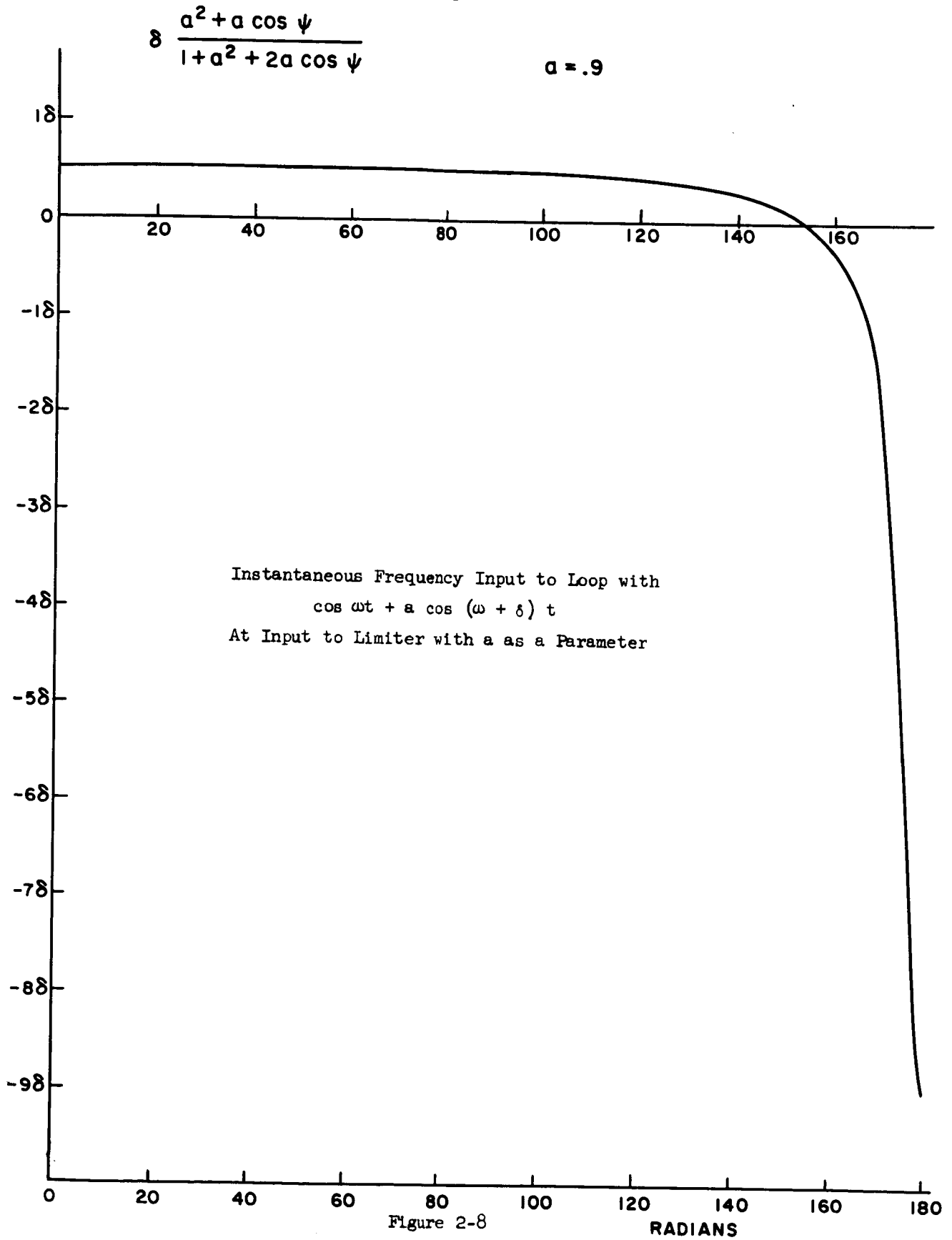


The Acquisition Process: The Spectral Analysis Viewpoint
and the Composite Signal Viewpoint
Figure 2-6



Limiter Output Spectrum with Loop Filter
Characteristic Superimposed

Figure 2-7



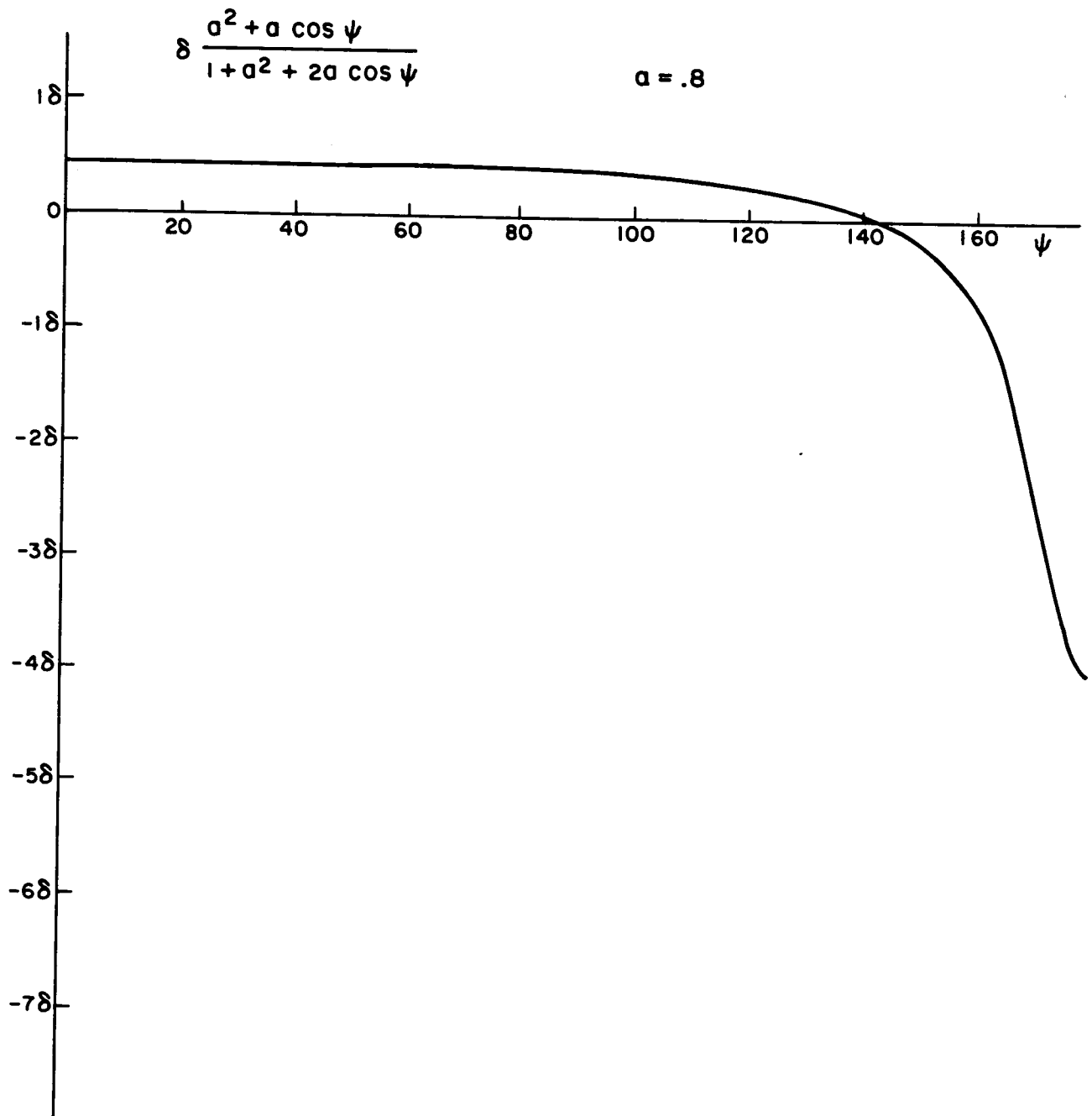


Figure 2-9

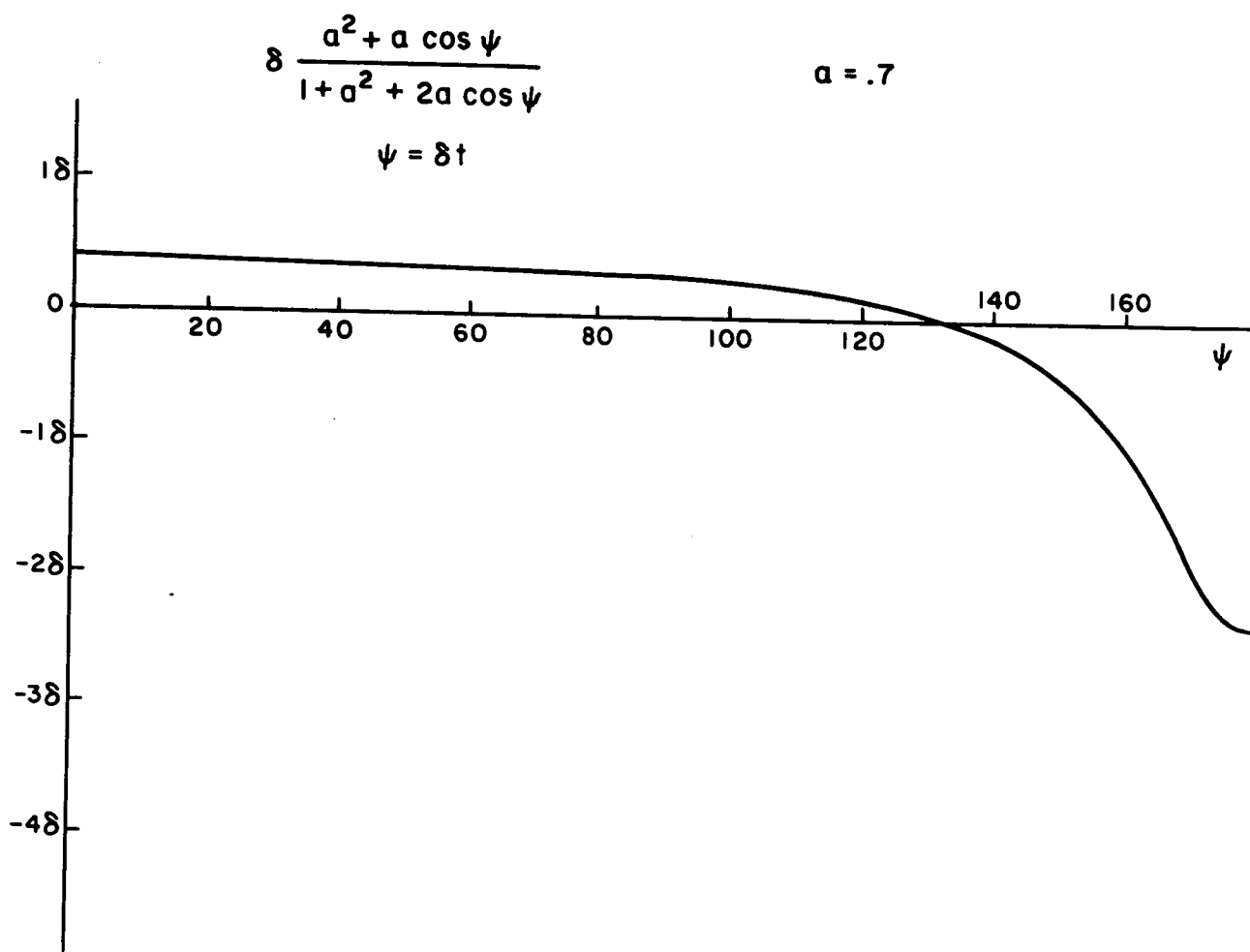


Figure 2-10

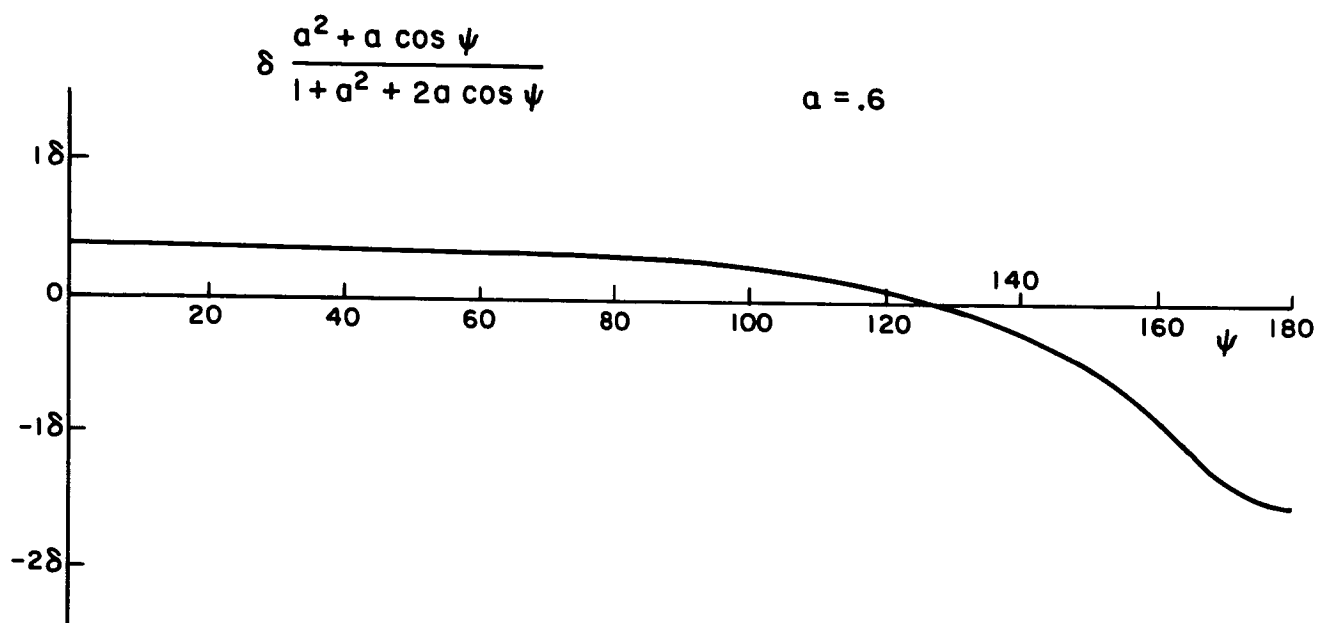


Figure 2-11

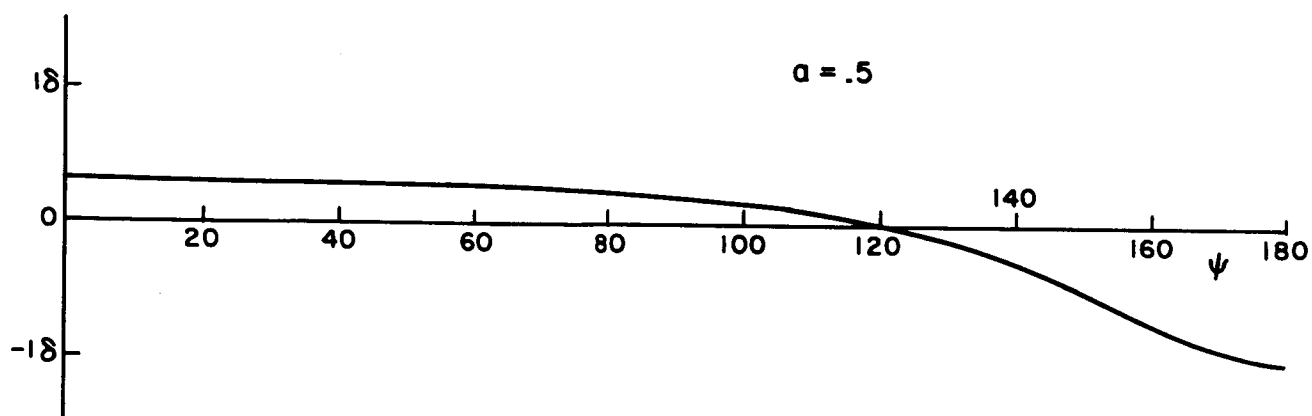


Figure 2-12

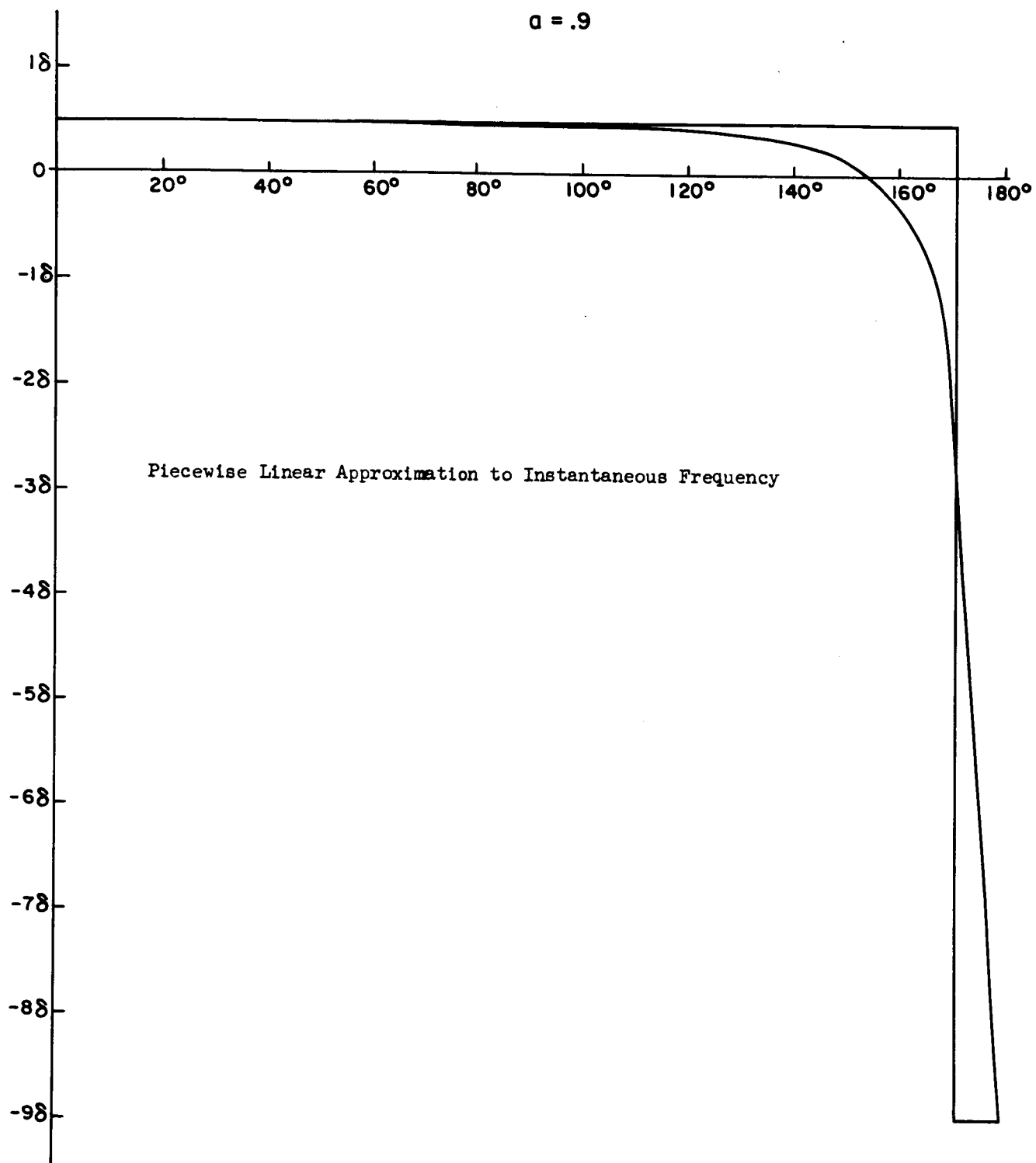
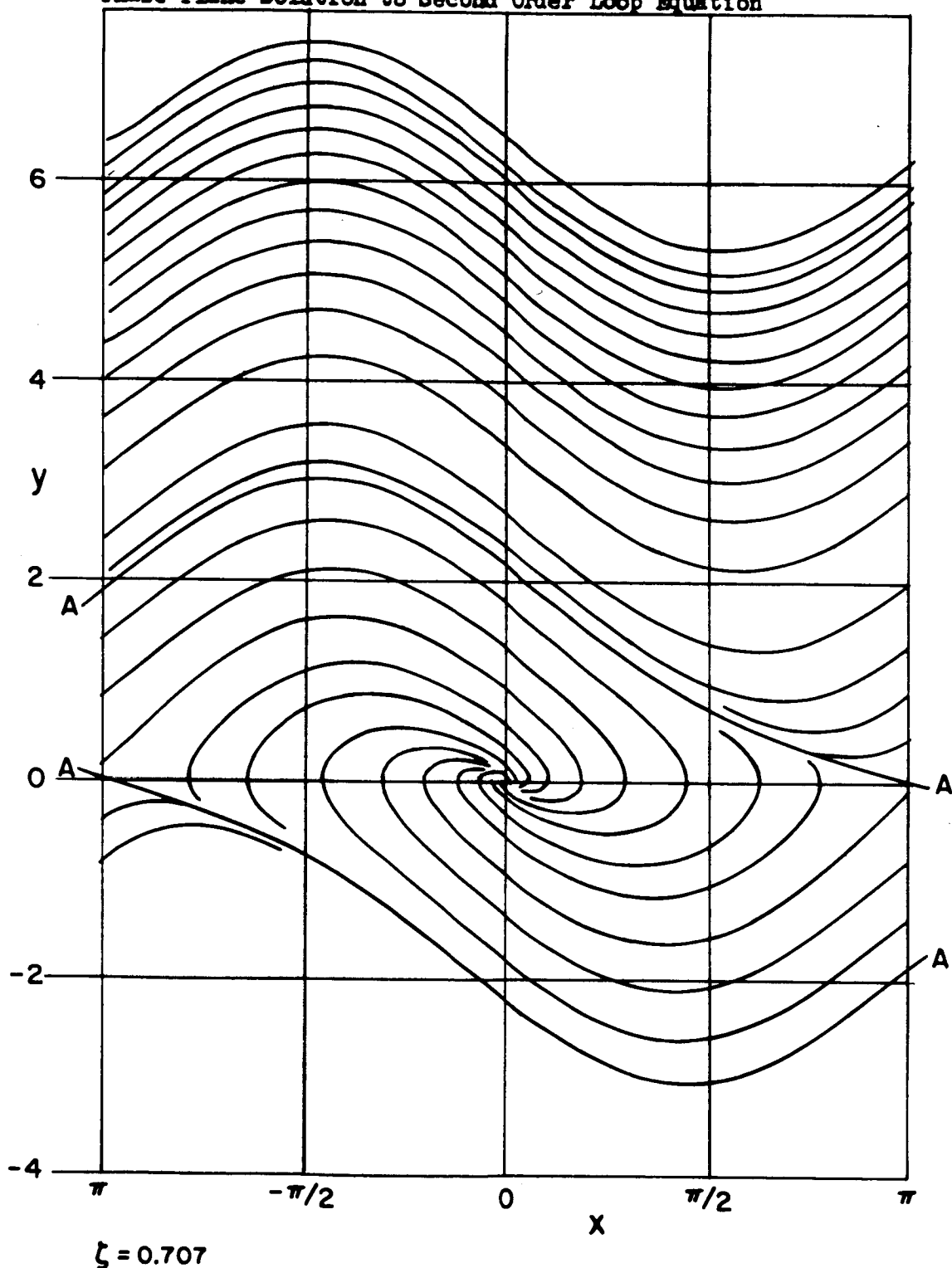


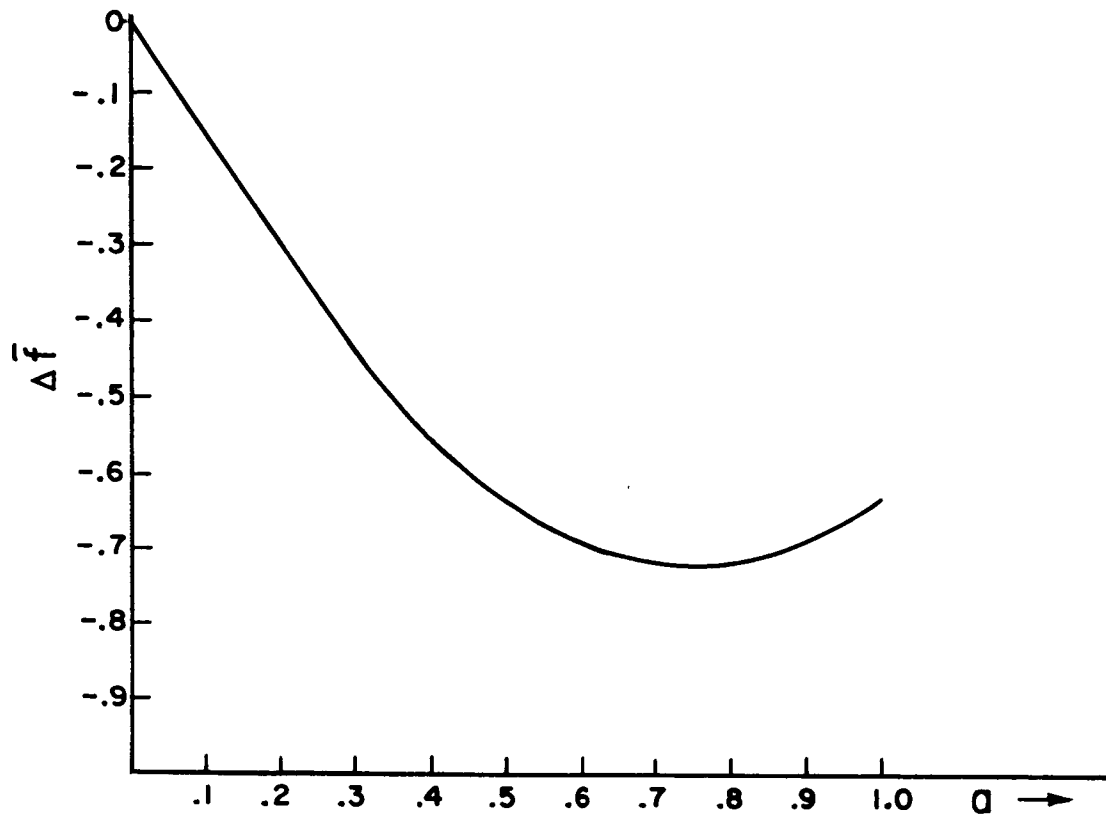
Figure 2-13

Phase Plane Solution to Second Order Loop Equation



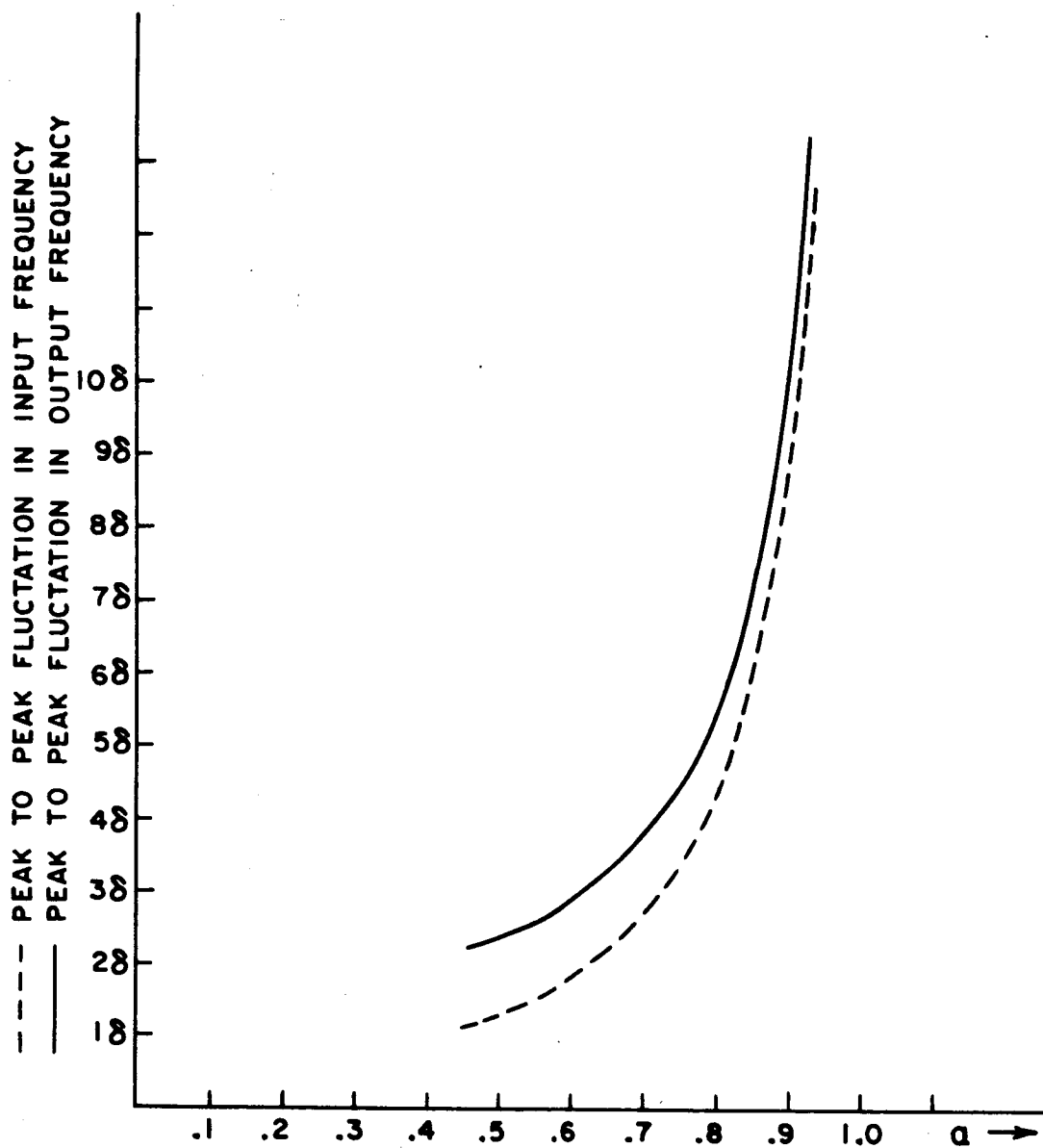
In the frequency acquisition region, only every third trajectory is drawn.

Figure 2-14



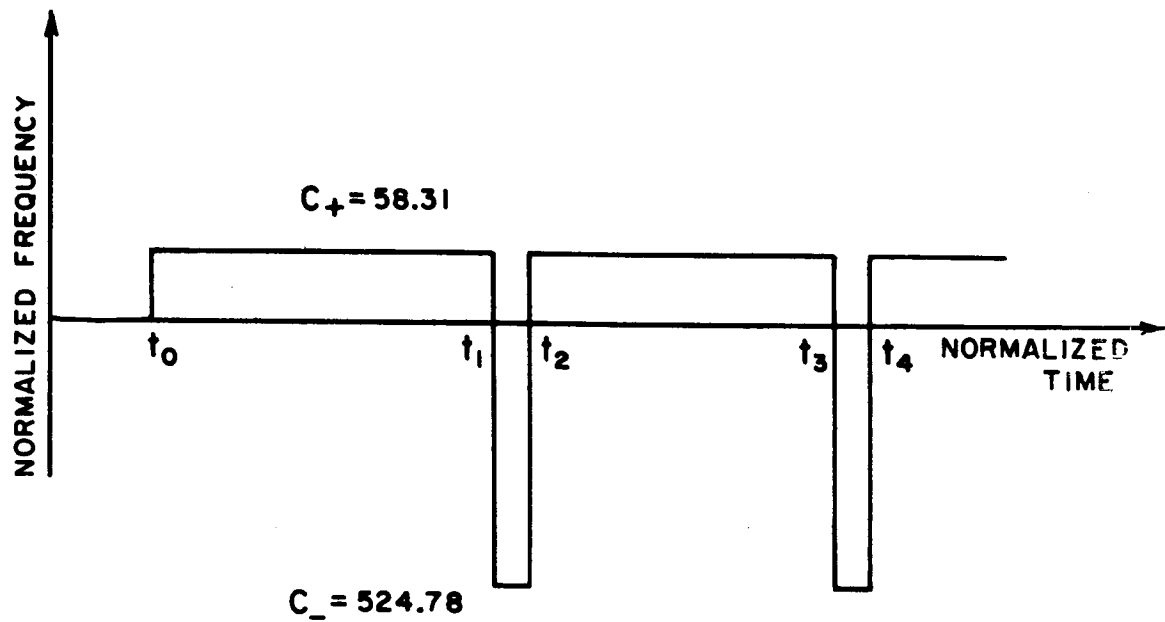
Change in Average Frequency
Caused by Phase Locked Loop

Figure 2-15



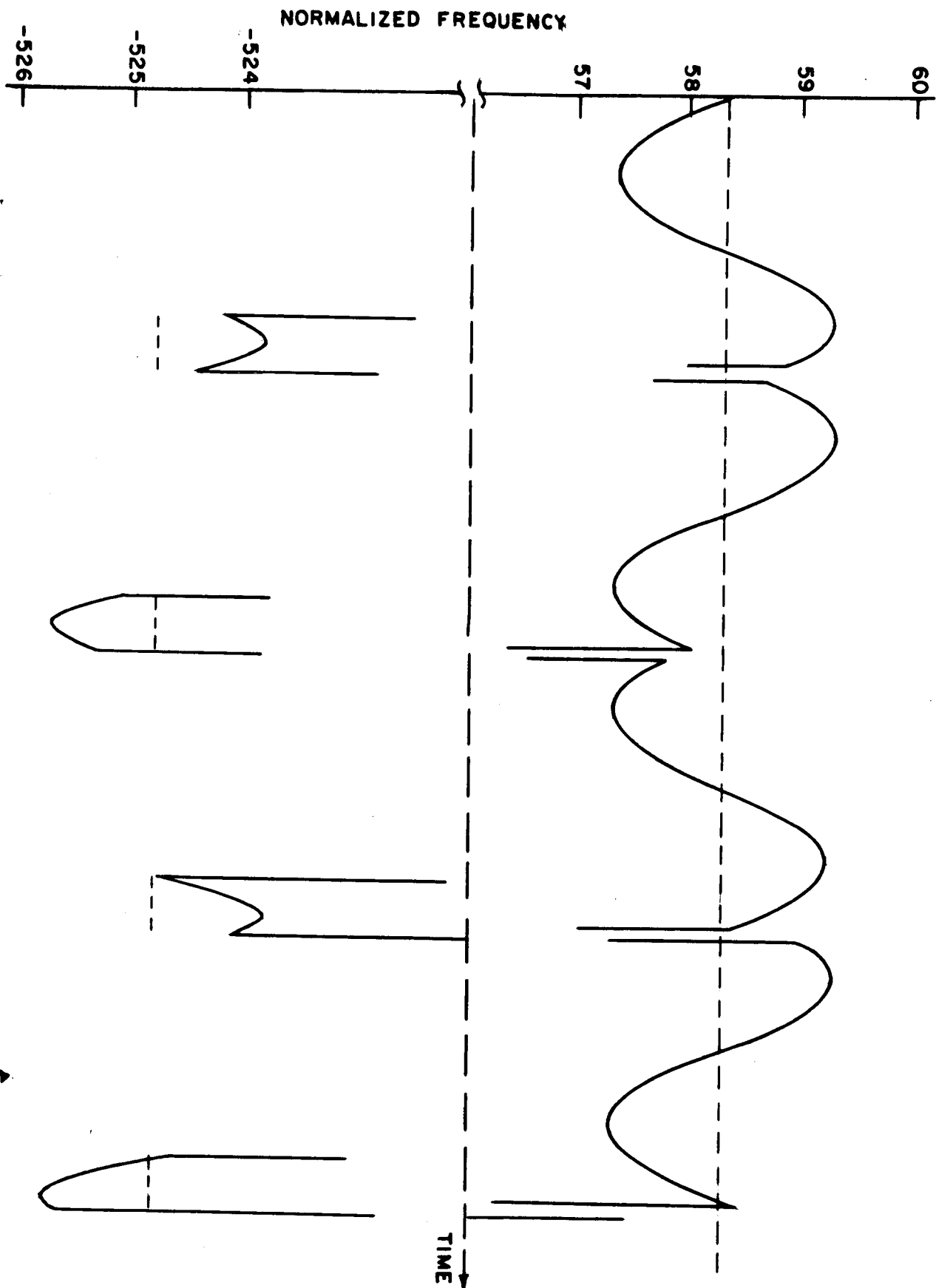
Peak to Peak Fluctuation in Input and Output Frequency
As a Function of a.

Figure 2-16



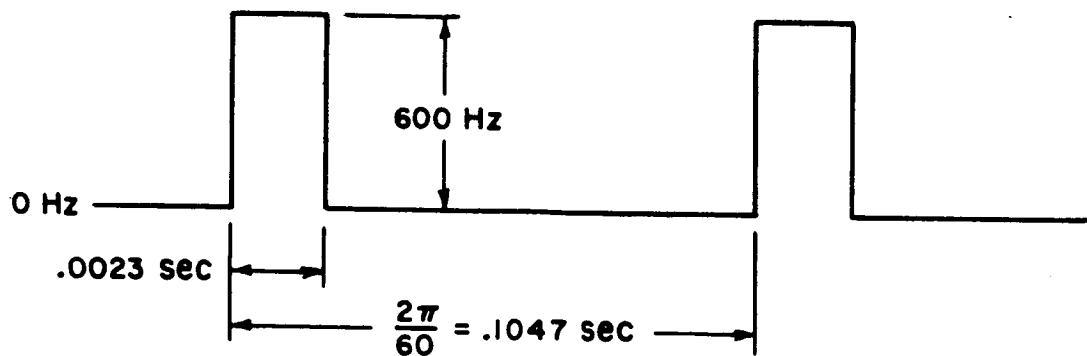
Approximate Frequency Input

Figure 2-17



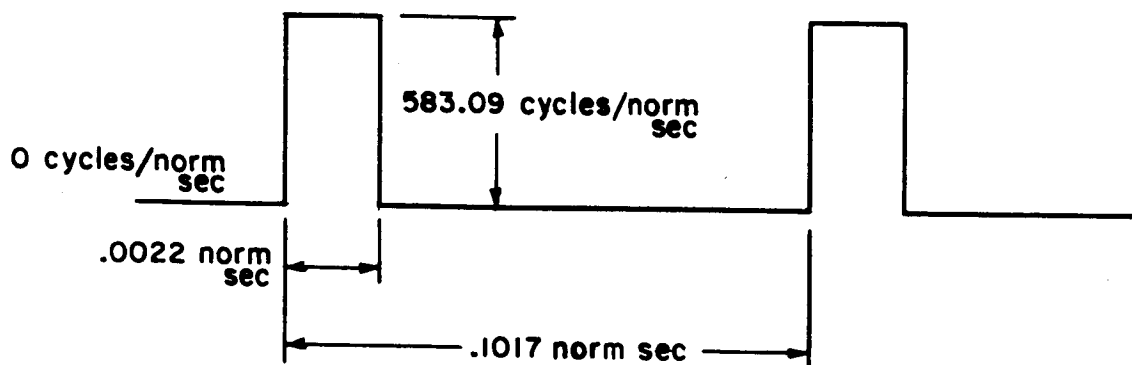
Output Frequency Error for Input of Fig. 2-17

Figure 2-18



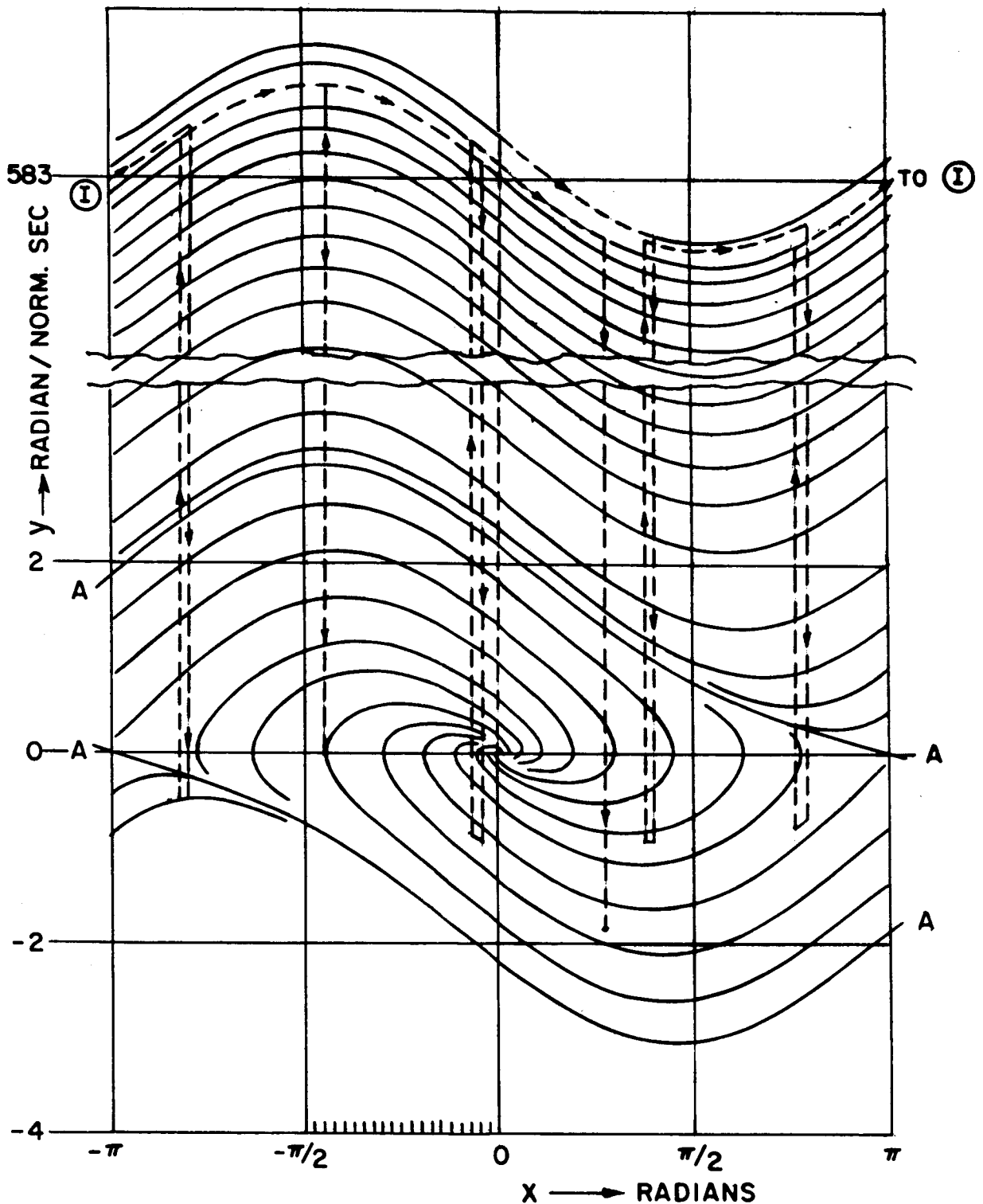
Approximate Input Frequency

Figure 2-19



Normalized Approximation to Input Frequency

Figure 2-20



Phase Plane Solution to Second Order Loop Equation with
Trajectory for Input of Figs. 2-19 and 2-20 Superimposed

Figure 2-21

Graphical Integration

1 sec = 3277 sq. units

1 normalized sec = 3184 sq. units

Therefore the second pulse strikes after
318 sq. units.

$$52x = 318$$

$$x = 6.11$$

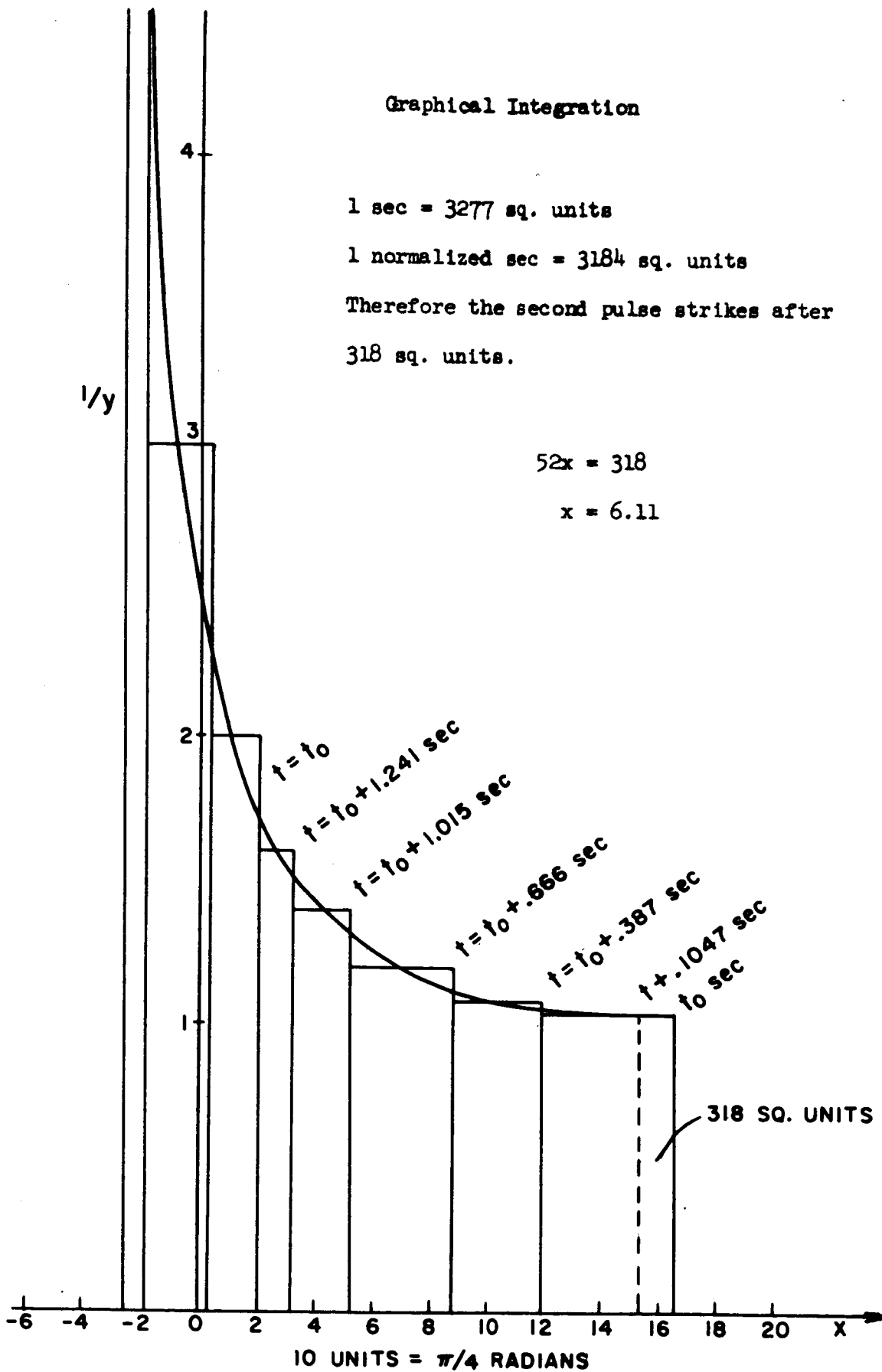


Figure 2-22

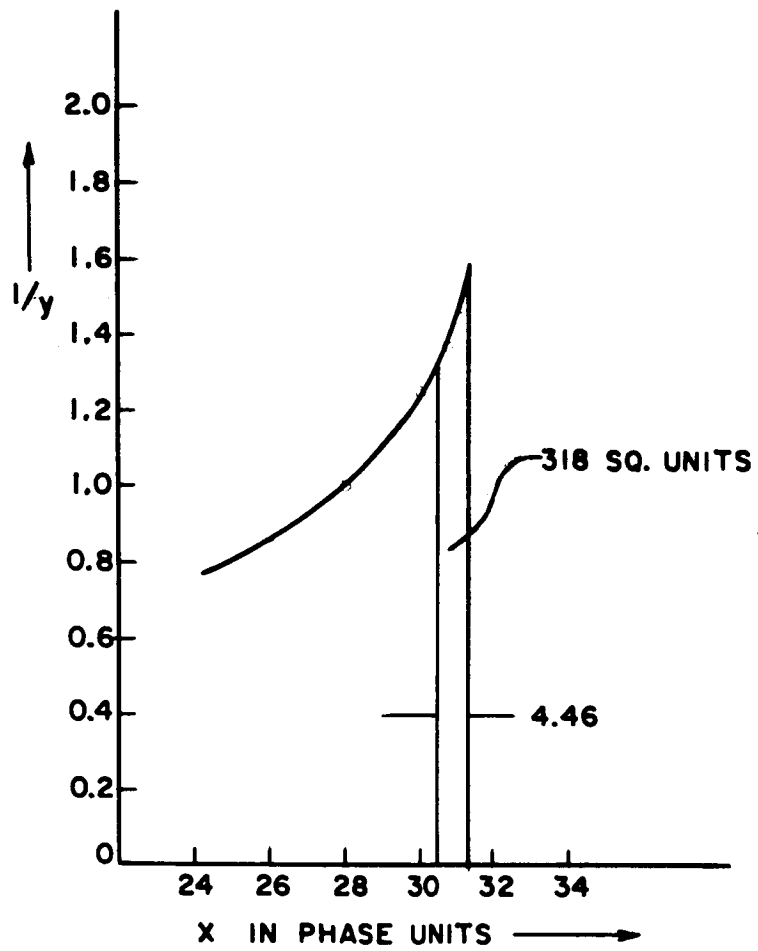


Figure 2-23

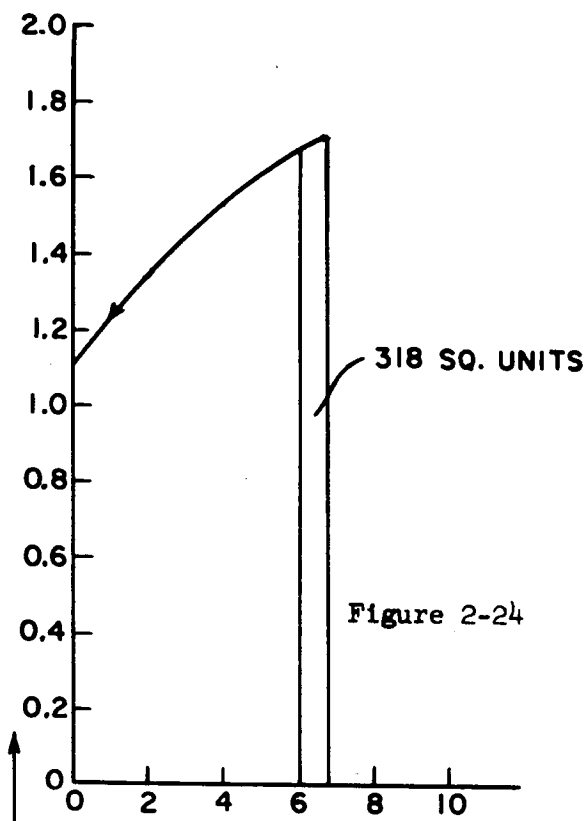


Figure 2-24

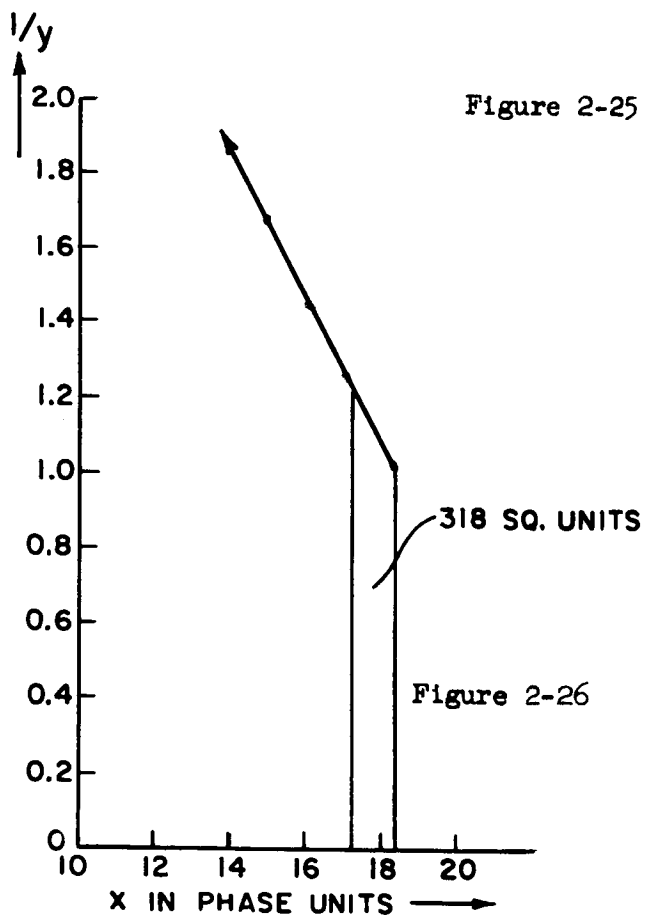
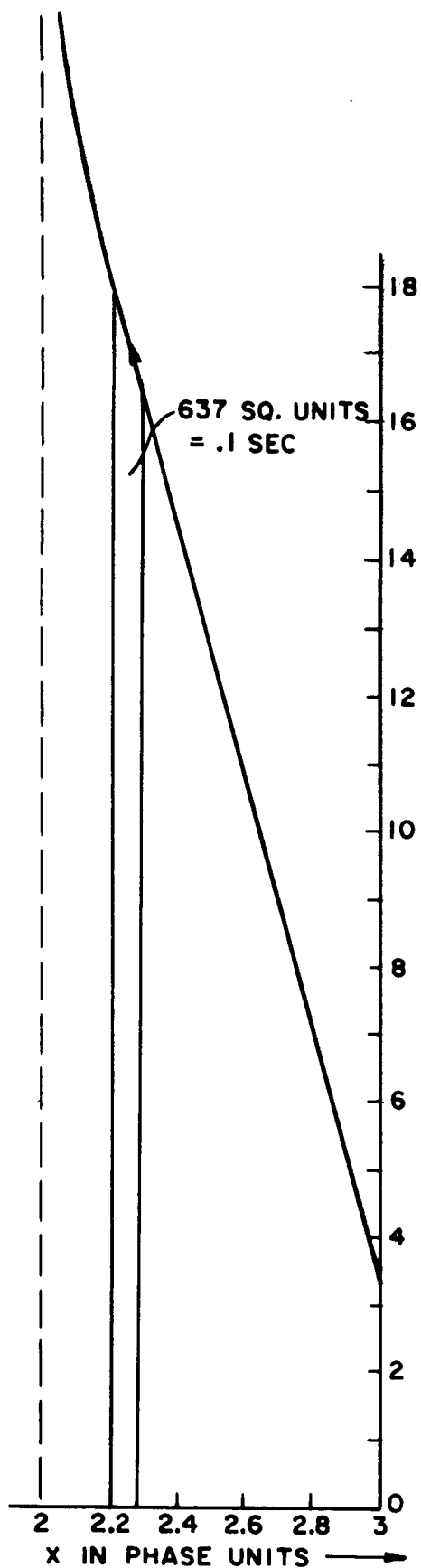


Figure 2-26



SPIKES ARE SHOWN LASTING 9 TIMES
AS LONG AS THEY ACTUALLY DO.

Output Frequency Error for
Input of Figs. 2-19 and 2-20
Fig. 2-27

